DIAGENETIC CHANGES IN LONG BONES IN CENTRAL FLORIDA: A PRELIMINARY
MACRO- AND MICROSCOPIC COMPARISON OF SUN AND SHADE
MICROENVIRONMENTS

by

MIKAYLA MAY OVERHOLTZER
B.A. University of Montana, 2012

A thesis submitted in partial fulfillment of the requirements
for the degree of Master of Arts
in the Department of Anthropology
in the College of Sciences
at the University of Central Florida
Orlando, Florida

Fall Term
2015

Advisor: John J. Schultz

ABSTRACT

In forensic investigations, the estimation of time since death is of utmost importance when examining decomposing bodies and skeletal remains. Current methodology typically focuses on the gross and macroscopic changes to human remains. Surprisingly, microscopic analysis of diagenetic change has not been fully researched in regards to time since death. The current study involved the analysis of diagenetic change in 15 pig (*Sus scrofa*) long bones from two microenvironments (sun and shade) in the subtropical environment of Central Florida. While the control bone was not placed in the field, seven bones were placed in the sun microenvironment and seven in the shade microenvironment. One bone was collected from each micro environment every other week for a duration of 14 weeks. The samples were then analyzed for gross and macroscopic taphonomic changes, which included soil staining, hemolysis staining, loss of bone grease, and penetration of hemolysis staining into the bone cortex. Microscope slides were then prepared using thin sections of the 15 long bones. Slides were then stained with Periodic Acid Schiffer's stain and Hemotoxylin and Eosin stain and analyzed for Non-Wedl microscopic focal destruction (MFD), Wedl tunneling, and Haversian canal inclusions using standard light microscopy. While gross and macroscopic changes were not significant due to the short time interval studied, microscopic diagenetic changes that were observed included MFD and Wedl tunneling as early as four and six weeks, respectively. Group A (sun) demonstrated a greater occurrence of diagenetic change and greater diameter of MFD. Additionally, the maximum diameter of MFD steadily increased over time, suggesting a correlation between size of MFD and time since death. This pilot study demonstrates the possibility for future research to establish standards for estimating time since death using microscopic analysis. For example,

further research should consider implementing a larger sample size, a longer postmortem

interval, additional environments, comparative human samples, and a standardized methodology

for preparing and analyzing the histological samples.

ACKNOWLEDGMENTS

Thank you to the Arboretum staff, particularly John and Jacques, for driving us out to the research site and being willing to help us out.

Garrett Kelly, for responding to my distress call for an artist to draw a bone biology diagram.

Finally, thank you to everyone in the UCF Anthropology department. I sincerely appreciate all of the help and encouragement throughout graduate school. I am proud to be a UCF Knight.

TABLE OF CONTENTS

LIST OF FIGURES

LIST OF TABLES

CHAPTER ONE: INTRODUCTION

In forensic investigations, time since death estimation is of paramount importance when examining decomposing bodies and skeletal remains. It allows investigators to establish a timeline of events and identify the decedent. Therefore, having methodologies for estimating the postmortem interval throughout all stages of decomposition into skeletonization is necessary. The rate and stages of soft tissue decomposition have been widely studied and reviewed (e.g., Galloway et al., 1985; Dix and Graham, 2000, Megyesi et al., 2005; Christensen et al., 2014; Damann and Carter, 2014); however, methods for estimating the postmortem interval using the hard tissues of the body remains imprecise.

Weathering standards were originally set forth by Behrensmeyer (1978) as a way to correlate the gross destruction of bone with the postmortem interval. As taphonomic research has advanced, the influence of the environment on the physical changes the bone has become the focus of weathering studies. However, since weathering studies require years of field work for gross changes to occur, many researchers have found this line of inquiry to be arduous with little reward (Beary and Lyman, 2012). Macroscopic and microscopic techniques have been proposed in recent years as a potential line of inquiry to refine the early postmortem interval estimation beyond the Behrensmeyer (1978) scale (Christensen et al., 2014; Damann and Carter, 2014; Jans, 2014).

Histological analysis of bone has been concentrated on two foci: the identification of diagenetic changes in archaeological samples and distinguishing between human and non-human bone tissues. Overwhelmingly, the literature correlates diagenetic changes with archaeological bone (e.g., Child, 1995; Nielsen-Marsh and Hedges, 2000; Trueman and Martill, 2002; Jans et

al., 2004). Challenging this notion, a few studies demonstrate the presence of diagenetic changes in bone with a much shorter postmortem interval. Yoshino et al. (1991) examined human bone with known postmortem intervals and found diagenetic changes within five years postmortem. Refining this, Bell et al. (1996) discovered diagenetic changes within three months postmortem. Additional studies have found diagenetic changes within a forensically significant time interval (Turner-Walker, 2012; White and Booth, 2014), but have failed to correlate postmortem interval with diagenetic changes.

The other foci of histological analysis of bone has been the distinction between human and animal bone for archaeological and forensic contexts. There have been many differences noted between human and non-human bone, for example, osteon banding, size of osteons, density of primary and secondary osteons, and, in particular, the presence of plexiform bone (Mulhern and Ubelaker, 2001; Martiniakova et al., 2006a; Hillier and Bell, 2007; Crescimanno and Stout, 2012; Junod and Pokines, 2014). Plexiform bone is a type of primary bone tissue within the fibrolamellar bone tissue group, and is found commonly in fast-growing, large animals, such as cows, horses, dogs, and pigs (Cuijpers 2006; Martiniakova et al. 2006a; Hillier and Bell 2007). Plexiform bone can be found in humans during periods of growth, such as infancy and during bone remodeling from trauma (Hillier and Bell 2007; Martiniakova et al. 2006a), but has been used as a distinguishing feature to identify non-human remains. For this reason, researchers have questioned the usefulness of non-human proxies, pigs in particular, for experimental studies (Junod and Pokines, 2014). However, Aerssens et al. (1998) examined the quality of human bone compared to dog, pig, chow, sheep, chicken, and rat, and discovered that, while dog bone more closely resembled human bone, pig bone was a close second. Therefore, experimental research utilizing pig bone as a proxy for human bone does not necessarily limit the

applicability of the results. The utilization of pig bone in forensic anthropological studies has been widely accepted in the field, particularly due to the destructive nature of diagenetic studies and the rarity of human samples (e.g., Komar and Beattie, 1998; Janjua and Rogers, 2008; Huculak and Rogers, 2009; Cunningham et al., 2011; White and Booth, 2014), but interspecies variation in diagenesis is still not fully understood.

Current methodologies for histological analysis require the complete maceration of the soft tissue and cleaning of the bone (e.g., Caropreso et al., 2000; Beauchesne and Saunders, 2006; Martiniakova et al., 2006b; Crowder et al., 2012; de Boer et al., 2013). This rids the bone of grease, but also cleans the bacteria and fungi present in the bone matrix. The current study adapts the protocol of Crowder et al. (2012) to eliminate the destructive cleaning procedures in order to view the progression of bacterial and fungal invasion in the bone matrix, with the intent of providing insight into the progression of bacteria and fungi into the bone.

The purpose of this thesis is to examine the gross, macroscopic, and microscopic taphonomic changes to bone in a humid, sub-tropical environment. The three main objectives for the current research project are:

1. To identify the earliest time interval for diagenetic changes occurring microscopically.
2. To compare the diagenetic changes between the two microenvironments and evaluate if there are differences in the occurrence and size of diagenetic changes.
3. To determine if this method can be utilized to estimate time since death.

First, the current methods of estimating time since death will be overviewed. This will demonstrate the wealth of knowledge regarding soft tissue decomposition and the lack of information regarding skeletal deterioration. Then, the materials and methods will be outlined. As previously discussed, a new histological methodology will be presented to maintain the

integrity of the bacteria and fungi present in the bone matrix. Next, the results of the histological analysis will be detailed. Finally, a discussion of the implications of the results and the future avenues of research will be presented.

CHAPTER TWO: TIME SINCE DEATH ESTIMATION

Time since death estimation is one of the most important and most difficult aspects of forensic investigations (Mann et al., 1990; Buchan and Anderson, 2001). The minimum time interval the remains have been exposed in an environment can narrow down the potential pool of victims in forensic investigations. Historically, investigations into the postmortem interval have focused on gross observations of soft tissue changes, but forensic anthropologists frequently are asked to assist on cases where no soft tissue is present (Beary and Lyman, 2012). Despite the research that has been conducted, more precise methods for estimating the postmortem interval are necessary. Therefore, understanding the current methods of time since death estimation and the limitations of these studies will clarify the necessity of further research.

Decomposition

Decomposition begins at the cessation of life (Damann and Carter, 2014). Once the normal operations of the human body stop, the processes of decomposition begin. There are four broad stages that have been recognized based on the observable soft tissue changes: fresh, early decomposition, advanced decomposition, and skeletonization (Galloway et al., 1989; Megyesi et al., 2005). However, a decedent can present multiple stages of decomposition in different areas of the body (Dix and Graham, 2000).

The fresh stage occurs immediately after death. The cellular destruction caused by the lack of oxygen, called autolysis, is the hallmark of the fresh stage. Autolysis most often begins in the pancreas or stomach and causes the destruction of cells from their own enzymes, the decrease

in cellular adenosine triphosphate (ATP), and the presence of fluids around the mouth or nose (Komar and Buikstra, 2008; Christensen et al., 2014; Damann and Carter, 2014). These microscopic changes in the soft tissue initiate the macroscopic changes of the mortis triad (Damann and Carter, 2014).

The mortis triad, algor, livor, and rigor, occur in the late fresh stage and can persist into the early decomposition stage (Galloway et al., 1989; Megyesi et al., 2005). Algor mortis is simply the cooling of the body and begins at the moment of death. There is generally no associated discoloration. The cooling rate from 98.6°F to ambient temperature has been generally accepted at 1.5°F per hour (Dix and Graham, 2000; Christensen et al., 2014; Damann and Carter, 2014). This relationship is not linear, but has been used as an acceptable postmortem interval estimator for the first 10 to 12 hours postmortem (Christensen et al., 2014; Damann and Carter, 2014).

Livor mortis, or lividity, results from the intravascular concentration and hemolysis of blood cells. This results in the pooling of blood in the lowest points of the body, creating a reddish-purple appearance (Dix and Graham, 2000; Komar and Buikstra, 2008; Christensen et al., 2014; Damann and Carter, 2014). This begins between 30 minutes to four hours after death and is most pronounced after 12 hours (Komar and Buikstra, 2008; Christensen et al., 2014). Livor mortis can be unfixed or fixed, with these stages being defined by blood coagulation. Before the blood coagulates, livor mortis is unfixed, and if the body is moved, the pooling of blood will occur in the new location. Once the blood coagulates approximately eight to 12 hours after death, livor mortis is fixed, and movement of the body will not change the patterns of blood pooling (Komar and Buikstra, 2008; Christensen et al., 2014; Damann and Carter, 2014).

Rigor mortis is the result of the decrease in cellular ATP and pH, the accumulation of lactic acids, and the presence of calcium ions (Komar and Buikstra, 2008; Damann and Carter, 2014). This creates the stiffening of the muscles caused by the binding of muscle fibers. Muscles require ATP in order to release from the constriction, but the ATP in the body quickly declines after death (Christensen et al., 2014). Rigor can initiate by two to six hours postmortem in the face and hands and progresses to the large muscle groups after approximately 12 hours. This can continue for one to two days (Dix and Graham, 2000; Komar and Buikstra, 2008; Damann and Carter, 2014).

Early decomposition is marked by the appearance of skin slippage and discoloration of the body. This can be identified through the drying of extremities, marbling, or a green discoloration in the abdomen (Galloway et al., 1989; Komar and Buikstra, 2008). The process involved in this stage is putrefaction. The loss of homeostatic conditions of the living body and the transmigration of bacteria of the gut to the surrounding tissues cause this skin to go through a series of color changes (Damann and Carter, 2014). First, the skin will pale then go from green to dark brown. The green discoloration occurs on the right anterior abdominal wall from the buildup of sulfur compounds. The dark brown results from the drying of the skin and generally occurs first at the head (Damann and Carter, 2014). Marbling can also occur from intravascular hemolysis, which darkens the blood vessels from the influx of bacteria in the circulatory system (Komar and Buikstra, 2008; Christensen et al., 2014). Putrefaction is also marked by the production of gases in the body cavity, causing the body to bloat. This can cause areas of the body to expand rapidly, the dermis to separate from the epidermis, and the skin to slip (Komar and Buikstra, 2008; Christensen et al., 2014; Damann and Carter, 2014). Skin slippage usually

occurs at the neck, abdomen, hands and feet. The transition to advanced decomposition occurs when the body cavity ruptures, releasing the gases from putrefaction (Damann and Carter, 2014).

Advanced decomposition begins with tissue sagging from the release of gases and an increase in maggot activity (Galloway et al., 1989). Exposure of skeletal elements begin, but this stage is characterized by less than half of the skeletal elements exposed. Skeletonization usually begins with the head and neck. Additionally, any lesions or wounds will accelerate skeletonization (Damann and Carter, 2014). Skeletonization is the last stage in decomposition and is marked by the exposition of bone of more than half of the body (Galloway et al., 1989).

Saponification, or the formation of adipocere from the conversion of fatty tissues, can occur during any stage of decomposition. It had been previously linked with advanced decomposition (Galloway et al., 1989), but has since been found to be unrelated to the stage of decomposition and linked to environmental factors (Megysi et al., 2005; Christensen et al., 2014). Adipocere usually occurs in unoxygenated, wet environments and can preserve soft tissue once formed and can complicate the estimation of time since death (Thali et al., 2011; Christensen et al., 2014).

Cultural and environmental factors can change the rate of human decomposition. Cultural determinants include autopsy, removal of organs, presence of clothing, mummification, and purposeful burial. Environmental determinates include temperature fluctuations, moisture levels, and soil pH (Damann and Carter, 2014). These factors can slow or accelerate the rate of decomposition.

The stage of decomposition has been correlated with postmortem interval estimation, but is highly dependent on the environment (Table 1). Galloway et al. (1989) demonstrated the rate of decomposition in the arid environment of Arizona and how it differed from the previous

research conducted in Tennessee, necessitating further research into the interaction of the environment and decomposition. Megyesi et al. (2005) correlated the stages of decomposition in regions of the body with accumulated-degree-days (ADD) and found that more precise postmortem intervals were being produced with the linear regression formulae. This quantitative method moves beyond the typological decomposition studies and produces a more precise method to calculate the postmortem interval. Particularly, it takes into account different regions of the body individually, rather than scoring the body between stages as a whole (Megyesi et al., 2005). While this is an effective method to estimate time since death, it is not applicable beyond skeletonization of the entire body.

Table 1: Summary of time since death estimation methods (e.g., Behrensmeyer, 1978; Yoshino et al., 1991; Bell et al., 1996; Courtin and Fairgrieve, 2004; Buchan and Anderson, 2001; Ubelaker and Buchholz, 2005; Komar and Buikstra, 2008; Christensen et al., 2014; Damann et al., 2014).

Method	Description	Postmortem Interval Estimation	Time Interval
Algor Mortis	Cooling of the body from 98.6°F to ambient temperature.	1.5°F per hour for the first 10 to 12 hours.	Short
Livor Mortis	Lividity resulting from the intravascular concentration and hemolysis of the blood cells.	Begins 30 minutes to four hours after death and is most pronounced after 12 hours.	Short
Rigor Mortis	The stiffening of the muscles caused by the binding of muscle fibers.	Initiate by two to six hours postmortem in the face and hands and to the large muscle groups after 12 hours.	Short
Stages of Decomposition	The progression of the body from fresh to skeletonization.	Depends on the environment.	Middle
Entomology	The succession of insect larvae to adulthood.	Provides a minimum postmortem interval depending on the insect.	Short
Carbon-14	Measuring the amount of radioactive carbon-14 in bone.	Can age remains to before or after 1950, when testing for atomic bombs occurred.	Long
Weathering	The loss of organic content and moisture, surface cracking and flaking, exfoliation, bleaching, staining, splitting, and disintegration of bone.	Codified stages of weathering patterns correlated with postmortem interval based on the environment.	Long
Bone Diagenesis	The destruction of the microstructure of the bone by microorganisms, for example bacteria and fungi.	Diagenetic changes can occur as early as three months postmortem, however, further research is necessary.	Middle/Long
Botanical Analysis	Analysis of the annual growth of plants found in the deposit or directly associated with the remains.	Provides a minimum postmortem interval through the analysis of growth rings or segments of different plants.	Middle/Long

Decomposition research has focused on many different aspects to fully understand the interaction between the rate of decomposition, cultural determinates and environmental determinants. For example, the change in grave soil from decomposition (Hopkins et al., 2000), body mass of the individual (Komar and Beattie, 1998), microenvironment (Shean et al., 1993; Komar and Beattie, 1998; Turner and Wiltshire, 1999; Carter et al., 2010; White and Booth, 2014), effects of hanging (Shalaby et al., 2000), scavenging (Haglund et al., 1989; Steadman and

Worne, 2007; Kjorlien et al., 2009; Reeves, 2009) and cultural additions (Weitzel, 2005). Most

of these studies have utilized pig carcasses or human cadavers (Haglund et al., 1989; Shean et al.,

1993; Komar and Beattie, 1998; Turner and Wiltshire, 1999; Hopkins et al., 2000; Shalaby et al.,

2000; Weitzel, 2005; Steadman and Worne, 2007; Kjorlien et al., 2009; Reeves, 2009; White and

Booth, 2014), but some studies have used unconventional proxies, such as rats (Carter et al.,

2010). Decomposition studies continue to clarify the processes involved in the decay of the

human body, but can only be applied when soft tissue is present.

Entomology

Forensic entomology, or the study of necrophagous insects associated with human

decomposition, can be used to estimate the minimum postmortem interval through the analysis of

succession (Table 1). This can be done because female adult insects generally do not deposit

eggs on living hosts (Anderson, 1995; Buchan and Anderson, 2001; Wells and LaMotte, 2001;

Komar and Buikstra, 2008). Insects are attracted to remains almost at the time of death and can

arrive within hours depending on environmental factors, such as weather or location of the

remains. The succession of insect larvae through the instars to adulthood can provide a minimum

amount of time an individual has been dead (Anderson, 1995; Anderson, 2001; Buchan and

Anderson, 2001; Wells and LaMotte, 2001).

There are two orders of insects of forensic importance, Diptera (flies) and Coleoptera

(beetles). Flies are the most common insects and has over 86,000 known species. There are ten

families of flies that are commonly associated with decomposition: Calliphoridae,

Sarcophagidae, Muscidae, Piophilidae, Scathophagidae, Sepsidae, Sphaeroceridae,

Stratiomyidae, Phoridae, and Psychodidae (Byrd and Castner, 2001). Additionally, there are

eight beetle families associated with decomposition: Silphidae, Dermestidae, Staphylinidae, Histeridae, Cleridae, Trogidae, Scarabaeidae, and Nitidulidae. Therefore, the proper identification of insect species is crucial for estimating time since death (Byrd and Castner, 2001). In addition to identification of species, the reference data for succession rates must accurately reflect the environment in which the remains were discovered (Wells and Lamotte, 2001).

The life cycles of flies and beetles are very similar. The first stage is the egg. Females can lay up to 200 eggs at a time (Gennard, 2007). The eggs then hatch, beginning the larval stage. Flies have three larval instars, while beetles may have between three and five instars. During the final instar, larvae will migrate for pupariation (Gennard, 2007). The pupal stage is the final metamorphosis from a larvae to an adult insect. The rate at which flies grow is dependent on temperature and environment. This necessitates the experimental reference data for succession rates. Beetles can reach adulthood from eggs within ten days or over a year (Gennard, 2007). Identification of species and stages of development can be then used to estimate the minimum postmortem interval using succession matrices (Wells and Lamotte, 2001). Factors that can affect the species present and the succession rates include temperature, season, exposure to sun, location, burial, submersion in water, and clothing (Anderson, 2001).

Experimental studies have focused on succession rates in different environments (e.g., Goff, 1992; Anderson, 1995; Anderson and VanLaerhoven, 1996; Hobischak and Anderson, 1999) and standardization of methods for postmortem interval estimates (Schoenly et al., 1992; Amendt et al., 2007; VanLaerhoven, 2008). More recently, research has found that traumatic injuries were not more attractive to insects for egg laying and would, therefore, not speed the rate of decomposition (Charabidze et al., 2015). The limitations of entomological estimates include

the variability in succession rates for different microenvironments and the need for

entomological experts to rear and identify species present at crime scenes. Additionally, as the

postmortem interval increases, the accuracy and precision of entomological estimates decrease

(Buchan and Anderson, 2001; Komar and Buikstra, 2008).

Chemical Methods

Chemical analysis of skeletal human remains can distinguish between archaeological and

forensic significance. Radiocarbon concentrations in bone have been used to make this

distinction (Buchan and Anderson, 2001). This method cannot be used to estimate precise

postmortem intervals, but has been used to determine the era of skeletal remains (Table 1).

The half-life of carbon-14 is 5730 years, which limits the applicability of this dating method in

forensic contexts (Ubelaker and Buchholz, 2005). However, carbon-14 concentrations in the

biosphere have experienced a modern anomaly that allows researchers to separate between pre-

modern (before 1950) and modern (after 1950) remains (Ubelaker and Buchholz, 2005; Buchan

and Anderson, 2001). Testing of thermonuclear devices began in 1950, creating a rise in carbon-

14 levels in the atmosphere and food supply. The "bomb-curve" created from this testing reached

its peak in 1963, but has since declined. However, the carbon-14 levels have not returned to the

levels prior to 1950 and allow for the distinction between modern and pre-modern skeletal

remains (Ubelaker and Buchholz, 2005).

Experimental research using radiocarbon dating has found that distinguishing between

pre-modern and modern remains was not difficult. Radiocarbon dating of teeth was found to

produce an estimated year of birth in the modern era with high precision. This could prove useful

for identification of skeletal remains, however, it does not indicate the time of death (Alkass et

al., 2010). Forensic anthropological studies found that soft tissues and hair could provide valuable information regarding the year of death, but the slow turnover rate for bone collagen limited the applicability of radiocarbon dating for time since death (Wild et al., 2000; Ubelaker et al., 2006). The results of these studies indicate that radiocarbon dating of skeletal remains is limited to determining the era or year of birth rather than the time since death. Despite these limitations, some scholars argue that research should focus on applying new techniques to refine the postmortem interval beyond the dichotomous system already in place (Cattaeno, 2007).

Botany

Botanical evidence at a death scene can provide important information. For example, botanical evidence can provide information on the stomach contents of a decedent, pollen analysis for geographical information, and fungal analysis for postmortem interval and locality (Courtin and Fairgrieve, 2004). Importantly, the analysis of annual growth rates in plant roots can provide a minimum postmortem interval. Woody tissues have been used historically in archaeology, however, the growth rates of plant roots can also provide a postmortem interval estimation (Courtin and Fairgrieve, 2004; Cardoso et al., 2010). Woody tissues can provide a more precise postmortem interval, but bryophytes and plant roots can only provide a minimum postmortem interval because the moment of plant colonization cannot be determined (Courtin and Fairgrieve, 2004; Cardoso et al., 2010).

Analysis of the growth rings in the woody tissues consists of dendrochronological methods (Courtin and Fairgrieve, 2004). The measurements of the growth rings can be correlated with the year counting back from the outer ring as the present year. Excessive growth can be

correlated with the influx of a food source, the remains of an individual, and provide a general postmortem interval (Courtin and Fairgrieve, 2004).

Bryophytes and plant roots have also been used to estimate postmortem interval. Bryophyte shoots grow annually and can be used to estimate minimum postmortem interval by counting the number of segments on the stems (Cardoso et al., 2010). Plant roots have a similar morphology to woody tissues, however, they are not as resistant to necrosis and the organization of the rings is not as clear. Therefore, plant root diameter, root architecture, and topology can be analyzed using Fitter and Stickland's methodology for a minimum postmortem interval (Fitter and Stickland, 1992; Cardoso et al., 2010). This method requires enough botanical growth around the remains for analysis and is generally found in conjunction with advanced decomposition (Courtin and Fairgrieve, 2004; Cardoso et al., 2010). In addition to interspecies variation in plant growth rate, environmental factors, such as rainfall and sunlight, will change the growth rate in different contexts, thus requiring comparative data for analysis (Courtin and Fairgrieve, 2004). Botanical evidence can refine conclusions drawn from taphonomic analysis to provide a smaller postmortem interval (Table 1).

Gross Taphonomic Changes

Taphonomy is the study of the changes in biological remains from death through recovery and analysis (Nawrocki, 2009; Pokines, 2014). Taphonomy was originally developed in the 1930's by paleontologists to explain fossils found in the geological record. This field was adapted to prehistoric and modern human remains starting in the 1970's (Nawrocki, 2009). Taphonomic processes result in a loss of biological information, however, the imprint of the processes help reconstruct the depositional history (Nawrocki, 2009). Weathering, soil staining,

sun bleaching, and superficial fungal growth are the gross taphonomic processes that will be further explained.

Weathering

The process of weathering involves the loss of organic content and moisture, surface cracking and flaking, exfoliation, bleaching, staining, splitting and disintegration of bone (Madgwick and Mulville, 2012; Junod and Pokines, 2014). The process of bone weathering begins at the time of death and can be affected by the rate of soft tissue decomposition (Cunningham et al., 2011).

Sun bleaching, or the color change from exposure to UV radiation, occurs in the early postmortem interval and continues for as long as the bone is exposed (Dupras and Schultz, 2014; Junod and Pokines, 2014). This taphonomic modification appears as a variation of the color white, from gray to bright white, and is dependent on the length of exposure. Solar UV radiation breaks down chemical bonds within the structure of the bone (Dupras and Schultz, 2014; Junod and Pokines, 2014). Interpretations regarding sun bleaching can reveal if the bone was buried after being exposed, the position of the remains after skeletonization, and if the remains were disturbed (Dupras and Schultz, 2014).

Soil staining is very commonly observed on skeletal remains from outdoor contexts where the remains are buried or in direct contact with the ground (Dupras and Schultz, 2014). This is due to the porous structure of bone (Pokines and Baker, 2014). The color of the stain depends on the composition of the soil. Buried remains frequently display brown coloration and must be distinguished from cemetery or historical remains, which have been associated with uniform brown staining (Dupras and Schultz, 2014). Surface depositions will exhibit soil staining

16

on the surface that was in contact with the soil. This can be used to determine if the remains were disturbed from the primary location. For example, if the soil staining is not in contact with the ground, then the remains were likely disturbed (Dupras and Schultz, 2014). Another type of staining that occurs is hemolysis. It appears as a dark, reddish coloration due to the breakdown of red blood cells (Dupras and Schultz, 2014).

An important aspect of the analysis of weathering is the information that can be gained about the postmortem interval (Table 1) (Junod and Pokines, 2014). To determine PMI from weathering, research has been conducted on known time since death assemblages to create codified stages of weathering patterns (Behrensmeyer, 1978). Since bone can exhibit multiple stages of weathering, it is recommended that the most advanced one cm^2 should be examined when determining the stage, avoiding areas of physical damage (Behrensmeyer, 1978; Junod and Pokines, 2014).

Skeletal remains present a significant challenge for estimating time since death due to the absence of soft tissue and insects. Therefore, the postmortem changes from weathering may be the only data available (Junod and Pokines, 2014). Behrensmeyer (1978) established a six stage system that estimates time since death. Through the observation of the most advanced 1 cm^2, researchers can establish the stage of weathering and the associated time since death. Other environmental factors influence the rate of decay, such as microenvironment, weather extremes, bone density, and species of animal (Christensen et al., 2014).

However, since the effects of differing environments and microhabitats on the rates of weathering have been little researched throughout the world, the interpretations that can be made are limited by the experimental research that has been conducted (Cunningham et al., 2011; Junod and Pokines, 2014). The original Behrensmeyer (1978) study was conducted in Kenya and

based upon the decay of animal carcasses with known time of death. Since the environment and microenvironment can change how bone decays, recent research has been conducted to adapt the six stages to different environments (Junod and Pokines, 2014). For example, bone in cooler, temperate environments and rainforest environments have shown a longer duration of survival than bones found in semiarid, savanna climates (Behrensmeyer, 1978; Coe, 1978; Andrews and Cook, 1985; Tappen, 1994; Fiorillo, 1995; Tappen, 1995; Andrews and Whybrow, 2005; Potmesil, 2005; Janjua and Rogers, 2008; Todisco and Monchot, 2008). These studies demonstrate how different microenvironments change the rate of bone decay. Therefore, experimental research to establish standards of weathering for different microenvironments is necessary to properly estimate time since death with skeletal remains. Additionally, these studies utilize non-human proxies, despite the known differences in microstructure, necessitating comparative research between human and non-human bone weathering (Buchan and Anderson, 2001; Junod and Pokines, 2014).

Despite the extensive research to refine these stages of weathering, methods to estimate time since death on skeletal remains continues to be difficult and imprecise. Particularly, the correlation between microenvironment and weathering patterns necessitates the creation of reference data for all possible environments through experimental research. However, such research is limited by the time span that is required for these taphonomic changes to occur (Beary and Lyman, 2012). Researchers have suggested that future studies could refine the earliest interval at which soil staining appears to provide a general postmortem interval (Pokines and Baker, 2014). Since contact with the soil is a requirement for soil staining and factoring in differential patterns of decomposition and soil characteristics, this method may not provide an accurate estimate of postmortem interval. However, this would be a non-invasive, observational

method for time since death estimation. Further research to refine techniques to estimate time

since death in the early postmortem interval is necessary for the future of forensic anthropology.

These limitations necessitate macroscopic and microscopic analysis of the bone matrix as the

postmortem interval increases. While these methods do not eliminate the influence of

microenvironments, the time span at which these changes occur is considerably less, therefore

decreasing the time to create standards for microenvironments and increasing the applicability

for forensic cases.

Superficial Fungal Growth

Some fungi, including *Aspergillus, Penicillium, Pythium* and *Rhizoctoia*, grow

superficially on the surface of bone, cause discoloration, and produce localized surface erosion

(Piepenbrink 1986; Huculak and Rogers, 2009). Fungi require oxygen to grow; therefore, aerobic

environments facilitate fungal growth and will be found in contexts in which the remains were

exposed on the surface for some period of time (Child 1995; Huculak and Rogers, 2009). Fungi

can provide a minimum time interval of growth, but such estimates require the precise

identification of the specific fungi, storage methods of the body, and the conditions of the

environment, which can be difficult to ascertain (Hawksworth and Wiltshire, 2011).

Macroscopic Taphonomic Changes

Using cross-sectional analysis, Huculak and Rogers (2009) conducted an experimental

study of pig long bones that were buried and exposed to examine the taphonomic changes to the

surface and cross-section of a bone. The first 2.5 cm from midshaft were examined for color

changes associated with differential bone grease composition. Darker colors were associated with higher grease contents and lighter colors with lower grease contents. Bones that were exposed prior to being buried exhibited a light to dark pattern in cross-section and could be used as an additional tool to recreate the taphonomic history of remains (Huculak and Rogers, 2009). However, there was no way to correlate the amount of protein loss with the postmortem interval as all of the samples had the same PMI, but different levels of protein loss.

Microscopic Taphonomic Changes

Before discussing human bone diagenesis, or the microscopic changes to the bone microstructure during decomposition, a general overview of microscopic bone anatomy is necessary. There are two basic structures within bone, compact, or cortical bone, and spongy, or trabecular bone. Compact bone is the external hard, dense bone (Figure 1). This bone is composed of Haversian canal systems, or osteons (Safadi et al., 2009; White et al., 2011). Osteons consist of Haversian canals, which are surrounded by concentric lamellae and connected by Volkmann's canals (Figure 1). Spongy bone consists of thin trabeculae of bone in a honeycomb structure, with marrow spaces in between and is located in the endosteal region of bone (Safadi et al., 2009; White et al., 2011).
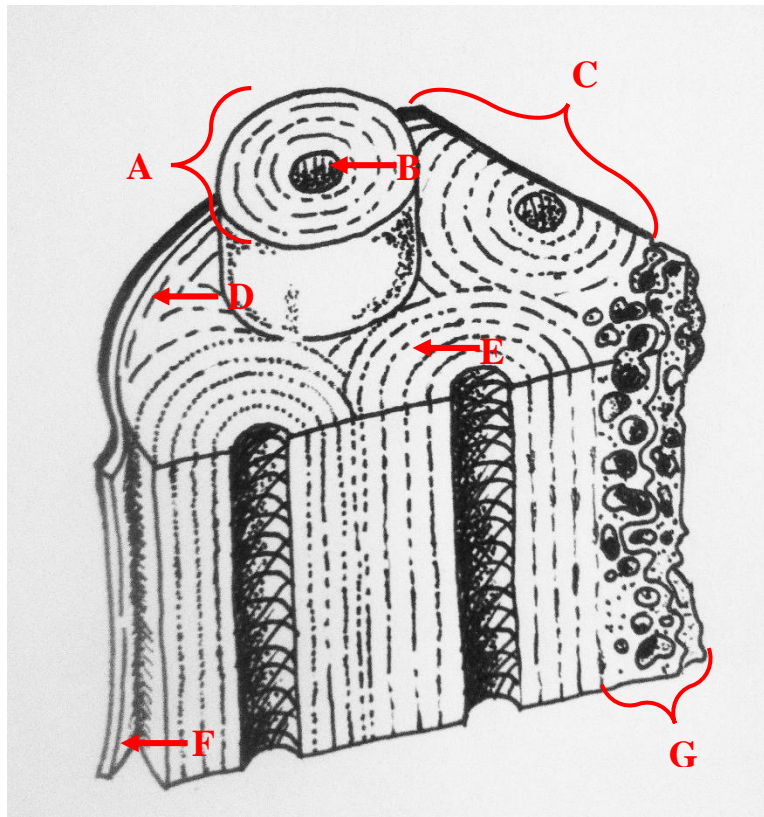
Figure 1: Bone biology diagram. A: Osteon B: Haversian Canal C: Cortical Bone D: Circumferential Lamellae E: Concentric Lamellae F: Periosteum G: Trabecular Bone

The microstructure of a typical human long bone consists of circumferential lamellae bone at the periosteal and endosteal regions (Figure 1). The middle portion of the cortical bone is generally composed of secondary osteons and interstitial lamellae in a densely packed, random arrangement (Mulhern and Ubelaker, 2001; White et al., 2011; Crescimanno and Stout, 2012). These secondary osteons may appear whole or as remnants that were partially replaced through remodeling (Crescimanno and Stout, 2012). As humans age, the primary circumferential bone near the endosteum is replaced more rapidly as a result of simultaneous appositional growth. Osteons also become smaller and more abundant nearer the periosteum than the endosteum, and the number of incomplete osteons increases with age (Crescimanno and Stout, 2012). The

diaphyseal structure of long bones of late juvenile and adult humans show little variation and the primary bone tissue is lamellar bone (Cuijpers, 2006).

A microscopic feature rarely observed in human bone, but more common in non-human bone is osteon banding, defined as a liner arrangement of complete, usually primary, osteons in rows or layers (Mulhern and Ubelaker, 2001). Some adults may exhibit a linear pattern of osteon arrangement, but this configuration has been noted in relatively few individuals, is isolated within the bone structure (Mulhern and Ubelaker, 2001). Analyses of young, juvenile human bone microstructure have not been performed, but could exhibit osteon banding similar to non-human mammals (Mulhern and Ubelaker, 2001).

Comparatively, the microstructure of adult and juvenile pig bone (*Sus scrofa*) consists of plexiform bone tissue and Haversian bone tissue, with the primary focus of Haversian tissue located near the endosteal margin (Hillier and Bell, 2007). Plexiform bone is a type of primary bone tissue within the fibrolamellar bone tissue group, and is found commonly in fast-growing, large animals, such as cows, horses, dogs, and pigs (Cuijpers, 2006; Martiniakova et al., 2006a; Hillier and Bell, 2007). Plexiform bone tissue is not found in smaller animals, such as rats and rabbits (Martiniakova et al., 2006a).

Plexiform bone has a similar structure to lamellar bone, but has a more dense system of vascularization. This bone tissue is rectilinear, which forms a "brick wall" structure (Cuijpers, 2006, Hillier and Bell, 2007; Junod and Pokines, 2014). Plexiform bone is placed in radial bands and consists of layers of parallel-fiber woven bone. This tissue is laid down quickly and the cavities are then later filled in with lamellar bone (Junod and Pokines, 2014). As non-human mammals age, plexiform bone is replaced with Haversian bone. The replacement begins near the endosteal surface and moves gradually to the periosteum (Hillier and Bell, 2007; Junod and

22

Pokines, 2014). Full replacement is rarer, but does occur in some mammals (Hillier and Bell, 2007). This distribution of plexiform and Haversian bone has been attributed to the mechanical stress on the bone, dictating the rate of remodeling (Katz et al., 1984). This bone tissue is frequently located within the cortical bone of long bones (Hillier and Bell 2007). However, while plexiform bone is noted as a non-human characteristic, multiple authors have noted plexiform bone in humans during periods of growth, such as infancy and during bone remodeling from trauma (Martiniakova et al., 2006a; Hillier and Bell, 2007; Junod and Pokines, 2014).

Various researchers have noted differences between human and pig bone microstructure. The Haversian system size and canal diameter in pigs is similar to humans (Hillier and Bell, 2007). The cortical bone is also typically thicker than seen in humans (Hillier and Bell, 2007; Coelho and Cardoso, 2013). Immature pig cortical bone normally consists of plexiform bone on the periosteal margin and layers of osteon banding and lamellar bone. However, juvenile bone demonstrates less Haversian bone tissue and previous experimental studies have observed immature pig long bone tissue consisting entirely of plexiform bone (Mulhern and Ubelaker, 2001; Hillier and Bell, 2007). Furthermore, when using a statistical evaluation of the hardness of human bone and pig bone, Saville et al. (2007) discovered the hardness across the cortex of the bone was comparable to humans, but the surface hardness was significantly less. Comparing the hardness between four species (sheep, calf, pig, and cow) led the authors to conclude that pig was the most comparable analog for human bone (Saville et al., 2007).

Bone diagenesis can provide important information regarding burial environment and postmortem interval. There are three mechanisms of bone diagenesis: protein deterioration, extreme environments, and microbial diagenesis (Collins et al., 2002). Protein degradation is a process that begins in the antemortem period and continues throughout life and death. As an

individual ages, bone increases in porosity and decreases in collagen content. This creates minute interconnected pores less than 30nm in diameter. The rate of postmortem collagen loss is dependent on environment and time (Collins et al., 2002). High temperatures and extreme alkaline or acidic soils will increase the rate of collagen loss. In general, acidic, aerated, and well drained soils are the most corrosive to osseous materials (Collins et al., 2002; Jans, 2014). Bone will also deteriorate more rapidly when exposed to extreme environmental changes. Fluctuations between freezing and thawing and wet and dry environments, as well as the process of cooking, will increase the speed at which bone decays (Collins et al., 2002; Jans, 2014).

Bioerosion, or microbial alteration, is the most common mechanism of bone deterioration (Collins et al., 2002; Jans, 2014). Soil with a neutral pH facilitates microbial activity, although these conditions would normally protect bone from chemical deterioration (Child, 1995; Nicholson, 1996; Collins et al., 2002). The microorganisms rely on demineralized tissues for sustenance and excrete secondary metabolites, which can lower the pH of the soil (Child, 1995). To facilitate osseous decomposition, microorganisms must feed on collagen, which is an insoluble protein under normal conditions; therefore, the organisms must secrete enzymes known as collagenases (Child, 1995; Trueman and Martill, 2002). There are two types of terrestrial microorganisms that participate in bioerosion that will be discussed later: fungi and bacteria.

The microstructure of bone determines the pathways that microorganisms will travel in order to penetrate the skeletal tissue (Turner-Walker, 2008). Therefore, an understanding of the distinction between human and pig bone microstructure is essential to interpret results of experiments (Nicholson, 1996). Nicholson (1996) investigated bone diagenesis of cow, sheep, rat, pigeon, cod, plaice, herring, and whiting over a seven year period. He discovered that mammalian bone was more vascular than fish and bird bone, which made it particularly more

24

susceptible for invasion by microorganisms, especially fungi, than the more compact bird and fish bones (Nicholson, 1996). Nicholson (1996) concluded that Haversian bone structure facilitates the invasion of microorganisms and the degradation of bone. However, he did not compare human or pig bone microstructure, and pig bone is the most commonly used analog for human bone (Janjua and Rogers, 2008; Huculak and Rogers, 2009). Microstructural differences have been acknowledged as a significant variable in the application of nonhuman bone weathering patterns to that of humans, but research has not been conducted to address this issue (Junod and Pokines, 2014).

Fungal Diagenesis

In 1864, Wedl discovered tunneling in the bone matrix (Hackett, 1981). This tunneling was later attributed to fungal invasion of the bone matrix. They appear moving away from surface of the cortex or Haversian canals and never increase in diameter. The path is never smooth, straight or longitudinal (Hackett, 1981). These fungi tunnel through natural pathways and vascular channels, and can produce focal destruction similar to bacteria (Piepenbrink, 1986; Child, 1995). There are two forms of tunneling that have been identified in bone, Type 1 and Type 2 (Trueman and Martill, 2002). Type 1 is the most common and has tunnels between 10 and 15 μm, whereas Type 2 is smaller and form more complex networks, however, both are attributed to fungal diagenesis (Trueman and Martill, 2002).

Two fungi genera, *Mucor* and *Fusarium*, are commonly found associated with human remains and excrete metabolites to erode cortical bone and destroy collagen (Marchiafava et al., 1974; Piepenbrink, 1986). As previously discussed, some fungi grow superficially on the surface of bone, cause discoloration, and produce localized surface erosion (Piepenbrink, 1986). Fungi

require oxygen to grow; therefore, burials in aerobic environments facilitate fungal diagenesis (Child, 1995).

Bacterial Diagenesis

The bacteria involved in bone diagenesis are collagenase-producing bacteria, which secrete collagenase enzymes that break down the collagen for consumption (White and Booth, 2014). These bacteria are present in both aerobic and anaerobic environments, as well as within mammalian intestinal tracks and most soils. As such, bacterial diagenesis is more common than fungal (Nicholson, 1996; White and Booth, 2014). Bacterial invasion of the bone matrix is characterized by non-Wedl microscopical focal destruction (MFD) and tunneling (Hackett, 1981; White and Booth, 2014).

MFD are localized changes in the bone matrix and are identified through presence of stippled or grainy infill, a mineralized rim, presence of bacteria, and the correlation with the microanatomy of the bone (Garland et al., 1988; Jans et al., 2002; Jans, 2008). Bacteria cannot cross the cement lines of Haversian canals and will frequently develop adjacent to Haversian canals (Trueman and Martill, 2002; Jans, 2008). Osteocyte canaliculi likely play a role in the infiltration of bacteria into the bone matrix (Jans, 2008)

The origin of the bacteria involved in the process of diagenesis has been the topic of much debate in the anthropological literature. Some studies believe bacteria present in the environment have the greatest effect (Child, 1995). Others have claimed that bacteria endogenous to the body have the greatest effect on bone diagenesis (Turner-Walker, 2008; White and Booth, 2014).

Child (1995) argues that the bones of the thorax decompose more quickly due to the presence of gut flora, which facilitates demineralization. However, the microflora of the burial environment outcompete the endogenous microorganisms of the limbs and skull (Child, 1995). This would suggest that the exogenous microflora are more important for bone diagenesis of the limbs and skull than the microflora of the soft tissue, which would eliminate the necessity for the soft tissue to decompose with the bone. Since many forensic anthropological studies utilize partially de-fleshed pig bones, this could indicate that maceration of the soft tissue prior to burial would not negatively affect experimental results (Child, 1995). This exogenous model suggests that the bones maintain their structural integrity until skeletonization, thus validating studies using partially de-fleshed bones (White and Booth, 2014).

However, it has been shown that as the autolysis phase concludes, an anaerobic environment is created within the remains, which facilitates proliferation of the bacteria endogenous to the thorax (Turner-Walker, 2008). When analyzing bone diagenesis of slaughtered domestic animals, the bacterial diagenetic changes were less pronounced when compared to human remains of similar postmortem intervals (Jans et al., 2004; Turner-Walker, 2008). This implies that the lack of soft tissue reduced the presence of endogenous bacteria, which in turn decreased the bacterial diagenetic changes. This would contrast with Child's (1995) implication that the endogenous bacteria have an impact on the early stages of bone diagenesis of long bones.

White and Booth (2014) sought to clarify this issue through the investigation of diagenetic changes to juvenile and stillborn pig carcasses. The authors buried six carcasses and deposited another six on the surface. They sampled the femora of each buried pig following one year of decomposition and each exposed pig every six months. The stillborn pigs did not

demonstrate any diagenetic changes, which was attributed to the lack of intestinal microflora (White and Booth, 2014). This was compared to the diagenetic changes in the more mature juvenile pigs, which displayed bioerosion consistent with the presence of intrinsic bacteria. The results firmly supported endogenous bacteria as the primary diagenetic agent until skeletonization (White and Booth, 2014).

These findings are important to forensic anthropological analysis because many experimental taphonomic studies utilize de-fleshed, nonhuman skeletal remains (Janjua and Rogers, 2008; Huculak and Rogers, 2009; Coelho and Cardoso, 2013). If the bacteria most involved with diagenesis are endogenous, then these studies do not fully reflect the experience of decomposition and taphonomy. Therefore, they cannot be accurately applied to cases involving human remains. A comparative study of the bioerosion of fleshed and de-fleshed pig long bones is necessary to fully ascertain whether the bacteria most involved in bone diagenesis are endogenous or exogenous. However, investigation into the bacterial concentration in de-fleshed bones at various postmortem intervals could reveal when bacteria are most active in diagenesis.

Time Since Death Estimation

The postmortem alteration to the microstructure of bone has only recently been investigated as a potential source of information about time since death in the early postmortem interval (Table 1) (Buchan and Anderson, 2001). Yoshino et al. (1991) sampled human humeri and observed that bacterial destruction of remains left in the open air was not present for short postmortem intervals. However, buried human remains exhibited diagenetic changes with a postmortem interval of two and a half years. Bacterial microscopical focal destruction was found as early as five years postmortem (Yoshino et al., 1991; Jans, 2014). The authors attempted to

correlate time since death with the intensity of UV-fluorescence and had a high correlation coefficient, but the standard error was more than two years and had a wide range of values for the earliest postmortem intervals.

Contrary to the findings of Yoshino et al. (1991), Bell et al. (1996) discovered postmortem diagenetic changes within a postmortem interval of three months. This tibia fragment was exposed and had experienced scavenging, as it was found in bear scat. Despite the absence of soft tissue in the tibia fragment, the authors argued that these changes occurred due to the presence of endogenous bacteria, but note that more research is necessary to understand the correlation between bioerosion and time since death. Changes were next identified in the 15 months postmortem period in a fourth rib (Bell et al., 1996). Turner-Walker (2012) demonstrated the potential for diagenetic changes in buried and aquatic specimens within a year, but collection of data did not occur until one year had passed. Therefore, these changes could have begun at an earlier time interval. White and Booth (2014) studied the bacteria involved in diagenesis and observed diagenetic changes in the microstructure of pig bone by the first sampling period, which was six months. This study confirms the assertions of Bell et al. (1996), that endogenous bacteria are more active in diagenesis. However, the authors did not correlate their findings with postmortem interval estimation.

This research suggests diagenetic changes can occur at a much more rapid pace than previously thought. However, research at the Anthropological Research Facility at the University of Tennessee did not find any diagenetic changes to human ribs with postmortem intervals up to 49 months (Jans, 2014). This could have been the result of a multitude of reasons, however, the studies that have found diagenetic changes have been examining long bones (Yoshino et al., 1991; Bell et al., 1996; Turner-Walker, 2012; White and Booth, 2014). Therefore, the contrary

findings of the Anthropological Research Facility could be the result of sampling the smallest ribs rather than long bones.

Hedges (2002) called for more research into the timing of diagenetic changes in order to better understand archaeological samples, but this can be directly applied to forensic anthropology. The estimation of the postmortem interval becomes increasingly difficult once skeletonization has occurred (Janjua and Rogers, 2008). Knowing the earliest point at which diagenetic changes occur could refine postmortem interval estimations beyond the Behrensmeyer (1978) weathering standards. The current published research has not been tested and cannot be considered reliable until more experimental research is conducted (Cattaneo, 2007). However, forensic scholars agree that the role microbes play in the bioerosion of bone is poorly understood and future research should investigate the early skeletonization stage of decomposition (e.g., Christensen et al., 2014; Damann and Carter, 2014; Jans, 2014). Creating standards that can estimate the minimum amount of time an individual has been dead through the presence or absence of diagenetic changes could aid in the investigation of forensic cases.

Damann et al. (2015) studied the origin of bacterial communities within bone samples in an attempt to estimate postmortem interval. The authors sampled a single lower rib from 12 different human cadavers in three stages of decomposition, partially skeletonized, fully skeletonized, and dry remains, at the Anthropological Research Facility (ARF) at the University of Tennessee (Damann et al., 2015). Additionally, soil samples were collected from a location one kilometer from the ARF with the same soil complex. By using PCR DNA analysis of the bacteria, the authors discovered that the bacteria in the bones of the partially skeletonized and fully skeletonized were most similar with bacterial families most commonly found within the human body. The bacteria from the bones of the dry remains were most similar to the bacteria

found in the soil samples (Damann et al., 2015). The authors determined that PCR analysis of the DNA of the bacteria could be a viable option for decaying bone, however, the system would require calibration for each environment to determine the type of natural bacteria found in the soil. Additionally, this method may only be effective for studies on human remains, as the endogenous bacteria in pigs more than likely differs from endogenous bacteria in humans.

The present study will contribute to the estimation of postmortem interval through the histological analysis of bone at specific postmortem intervals. The 14-week period encompasses the earliest time interval seen for diagenetic changes of three months (Bell et al., 1996). This will allow for the experimental analysis of diagenetic changes, rather than observations of remains found at varying time intervals in a case study format. In addition, the histological thin sections of bone from midshaft will be stained to observe the bacterial and fungal invasion of the cortical bone as the postmortem interval increases. This could provide a minimum time since death should a recognizable pattern of bacterial succession be present or if fungal invasion occurs in both sun and shade microenvironments.

CHAPTER THREE: MATERIALS AND METHODS

Bone Sample

Fifteen de-fleshed long bones from juvenile pigs (*Sus scrofa*) were obtained from Nettle's

Sausage Slaughterhouse in Lake City, Florida immediately after death. Pig bone is forensically

considered an acceptable proxy for human bone tissue in taphonomic study (Janjua and Rogers,

2008; Huculak and Rogers, 2009). The pigs were slaughtered for human consumption following

the standards set by the USDA (USDAFSIS, 2003). The femora and humeri were de-fleshed by

the slaughterhouse with butchered radii and ulnae or tibiae and fibulae still attached. Small

amounts of muscle tissue and connective tissue were still present at the proximal and distal ends.

All samples were frozen (-40°C) immediately after collection prior to the start of the study, a

process that does not alter the integrity of the microstructure of bone (Evans, 1973; Tersigni,

2007). All bones were wrapped in plastic and in paper bags to prevent freezer burn (Shattuck,

2010; Wieberg, 2005; Wieberg and Wescott, 2008). The long bones were then frozen between

105 and 126 days after the pigs were slaughtered. Additionally, the bones were thawed for 24

hours prior to placement in the field on October 13, 2014. The sample of 15 pig bones consisted

of five humeri and two femora placed in the sun, five humeri and two femora placed in the

shade, and one humerus serving as a control (Table 2). The mixed long bone sample was a

product of bone availability, as the study was conducted in conjunction with Green (2015), who

was also using humeri and femora.

Table 2: Pig bone elements analyzed for each week by group.

	Group A	Group B
Week 2	Humerus	Humerus
Week 4	Humerus	Humerus
Week 6	Femur	Humerus
Week 8	Humerus	Femur
Week 10	Humerus	Femur
Week 12	Femur	Humerus
Week 14	Humerus	Humerus

Field Methods

The experimental site consisted of two microenvironments, full sun and shade, in the subtropical environment of Central Florida. The long bones were placed on the ground surface outside at University of Central Florida's Deep Foundations Geotechnical Research Area at the Arboretum (Figures 2 and 3). The field samples were placed under hardware cloth that was secured using tent stakes to allow for natural scavenging and entomological activity, but prevent the loss of samples. Bones were collected every other week, one from each group, for 14 weeks (October 13, 2014 – January 19, 2015). This study was conducted in conjunction with Green (2015), which dictated the length of the field component. Upon collection, samples were photographed, wrapped in plastic wrap, placed in paper bags, and returned to the freezer. This process ensured the postmortem interval was maintained upon collection. The field component was completed on January 19, 2015.
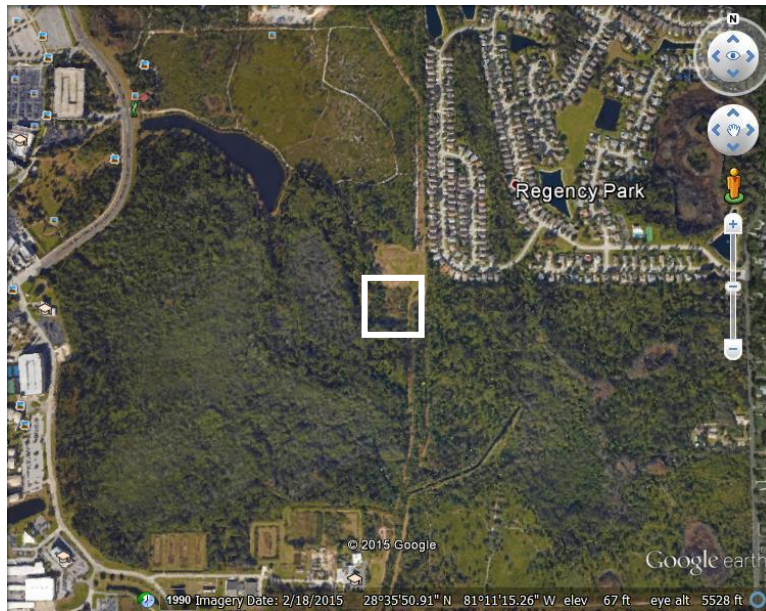
Figure 2: Aerial view of the research site at the University of Central Florida.

Figure 3: Aerial view of the research site and field locations of Group A and Group B bone samples.

<u>Laboratory Methods</u>

Laboratory preparation of the samples was conducted over two days. However, the samples had been frozen directly after collection for a period ranging from 102 to 186 days, prior to being thawed for processing and the embedding procedure. Histology cups were prepped 24 hours prior to embedding using Epothin Epoxy Resin and Epothin Epoxy Hardener (39 parts hardener to 100 parts resin) (Crowder et al., 2012). The bones from Group A were embedded on the first day and the bones from Group B and the control were embedded on the second day. First, any remaining soft tissue was removed using clay tools at mid-diaphysis. Then, the upper limit of the cross section at midshaft was cut using a Dremel and a 1.5 inch metal blade. The lower limit was then cut, creating a cross section from mid-diaphysis approximately 3 cm in length (Figure 4). Photographs were taken of the cross section and the surface of the bone. Then, observations were recorded regarding gross and macroscopic taphonomic changes. Next, a longitudinal section was cut from the medial aspect of the cross section approximately 1 cm in width (Figure 5). Finally, the samples were embedded in a 39:100 hardener to resin ratio, placed in the vacuum desiccator for 15 minutes, then left in the chemical hood overnight to harden (Figure 6).

Figure 4: Mid-diaphysis cut from Group A, Week 2 pig humerus.

Figure 5: Longitudinal section cut from the medial aspect of the large section from mid-diaphysis of Group A, Week 2 pig humerus.

Figure 6: Embedded longitudinal section from mid-diaphysis of Group B, Week 2 pig humerus.

Slide thin sections were prepared by cutting 1 mm thin sections from the embedded

sample using an IsoMet 1000 Precision Saw and a diamond wafer blade, using a protocol

adapted from Crowder et al. (2012). A waste cut was made first to create a smooth edge for the

first thin cut (Figure 7). Then, four sections were cut from the sample (Figure 8). Each cut was

wrapped in paper and placed in a labelled plastic bag. Three thin sections for each sample were

then mounted onto glass microscope slides using Permount or the embedding resin (Figure 9).

The Permount required an extended period of time to cure, likely due to the modified protocol

and the retention of bone grease in the samples. Additionally, the fourth thin section for each
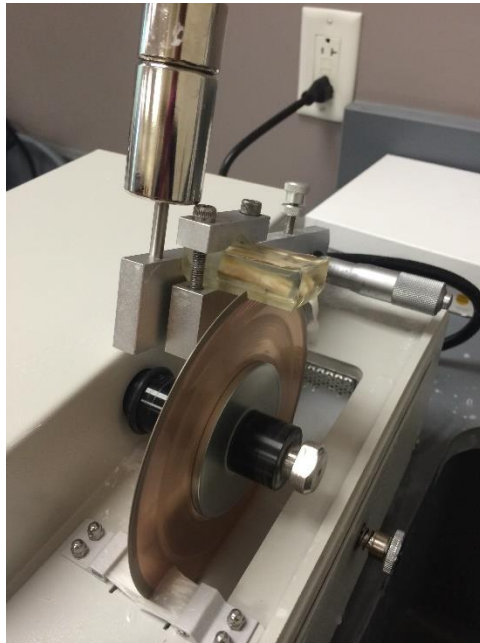
bone was not mounted and was retained as a backup.

Figure 7: Waste cut sectioning using an IsoMet 1000 Precision Saw and a diamond wafer blade.

Figure 8: Thin sectioning using an IsoMet 1000 Precision Saw and a diamond wafer blade.

Figure 9: Thin section of Group B, Week 6 pig humerus mounted to a microscope slide.

The samples were then ground down to approximately 0.30 mm thickness using an

Ecomet 400 Variable Speed Grinder with Microcut Discs 12″ Grit 800 (Figure 10). The thin

sections were then polished for five minutes using MetaDi Supreme Polycrystalline Diamond

Suspension 9 μm grit and five minutes using MetaDi Supreme Polycrystalline Diamond
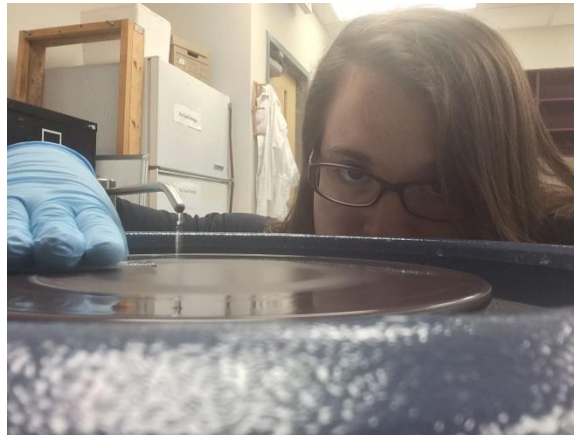
Suspension 3 μm grit.

Figure 10: Author using the Ecomet 400 Variable Speed Grinder.

The first set of the sample slides were then stained using a standardized procedure for Periodic Acid-Shiff (PAS) staining system (Sigma-Aldrich, Procedure No. 395-2014, St. Louis, www.sigmaaldrich.com). The samples were submerged in room temperature formalin-ethanol fixative solution for one minute then rinsed in distilled water. The slides were then immersed in room temperature PAS for five minutes and then rinsed in distilled water. Subsequently, the slides were placed in Schiff's Reagent for 15 minutes then washed in running tap water for five minutes. The slides were then counterstained in Hematoxylin Solution (Mercury Free) for three minutes and rinsed in running tap water for 30 seconds.

The second set of slides were stained using a standardized procedure for a Hematoxylin and Eosin (H and E) stain (Sigma-Aldrich, Procedure No. GHS-2013, St. Louis, www.sigmaaldrich.com). The samples were submerged in the Hematoxylin Solution (Mercury Free) for one minute then immediately rinsed in distilled water. The samples were then submerged in a differentiation solution of 0.3% HCL mixture and then rinsed in distilled water. Next, the slides were submerged in Scott's Tap Water Substitute for two minutes, rinsed in distilled water, submerged in Eosin Y Solution, Alcohol for one minute, and then finally rinsed in distilled water.

One set of sample slides remained as a control for comparison with the stained samples.

Analysis

An overview picture of each thin section was created and used as a guideline for in-depth analysis of diagenetic changes. This overview picture was created by using a 2MP USB digital zipScope microscope at approximately 17x magnification. The images were then stitched together using Adobe Photoshop©. The slides were then analyzed under a polarizing light microscope using a 10x objective lens and an 8MP digital camera, producing a magnification of 280x. Areas of potential diagenetic changes were measured and documented for the location within the bone. The Oxford Histological Index (OHI) was not utilized because the diagenetic changes within the bone were too limited in number for the OHI to meaningfully describe (Hedges et al., 1995).
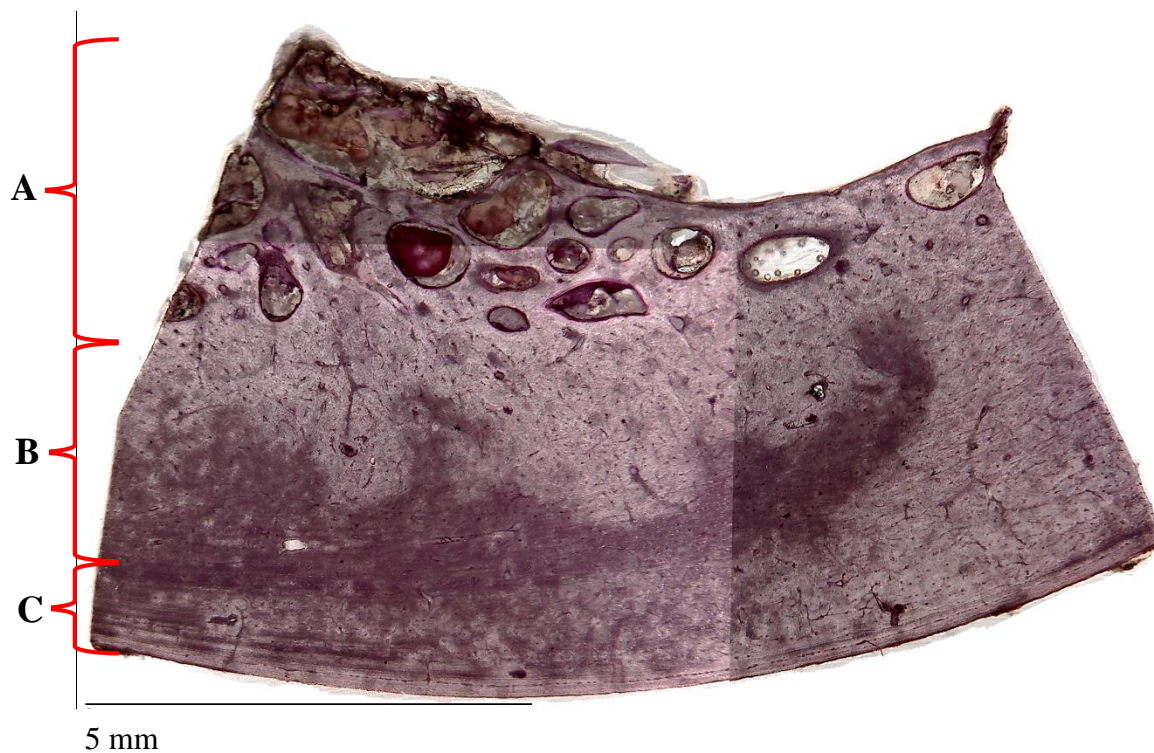
Figure 11: Thin section of cortical bone of Group A, Week 4 from mid-diaphysis of a pig humerus and stained with PAS. A: Endosteal region. B: The middle region. C: The periosteal region (Jans et al., 2002).

Each thin section was divided into three general regions: endosteal, middle cortical, and periosteal (Figure 11) (Jans, 2008). The thin sections were then analyzed for non-Wedl microscopical focal destruction, inclusions, Wedl tunneling, and presence of bacteria. The samples were assessed for location of diagenetic changes and the greatest diameter of microscopical focal destruction structures.

Non-Wedl microscopical focal destruction (MFD) are localized changes in the bone matrix and are identified through presence of stippled or grainy infill, a mineralized rim, presence of bacteria, and the correlation with the microanatomy of the bone (Figure 12) (Garland et al., 1988; Jans et al., 2002; Jans, 2008). Bacteria cannot cross the cement lines of Haversian canals and will frequently develop adjacent to Haversian canals (Trueman and Martill, 2002; Jans, 2008). Osteoclastic activity should be considered as a differential diagnosis with MFD.

41

Areas of osteoclastic activity are characterized by scalloped edges (Figure 13), whereas MFD has a mineralized rim (Bell, 1990; Bass, 2006). MFD was not assessed along the endosteal margin due to the transition to trabecular bone and the large structures that accompanied this change, called "trabecularized" cortical bone (Maggiano, 2012). Therefore, the focus of the analysis for MFD was in the middle cortical and periosteal regions.
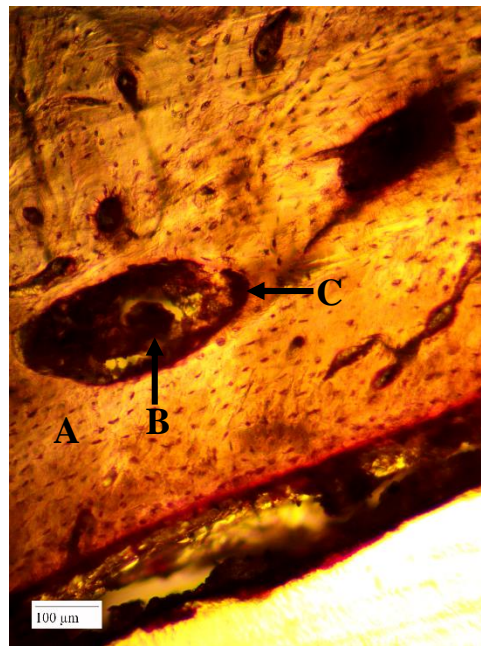

Figure 12: Thin section of Group A, Week 14. A: No concentric lamellae. B: Grainy infill. C: Mineralized rim.
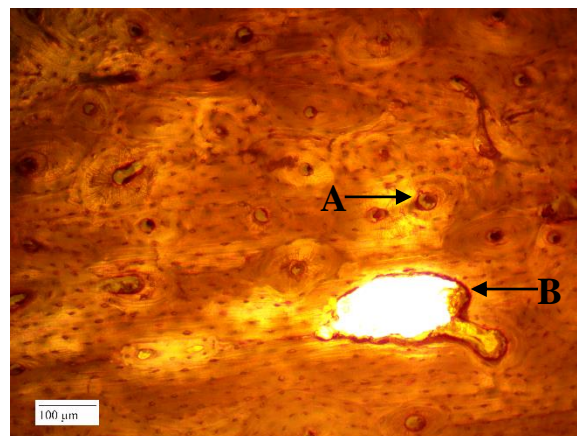

Figure 13: Example of a Haversian canal with inclusions (A) and osteoclastic activity (B) from a thin section of pig bone.

Inclusions, or the presence of non-osseous material within the spaces in the bone, were identified through the PAS and H and E staining (Figure 13) (Garland et al., 1988; Grupe, 1993). The positively charged hematoxylin stain, used as a counterstain in the PAS stain and as the primary stain in the H and E stain, reacts with the negatively charged phosphate groups in the nuclear DNA, thus dying the nucleus of bacteria blue (Sigma-Aldrich). The PAS stain reveals the presence of fungi within tissues by staining glycogen (Sigma-Aldrich). Presence of tunneling was assessed throughout all regions of the bone.

Wedl tunnels are attributed to fungal diagenetic changes to the bone matrix. They appear moving away from surface of the cortex or Haversian canals and never increase in diameter. The path is never smooth, straight or longitudinal (Hackett, 1981). Wedl tunneling was further refined into two forms, Type 1 and Type 2 by Trueman and Martill (2002). Type 1 is the most common and has tunnels between 10 and 15 µm, whereas Type 2 is smaller and form more complex networks (Trueman and Martill, 2002). Wedl tunneling was identified using these characteristics, but since a differential diagnosis for Volkmann's canals is not available, the classification is labeled as probable (Figure 14).
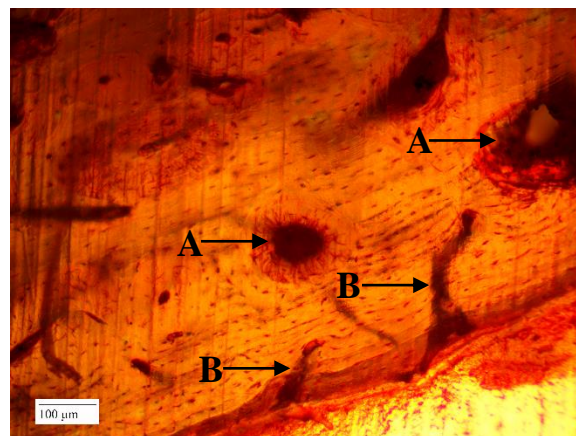

Figure 14: Example of microscopical focal destruction caused by bacteria in the periosteal region (A) and possible Wedl tunneling (B).

CHAPTER FOUR: RESULTS

Weather Data

Weather data was collected daily throughout the length of this study, from October, 2014 through January, 2015. Using the HOBO link at the University of Central Florida Arboretum, the daily high and low temperatures, rainfall, and humidity were recorded (Table 3). During the experimental period, the average temperature ranged from 54º to 87º Fahrenheit.

Table 3: Summary of average temperatures (ºF), total rainfall (inches), and average humidity by month. Data extrapolated from Green (2015).

Month	Average Low (ºF)	Average High (ºF)	Total Rainfall (Inches)	Average Humidity
October 2014	65.11	86.68	0.17	94%
November 2014	56.23	74.67	6.61	92%
December 2014	58.06	75.71	2.22	99%
January 2015	54.35	72.88	2.40	94%

Observations and Gross Taphonomic Changes

As expected, there was no change in the Behrensmeyer (1978) stage over fourteen weeks for both groups. The decomposition of the adhered soft tissue in Group A was immediately more obvious. Over time, Group A showed a marked increase in the fungal activity on the surface of the bone starting in Week 6, identified through fuzzy appearance, and increased each week (Table 4). The insect activity at the location covered the remains with soil causing superficial adherence and slight soil staining (Figure 15). Soil staining was recognized through the brown

discoloration on the exterior of the bone diaphyses (Dupras and Schultz, 2014). The humeri in the group demonstrated a pink coloring on the periosteal surface of the bone (Figure 16). This could be due to hemolysis, or the breakdown of red blood cells during decomposition or the freezing process causing the blood cells to burst (Dupras and Schultz, 2014; Sowemimo-Coker, 2002).
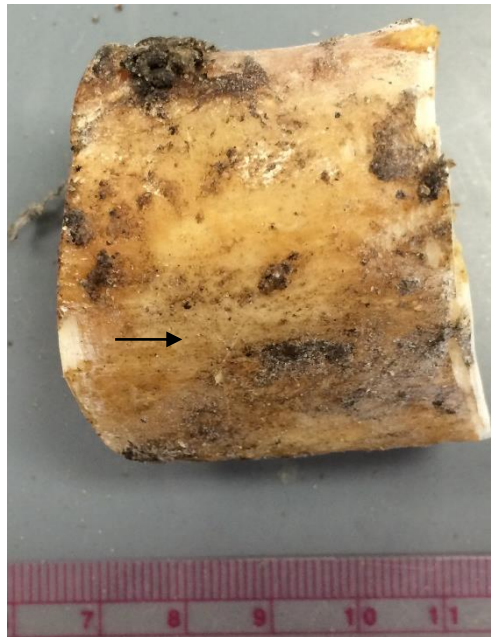

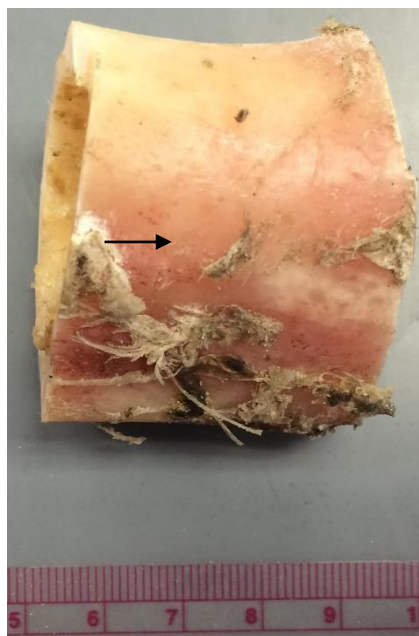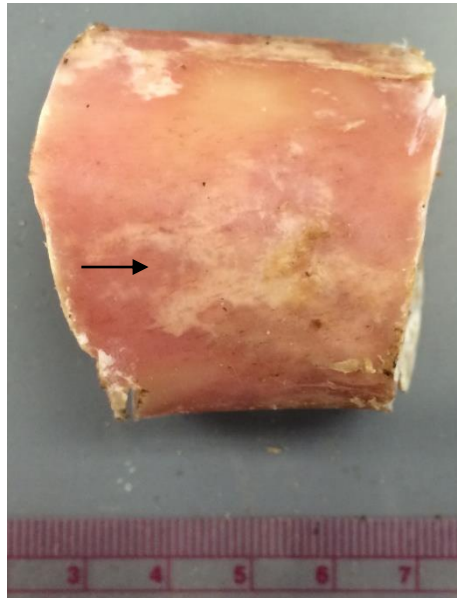Figure 15: Soil staining on the exterior of the mid-diaphysis cut of a pig humerus from Group A, Week 10.

Figure 16: Possible hemolysis staining on the exterior of the mid-diaphysis cut of a pig humerus from Group A, Week 4.

The adhered soft tissue decay was initially slower for Group B, but resulted in similar tissue desiccation by the end of the fourteen weeks. However, insect activity was greater in Group B, which corresponds with the quick skeletonization of the side of the bone in contact with the soil. Group B demonstrated minimal fungal activity beginning in Week 6, but fungal activity did not increase over time (Table 5). The slight presence was coupled with soil staining on the surface in contact with the ground (Dupras and Schultz, 2014). There was pink coloring from hemolysis on the humeri from Weeks 2 and 6 (Figure 17).

Figure 17: Possible hemolysis staining on the exterior of the mid-diaphysis cut of a pig humerus from Group B, Week 2.

Macroscopic Taphonomic Changes

The macroscopic changes to the bone cross sections were minimal in both groups. The possible hemolysis staining present on the exterior of the bone did penetrate into the cortex in Weeks 4, 6, 10, and 14 in Group A (Table 4) based on criteria provided by Dupras and Schultz (2014). Additionally, Weeks 2 and 6 of Group B exhibited pink coloration in the cortex (Figure 18) (Table 5). However, as time progressed, the presence diminished and yielded to the natural bone color.
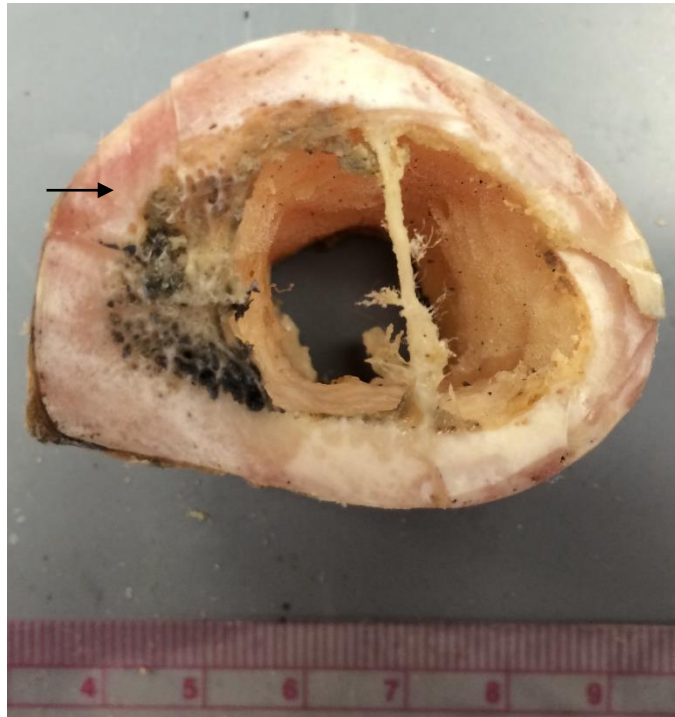
Figure 18: Hemolysis staining penetrating into the cortex of the cross section of mid-diaphysis of a pig humerus from Group B, Week 2.

The bone cortex also demonstrated the loss of bone grease within the bone cortex as evidenced by the dark and light cream color, identified based on criteria provided by Huculak and Rogers (2009). There was discoloration indicating bone grease loss in both groups. In Group A, Weeks 2, 4, 8, 12, and 14 demonstrated the dark and light discoloration described by Huculak and Rogers (2009). Weeks 8, 10, and 12 in Group B also demonstrated these discolorations (Figure 19).
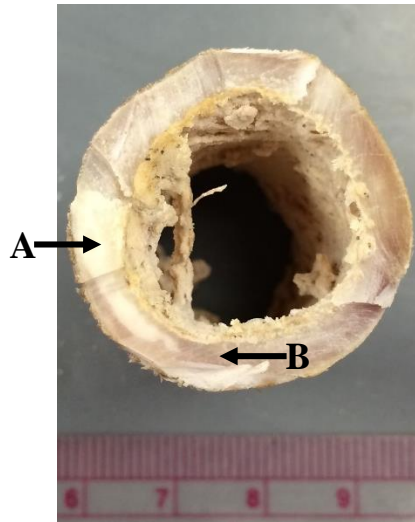
Figure 19: Loss of bone grease in the cortex of the cross section of the mid-diaphysis of a pig femur from Group B, Week 10. A: Areas indicating a loss of bone grease are lighter in color. B: Areas maintaining bone grease are darker in color.

Despite the presence of the soil staining on the exterior bone surface, there was no evidence that the soil staining penetrated the cortex of the bone. Since the experiment was limited to 14 weeks, the time constraints likely restricted the staining to the exterior surface (Huculak and Rogers, 2009; Dupras and Schultz, 2014).

Table 4: Summary of observations, gross taphonomic changes, and macroscopic taphonomic changes over time for the pig bones of Group A (sun) (* indicates femur).

Sample	Group A		
	Observations	Gross Changes	Macroscopic Changes
Control	De-fleshed bone with adhered soft tissue	Natural bone color	Pink medullary cavity; natural bone coloring
Week 2	Superficial soil adherence	Minimal soil staining; pink coloring	Slight discoloration around the periosteal margin
Week 4	Superficial soil adherence	Minimal soil staining; pink coloring	Slight color changes Pink coloring
Week 6*	Superficial fungi and soil adherence	Slight soil staining	Slight pink coloring
Week 8	Superficial fungi and soil adherence	Slight soil staining; pink discoloration	Discoloration throughout cross section
Week 10	Superficial fungi and soil adherence	Slight soil staining; pink coloring	Pink coloring to natural bone
Week 12*	Superficial fungi (Dark green) and soil adherence	Soil staining	Dark discoloration; natural bone color
Week 14	Fungus adherence (Dark green, light orange, bright orange); Abundance of trabecular bone	Slight soil staining; pink coloring.	Pink coloring; dark discoloration; natural bone color.

Table 5: Summary of observations, gross taphonomic changes, and macroscopic taphonomic changes over time for the pig bones of Group B (shade) (* indicates femur).

| Sample	Group B		
	Observations	Gross Changes	Macroscopic Changes
Control	De-fleshed bone with adhered soft tissue	Natural bone color	Pink medullary cavity; natural bone coloring
Week 2	Minimal activity; abundance of soft tissue	Pink coloring	Pink and natural coloring
Week 4	Decrease in soft tissue	Slight soil staining	Natural coloring
Week 6	Slight fungal growth	Slight soil staining; pink coloring	Pink and bone color
Week 8*	Slight fungal growth	Slight soil staining	Dark discolorations in cross section
Week 10*	Slight fungal growth and soil adherence	Soil staining	Dark discolorations in cross section
Week 12	Slight fungal growth (white); Marked soil staining; desiccated tissue	Soil staining	Dark discolorations in cross section; natural bone color
Week 14	Slight fungal growth; desiccated tissue	Soil staining	Natural bone color; no discolorations
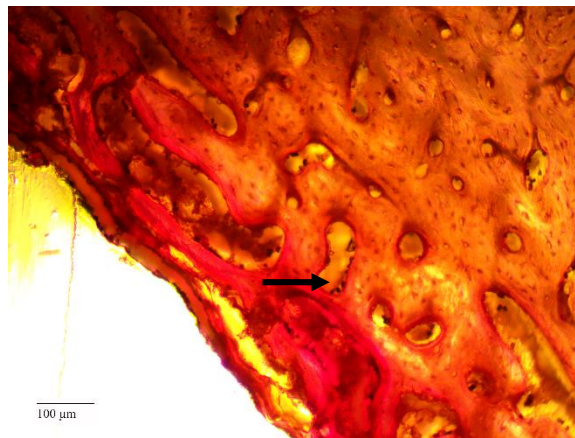
Figure 20: Example of the presence of bacteria (dark nodules) in the periosteal region of a thin section of a pig femur from Group B, Week 10 (arrow).
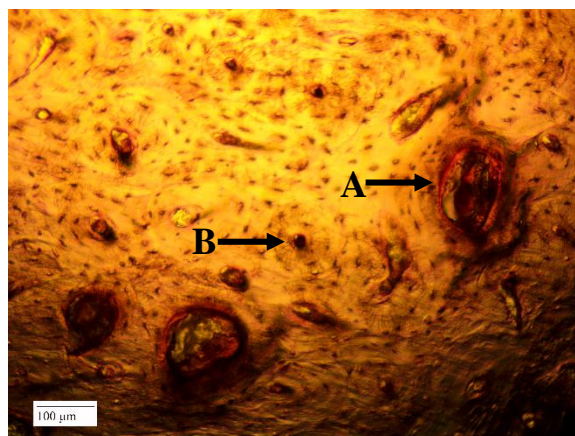

Figure 21: Example of non-Wedl microscopical focal destruction (A) and a regular Haversian canal with inclusions (B) on a thin section of a pig humerus from Group A, Week 14.
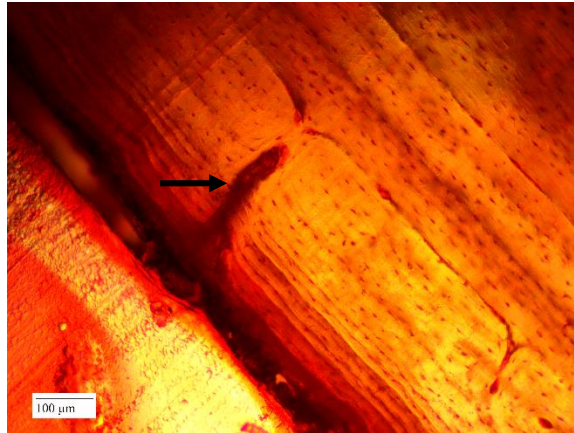
Figure 22: Example of Wedl tunneling from the periosteal margin into the cortical bone on a thin section of a pig humerus from Group A, Week 10. Note the plexiform bone tissue arranged linearly.

Control

The microstructure of the control consisted of entirely plexiform bone tissue. There were no diagenetic changes observed in the periosteal region, the middle cortical region, or in the endosteal region (Appendix A, Tables 10, 11, and 12). There were bacteria present in the periosteal and endosteal regions, however, the presence was limited in number.

Group A

The periosteal region of Week 2 contained minimal amounts of bacteria and no other diagenetic changes were observed (Appendix B, Tables 13 and 14). The middle cortical region contained minimal amounts of bacteria, inclusions in Haversian canals, and one possible locus of MFD (Tables 6 and 7). However, this structure was aligned with other large circular structures in the plexiform bone, suggesting that this was a large Haversian canal rather than MFD. The endosteal region contained bacteria and inclusions in Haversian canals, but no other diagenetic changes were observed.

The periosteal region of Week 4 contained minimal amounts of bacteria and small loci of MFD (Appendix B, Tables 15 and 16). The middle cortical region contained minimal amounts of bacteria, inclusions in Haversian canals, and small loci of MFD (Tables 6 and 7). Osteoclastic activity was also noted in the middle cortical region. The endosteal region contained bacteria and inclusions in Haversian canals, but no other diagenetic changes were observed.

The periosteal region of Week 6 contained bacteria and loci of MFD (Appendix B, Tables 17 and 18). There was definitive and possible Wedl tunneling from the periosteum into the bone. The middle cortical region contained bacteria, inclusions in Haversian canals, and loci of MFD (Tables 6 and 7). The endosteal region contained bacteria and inclusions in Haversian canals, but no other diagenetic changes were observed.

The periosteal region of Week 8 contained bacteria, but no other diagenetic changes were observed (Appendix B, Tables 19 and 20). The middle cortical region contained bacteria, inclusions in Haversian canals, and small loci of MFD (Tables 6 and 7). The endosteal region contained bacteria and inclusions in Haversian canals, but no other diagenetic changes were observed. This bone displayed layers of plexiform and cortical bone. The majority of the diagenetic changes were noted in the cortical bone layer.

Table 6: Summary of the locations of diagenetic changes of pig bones by region for each week of Group A (sun) (* indicates femur).

Group A			
Week	Periosteal Region	Middle Cortical Region	Endosteal Region
Control	Bacteria	-	-
Week 2	Bacteria	Bacteria, inclusions, MFD	Bacteria, inclusions
Week 4	Bacteria, MFD	Bacteria, inclusions, MFD, osteoclasts	Bacteria, inclusions
Week 6*	Bacteria, MFD, definitive and possible Wedl tunneling	Bacteria, inclusions, MFD	Bacteria, inclusions
Week 8	Bacteria	Bacteria, inclusions, MFD	Bacteria, inclusions
Week 10	Bacteria, MFD, definitive Wedl tunneling	Bacteria, inclusions, MFD, possible Wedl tunneling	Bacteria, inclusions
Week 12*	Bacteria, MFD	Bacteria, inclusions, MFD, definitive Wedl tunneling	Bacteria, inclusions
Week 14	Bacteria, inclusions, MFD	Bacteria, inclusions, MFD, definitive and possible Wedl tunneling	Bacteria, inclusions

The periosteal region of Week 10 contained bacteria, loci of MFD, and definitive Wedl tunneling (Appendix B, Tables 21 and 22). The middle cortical region contained bacteria, loci of MFD, inclusions in Haversian canals, and possible Wedl tunneling. The endosteal region contained bacteria and inclusions in Haversian canals, but no other diagenetic changes were observed (Tables 6 and 7). There was likely the presence of MFD in the endosteal region, however, due to the transition from cortical bone to trabecular bone, MFD was not distinguished from the natural bone structures.

The periosteal region of Week 12 contained bacteria and loci of MFD (Appendix B, Tables 23 and 24). The middle cortical region contained bacteria, inclusions in Haversian canals, loci of MFD, and definitive Wedl tunneling (Tables 6 and 7). The endosteal region contained bacteria and inclusions in Haversian canals, but no other diagenetic changes were observed. There was likely the presence of MFD in the endosteal region, however, due to the transition from cortical bone to trabecular bone, MFD was not distinguished from the natural bone structures.

The periosteal region of Week 14 contained bacteria, inclusions in Haversian canals, and large loci of MFD (Appendix B, Tables 25 and 26). The middle cortical region contained bacteria, inclusions in Haversian canals, large loci of MFD, and definitive and possible Wedl tunneling (Tables 6 and 7). The endosteal region contained bacteria and inclusions in Haversian canals, but no other diagenetic changes were observed. There was likely the presence of MFD in the endosteal region, however, due to the transition from cortical bone to trabecular bone, MFD was not distinguished from the natural bone structures.

Table 7: Summary of diagenetic changes to the microstructure of pig bone over fourteen weeks for Group A (sun) (* indicates femur).

Sample	Group A				
	Presence of Bacteria	Haversian Canals with Inclusions	Possible Wedl Tunneling (Type 1)	Microscopical Focal Destruction	Size of Focal Destruction
Control	+	-	-	-	-
Week 2	+	-	-	+	179µm
Week 4	+	+	-	+	207µm
Week 6*	+	+	+	+	220µm
Week 8	+	+	-	+	223µm
Week 10	+	+	+	+	225µm
Week 12*	+	+	+	+	483µm
Week 14	+	+	+	+	373µm

Group B

The observations of the periosteal region of Week 2 revealed a minimal presence of bacteria and small loci of possible MFD (Appendix C, Tables 27 and 28). The middle cortical region contained minimal amounts of bacteria, inclusions in Haversian canals, and small loci of MFD (Tables 8 and 9). The endosteal region contained bacteria and inclusions in Haversian canals, but no other diagenetic changes were observed.

The observations of the periosteal region of Week 4 displayed a minimal presence of bacteria (Appendix C, Tables 29 and 30). The middle cortical region revealed a minimal presence of bacteria, inclusions in Haversian canals, and small loci of MFD (Tables 8 and 9). The endosteal region contained bacteria, inclusions in Haversian canals, and areas of likely MFD, but the location excludes these MFD structures from analysis.

The periosteal region of Week 6 contained bacteria, small loci of MFD, and possible Wedl tunneling (Appendix C, Tables 31 and 32). The middle cortical region contained bacteria, inclusions in Haversian canals, possible Wedl tunneling, and small loci of MFD (Tables 8 and 9). Osteoclastic activity was also noted in the middle cortical region. The endosteal region contained bacteria and inclusions in Haversian canals, but no other diagenetic changes were observed.

The periosteal region of Week 8 contained bacteria and small loci of MFD (Appendix C, Tables 33 and 34). The middle cortical region contained bacteria, inclusions in Haversian canals, and small loci of MFD (Tables 8 and 9). Osteoclastic activity was also noted in the middle cortical region. The endosteal region contained bacteria and inclusions in Haversian canals, but no other diagenetic changes were observed.

Table 8: Summary of the locations of diagenetic changes of pig bones by region for each week of Group B (shade) (* indicates femur).

Group B			
Week	Periosteal Region	Middle Cortical Region	Endosteal Region
Control	Bacteria	-	-
Week 2	Bacteria, MFD	Bacteria, inclusions, MFD	Bacteria, inclusions
Week 4	Bacteria	Bacteria, inclusions, MFD	Bacteria, inclusions
Week 6	Bacteria, MFD	Bacteria, inclusions, MFD, osteoclasts	Bacteria, inclusions
Week 8*	Bacteria	Bacteria, inclusions, MFD, osteoclasts	Bacteria, inclusions
Week 10*	Bacteria, MFD, definitive and possible Wedl tunneling	Bacteria, inclusions, MFD, possible Wedl tunneling, osteoclasts	Bacteria, inclusions
Week 12	Bacteria, MFD	Bacteria, inclusions, MFD, possible Wedl tunneling, osteoclasts	Bacteria, inclusions
Week 14	Bacteria	Bacteria, inclusions, MFD, possible Wedl tunneling, osteoclasts	Bacteria, inclusions

The periosteal region of Week 10 contained bacteria, MFD, and definitive and possible Wedl tunneling (Appendix C, Tables 35 and 36). The middle cortical region contained minimal amounts of bacteria, inclusions in Haversian canals, possible Wedl tunneling, and loci of MFD (Tables 8 and 9). Osteoclastic activity was also noted in the middle cortical region. The endosteal region contained bacteria and inclusions in Haversian canals, but no other diagenetic changes were observed.

The periosteal region of Week 12 contained bacteria, but no other diagenetic changes were observed (Appendix C, Tables 37 and 38). The middle cortical region contained bacteria, inclusions in Haversian canals, possible Wedl tunneling, and loci of MFD (Tables 8 and 9).

Osteoclastic activity was also noted in the middle cortical region. The endosteal region contained bacteria and inclusions in Haversian canals, but no other diagenetic changes were observed.

The periosteal region of Week 14 contained bacteria, but no other diagenetic changes were observed (Appendix C, Tables 39 and 40). The middle cortical region contained minimal amounts of bacteria, inclusions in Haversian canals, possible Wedl tunneling, and loci of MFD (Tables 8 and 9). Osteoclastic activity was also noted in the middle cortical region. The endosteal region contained bacteria and inclusions in Haversian canals, but no other diagenetic changes were observed. The microstructure of the bone demonstrated layers of plexiform bone and cortical bone.

Table 9: Summary of diagenetic changes to the microstructure of pig bone over fourteen weeks for Group B (shade) (* indicates femur).

Sample	Group B				
	Presence of Bacteria	Haversian Canals with Inclusions	Possible Wedl Tunneling (Type 1)	Microscopical Focal Destruction	Size of Focal Destruction
Control	+	-	-	-	-
Week 2	+	+	-	+	174µm
Week 4	+	+	-	+	292µm
Week 6	+	+	+	+	190µm
Week 8*	+	+	+	+	264µm
Week 10*	+	+	+	+	326µm
Week 12	+	+	+	+	235µm
Week 14	+	+	+	+	234µm

CHAPTER FIVE: DISCUSSION

In forensic anthropology, time since death estimation is an integral part of forensic investigations. Methodologies currently focus on gross changes to soft tissue during decomposition and taphonomic changes to the surface of the bone (e.g., Behrensmeyer, 1978; Galloway et al., 1989; Christensen et al., 2014; Damann and Carter, 2014). Minimal attention has been paid to correlating histological diagenetic change with time since death (e.g., Yoshino et al., 1991; Bell et al., 1996). Therefore, the focus of this current study is to examine the progression of diagenetic change in the early postmortem interval. The implications of the gross analysis, macroscopic analysis, and microscopic analysis will be discussed further, followed by limitations and future considerations.

Gross Taphonomic Change Analysis

Weathering and bone staining were the gross taphonomic changes analyzed in this study. Research pertaining to gross changes in bone have focused on the Behrensmeyer (1978) six stage categorical system to estimate time since death (e.g., Andrews and Whybrow, 2005; Potmesil, 2005; Janjua and Rogers, 2008; Todisco and Monchot, 2008). However, gross changes in bone require extended time periods to manifest and are highly dependent on environmental factors (Beary and Lyman, 2012).The current experiment did not reveal any significant gross taphonomic changes. This is not unexpected due to the limited PMI upon which the field component was conducted. The duration of time required for large scale gross taphonomic changes to occur is beyond the scope of this research.

Two types of staining were observed on the remains: soil and hemolysis staining. The soil staining occurred on the surfaces of the bones that were in direct contact with the ground and began occurring in Week 2 for Group A and Week 4 for Group B. The staining was, however, superficial and did not penetrate into the cortex of the bone. Prolonged exposure, beyond the 14 weeks in this experiment, would be required to understand the link between soil staining penetration into the bone cortex and time since death estimation (Pokines and Baker, 2014).

The pink/red staining observed on the exterior of the bone was most consistent with hemolysis staining. This observation has not been widely documented in experimental literature (Huculak and Rogers, 2009) or correlated with time since death, but has been acknowledged as a surface stain (Dupras and Schultz, 2014). Upon placement in the field site, the remains had adhering soft tissue and retained red blood cells within the tissue. The bursting of these cells during decomposition is likely the source of staining, and as the red blood cells decomposed, a pink/red stain remained on the surface of the bone. Soil staining and hemolysis staining occurred on opposite sides of the exterior of the cut section. This suggests the soil staining occurred on the side of the bone in contact with the ground, which was skeletonized more rapidly, while the hemolysis staining occurred on the side of the bone with soft tissue adherence throughout the duration of the experiment.

Macroscopic Taphonomic Change Analysis

The loss of bone grease in the cortex of the bone and the penetration of hemolysis staining into bone cortex were the macroscopic taphonomic changes analyzed. Macroscopic changes to the bone cortex have not been widely researched in the forensic anthropological literature. Huculak and Rogers (2009) demonstrated that the areas of dark and light coloration

could be minimally related to depositional environment and represented the loss of bone grease. This was correlated to the mixed depositional environment that included exposed then buried, or buried then exposed (Huculak and Rogers, 2009).

The present study had two microenvironments, but only one depositional context, exposed, unlike the mixed context by Huculak and Rogers (2009). Despite the observed loss of bone grease within the samples in the present study, a discernible pattern was not observed within the 14 week study. Each week and microenvironment demonstrated different levels of bone grease and the changes from dark to light were not consistent across time. For example, Group A, Week 8 demonstrated discolorations throughout the cross section, but Week 10 did not demonstrate any loss of protein.

Hemolysis has been acknowledged in the literature as a surface stain, but has not been observed as a penetrating stain into the bone cortex (Dupras and Schultz, 2014). In the present study, the hemolysis staining did penetrate into the cortex of the bone, but was inconsistent across time. The microenvironment did appear to correlate the persistence and penetration of the hemolysis staining. Group A maintained pink staining throughout the fourteen week experiment, though inconsistently, while Group B had pink staining only in Week 2 and Week 6. This could demonstrate the greater retention of soft tissue and blood by Group A, however soft tissue changes were beyond the scope of this study and would require additional research. Conversely, this could represent the explosion of red blood cells when frozen into the cortex of the bone, as blood has been observed exploding in extreme cold temperatures in controlled settings (Sowemimo-Coker, 2002). Therefore, a direct comparison between fresh and frozen pig bone is necessary to ascertain the causal factor in the observed hemolysis staining.

Macroscopic changes to the bone cortex present a unique opportunity to study the postmortem interval. While there was no discernible pattern of bone grease loss in the present study, a longer longitudinal study with a larger sample size could demonstrate a quantifiable loss of bone grease. Hemolysis staining has not been widely acknowledged in the experimental literature, but could provide insights into the correlation of soft tissue decomposition and PMI. For example, if the presence of hemolysis staining persists into full skeletonization, does it diminish with time at a consistent rate, or is loss related to environment or microenvironment?

Methodological Considerations

Methodologically, throughout the study, there were several challenges. First, the standard protocol was adapted from Crowder et al. (2012) because their protocol cleansed the bone of bacteria and grease. For the purposes of the present study, the identification of bacteria within the bone matrix was a priority in order to understand the processes of diagenetic change more comprehensively. Utilizing this methodology allowed the intrusion of bacteria in vascular canals to gain access to the bone matrix to be observed (Child, 1995; Jans et al., 2004). However, the retention of bone grease extended the curation time of the Permount, from several hours to over three weeks. The embedding resin did not encounter this difficulty and should be considered as a mounting medium in future studies utilizing this protocol.

The second, and primary, challenge was the identification of diagenetic change. Specifically, one of the difficulties was the differential diagnosis of vascular canals with MFD and Volkmann's canals with Wedl tunneling. The use of pig bone increased this challenge for this type of study as plexiform bone is not similar to natural cortical bone found in human comparative studies (Cuijpers, 2006; Martiniakova et al., 2006a; Hillier and Bell, 2007; Junod

62

and Pokines, 2014). This complicated the identification of MFD, as Haversian canals were more

inconsistently sized and shaped in plexiform bone. Within cortical bone, identification of MFD

was simplified by the presence of concentric lamellae around Haversian canals (White et al.,

2011) and the presence of MFD within the lamellae. A flow chart depicting the criteria for

identification of MFD was created to demonstrate the analytical process based on multiple

researchers (Figure 23) (Hackett, 1981; Garland et al., 1988; Jans et al., 2002; Jans, 2008;

Maggiano, 2012; White et al., 2011). The identification of Wedl tunneling was complicated by

the presence of Volkmann's canals. Volkmann's canals connect Haversian canals (Hillier and

Bell, 2007; Maggiano, 2012; White et al., 2011) and could be distinguished if the path was

discernible in the thin section. However, the thin section can show the Volkmann's canal before

it reaches its final destination and fungi would use these canals to gain access to the bone.

Therefore, the widening of Volkmann's canals could be the result of fungal diagenetic change as

well (Child, 1995; Jans et al., 2004). A flow chart depicting the criteria for identification of Wedl

tunneling was created to demonstrate the analytical process based on multiple researchers

(Figure 24) (Hackett, 1981; Garland et al., 1988; Garland, 1993; Jans et al., 2002; Trueman and

Martill, 2002; Jans et al., 2004; Jans, 2008; White et al., 2011; Maggiano, 2012).
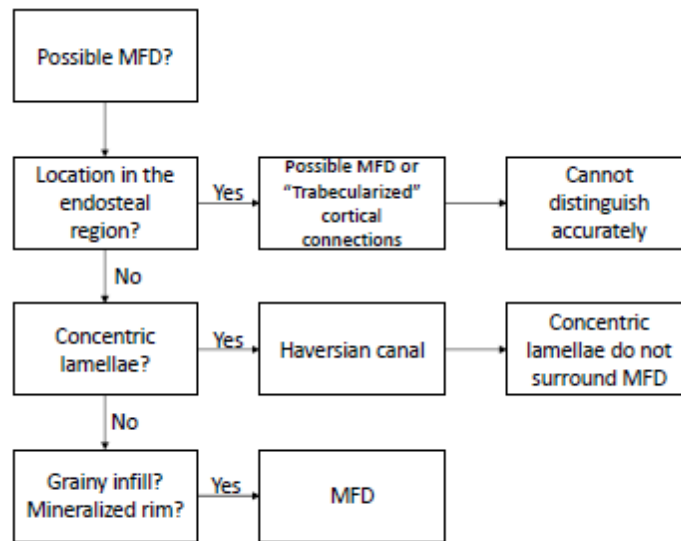
Figure 23: Flow chart demonstrating the criteria for identifying MFD and Haversian canals in the present study based on multiple researchers (Hackett, 1981; Garland et al., 1988; Jans et al., 2002; Jans, 2008; White et al., 2011; Maggiano, 2012).
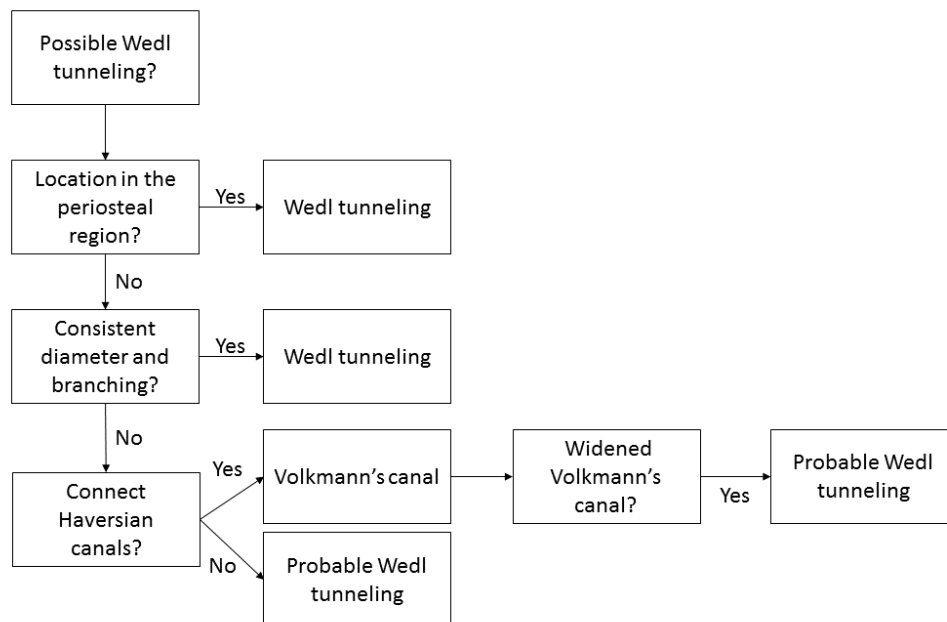
Figure 24: Flow chart demonstrating the criteria for identifying Wedl tunneling and Volkmann's canals in the present study based on multiple researchers (Hackett, 1981; Garland et al., 1988; Garland, 1993; Jans et al., 2002; Trueman and Martill, 2002; Jans et al., 2004; Jans, 2008; White et al., 2011; Maggiano, 2012).

Microscopic Taphonomic Change Analysis

In recent years, while there is an increasing number of articles in forensic anthropology dealing with diagenetic change, this research is still in its infancy regarding how to use diagenetic change when examining forensic bone with a short PMI. Therefore, the correlation with time since death has only been briefly explored in forensic literature (Yoshino et al., 1991; Bell et al., 1996; Jans, 2014). Other forensic inquiry has examined diagenetic change, but has not correlated the findings with time since death (e.g., Turner-Walker, 2012; White and Booth, 2014).

The present study examined diagenetic change in two microenvironments, full sun (Group A) and shade (Group B). The use of these two microenvironments have been widely used in experimental decomposition research, and, therefore, was used in the present study (Shean et al., 1993; Komar and Beattie, 1998; Kjorlien et al., 2008). There were notable differences in the size and occurrence of MFD between Group A and Group B (Tables 7 and 9). While the total number of MFD was not calculated, due to equipment limitations, observations of every sample revealed an overall greater occurrence of MFD in Group A than Group B. The MFD were larger in size in Group A than in Group B. This difference was most apparent in the samples from Week 14, which demonstrated a maximum MFD diameter of 373µm in Group A compared to 234µm in Group B (Figures 25 and 26). Additionally, the maximum diameter of MFD steadily increased from possible MFD in Week 2 through Week 14 in both environments. These results also highlight the impact of not only environment, but microenvironment. Diagenetic changes in Group A were significantly greater than those in Group B.
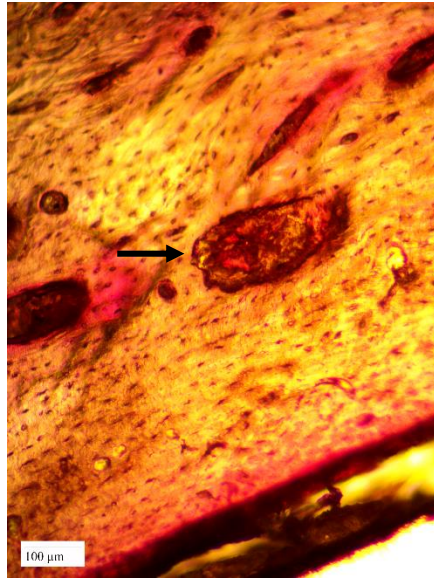
Figure 25: Example of MFD from a thin section of pig humerus from Group A, Week 14 (arrow).
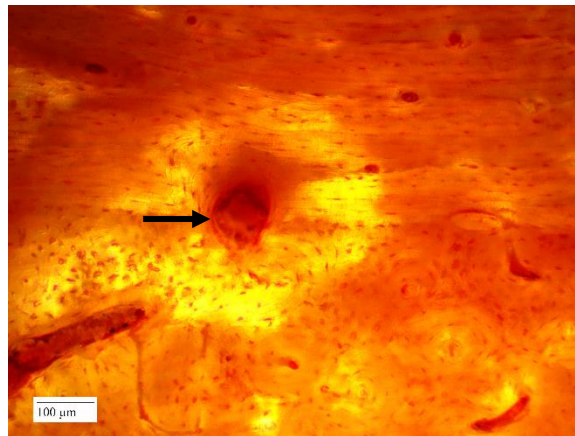
Figure 26: Example of MFD from a thin section of pig humerus from Group B, Week 14 (arrow).

In the limited work that has been undertaken with forensic cases and diagenetic change, there are a number of similarities between those studies and the present study. In this study, diagenetic changes not only occurred within 14 weeks, or three and a half months, but changes began to occur within four weeks postmortem. As a pilot study, these findings corroborate the findings of some previous studies examining long bones. Yoshino et al. (1991) examined human humeri from forensic cases with known postmortem intervals and observed diagenetic changes in buried human remains within two and a half years. However, open air diagenetic changes did not

occur within the early postmortem interval, with the first identification occurring 15 years postmortem (Yoshino et al., 1991). Bell et al. (1996) identified diagenetic changes within three months in scavenged human remains. These changes were observed within a tibia fragment found in the feces of a scavenger, which were partially attributed to this unusual deposition. Changes were next identified 15 months postmortem in a fourth rib of a surface deposition (Bell et al., 1996). The findings of the present study corroborate the accelerated timing of diagenetic changes described by Yoshino et al. (1991) and Bell et al. (1996) when compared to archaeological studies. The current study was conducted in the subtropical environment of Central Florida, which is characterized by increased heat, rain, and humidity. This could explain the difference in timing of diagenetic change in Japan (Yoshino et al. 1991) and Canada (Bell et al., 1996). However, the different rates of diagenetic change observed within the three studies demonstrate the effect of environment on diagenetic change. Furthermore, this variability highlights the necessity of more actualisitic studies in different environments to better understand the factors that influence diagenetic change.

There have been a number of actualistic studies, though not directly comparable with the current methodology, which demonstrate the value of experimental studies to understand the timing of diagenetic changes. Turner-Walker (2012) studied the potential for diagenetic changes in buried specimens in three different contexts and identified diagenetic change, but collection of data did not occur until one year had passed. Similarly, White and Booth (2014) studied the bacteria involved in diagenesis and observed diagenetic changes in the microstructure of pig bone by the first sampling period, which was six months. However, these changes could have begun at an earlier time interval. The observation of early diagenetic change by Turner-Walker (2012), and White and Booth (2014) corroborates the findings of the current experiment.

However, the current study specifically examined diagenetic change in an experimental setting with specific collection increments to analyze the progression of change, making this pilot study unique.

More recently, Jans (2014) reported on preliminary findings at the Anthropological Research Facility at the University of Tennessee. There was no diagenetic changes to the human ribs sampled with postmortem intervals up to 49 months. This directly contrasts with the findings of the present study. However, the researchers sampled the smallest rib, rather than long bones, as sampled by Yoshino et al. (1991), Bell et al. (1996), Turner-Walker (2012), White and Booth (2014), and the current study. Consistency of the bone and species sampled by researchers would make results more comparable.

The current study utilized one depositional context, surface, and two microenvironments, sun and shade. While comparison of microenvironment has been established in decompositional research (Shean et al., 1993; Komar and Beattie, 1998; Kjorlien et al., 2008), it has not been used in experimental histological analysis. As previously discussed, there were difference between Group A (sun) and Group B (shade), specifically the size and occurrence of MFD. Other studies have compared different depositional contexts, buried and surface (White and Booth, 2014) and different buried contexts and aquatic (Turner-Walker, 2012). White and Booth (2014) observed more diagenetic change in the buried specimens than those exposed, however, diagenetic change occurred in both contexts. Comparatively, Turner-Walker (2012) identified more diagenetic change in the aquatic context than in the dry soil and did not observe diagenetic change in the water-logged soil burial. These three studies demonstrate the utility of understanding how diagenetic change varies with the type of microenvironment in addition to depositional environment.

68

In an overview article about diagenetic change, Jans (2008) stated that microbial alteration likely occurs in the early postmortem interval, but that MFD would not occur in situations where the gut bacteria had no access to the bone or where bacterial growth was inhibited. This idea contrasts with the findings of this study as microscopical focal destruction was identified within four weeks and the presence of gut bacteria on the limb bones was unlikely. Additionally, the forensic anthropological literature supports a trend of diagenetic change occurring earlier in long bones than in ribs, which gut bacteria would have greater access to (Yoshino et al., 1991; Bell et al., 1996; Turner-Walker, 2012; White and Booth, 2014). However, comparative studies on human and nonhuman bone have not observed the levels of Wedl tunneling caused by fungal diagenesis as observed in the current study (Yoshino et al., 1991; Bell et al., 1996; Turner-Walker, 2012; White and Booth, 2014). The increased occurrence of Wedl tunneling in the current study could be could be the product a combination of factors, for example, the proliferation of fungi in the Central Florida environment, the sampling location of the cortical bone from mid-diaphysis for thin section analysis, or the larger sample size utilized.

The presence of bacteria was a diagenetic factor that was not contingent upon time since death, as the control had a limited presence of bacteria in the periosteal region. However, as time progressed, the presence of bacteria increased in number and spread to encompass all regions of the bone. This cannot be correlated with time since death, but it demonstrates the increasing penetration of bacteria into the bone cortex within a short time interval. It also shows that bacteria become active in the bone matrix almost immediately after death, therefore, it is not unexpected to find areas of bacterial MFD at early time intervals. Additionally, the unique protocol adapted from Crowder et al. (2012) did not cleanse the bone of proteins or bacteria, thus

allowing the progression of bacteria within the bone matrix to be viewed and assessed. This can be used to better understand the process of bacterial diagenesis. The Haversian canals with inclusions demonstrated the utilization of vascular canals within the bone matrix by bacteria and fungi to gain access to the middle cortical and endosteal regions of the bone (Child, 1995; Jans et al., 2004).

There were not many significant changes observed in Weeks 2 and 4 in the gross field observations. Superficial fungal growth appeared in Week 6 for both Group A and Group B, which has been observed in the literature (Piepenbrink 1986; Huculak and Rogers, 2009; Hawksworth and Wiltshire, 2011). This coincided with the appearance of possible Wedl tunneling from fungal diagenesis. Fungi had a continuous presence for the rest of the experiment, with a greater presence in Group A than Group B. This could be used to indicate diagenetic change without the destructive microscopic analysis, however, further research is necessary. Additionally, Volkmann's canals connecting Haversian canals appear to have been utilized by fungi to gain access to the bone matrix, as many Volkmann's canals appear enlarged by diagenetic change (Child, 1995; Jans et al., 2004).

Overall, when considering the four diagenetic changes observed, presence of bacteria, Haversian canals with inclusions, possible Wedl tunneling, and microscopical focal destruction, the size of MFD presents the most promising predictor of time since death. The results of the current study demonstrate an increasing trend in the maximum diameter of MFD (Figure 27). Unfortunately, previous literature has not examined the relationship of increasing maximum diameter of MFD and PMI. While this is highly dependent on environment, as the diameter of MFD from Group A and Group B differed significantly, research could examine diameter MFD with a larger sample size for other environments to establish a regression equation to estimate

time since death. Rudimentary graphing of the maximum diameter of MFD revealed the potential

for the estimation of time since death (Figure 27). However, the line of best fit presented in the

graph cannot be considered accurate with a total sample size of 15. This could be important for

forensic anthropology as an additional method for estimating time since death when remains are

fully skeletonized.
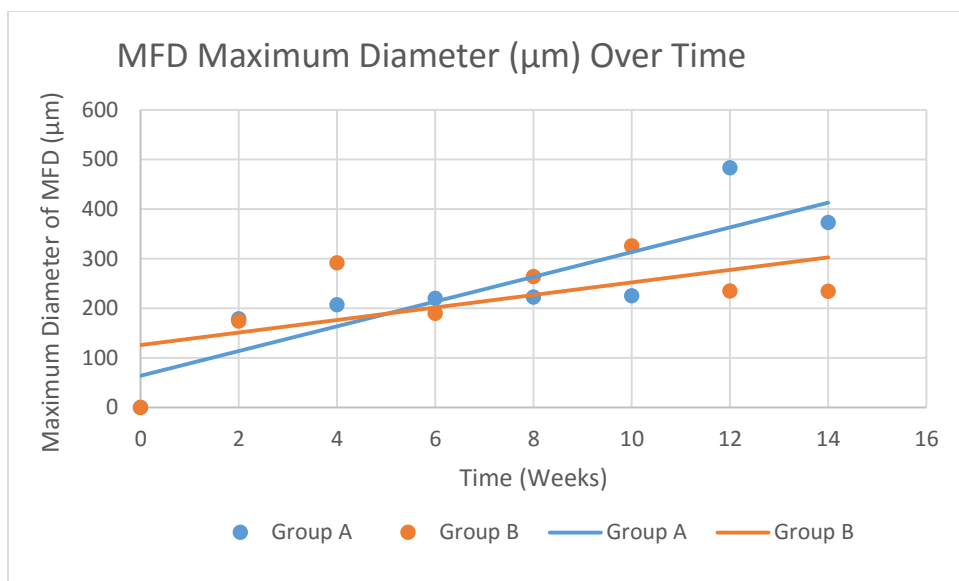
Figure 27: Graph of maximum diameter of MFD (µm) over time for Groups A and B. Lines of best fit represent the PMI estimation based on maximum diameter of MFD.

Limitations and Future Considerations

There were several limitations for this study, however, ways to overcome these

limitations for future studies are presented in addition to future considerations for similar

research. The primary limitation for this study was the mixed sample of long bone used. This

study utilized juvenile pig humeri and femora in a variety of different sizes, which could suggest

differences in developmental age. This could contribute to the heavy presence of plexiform bone

and the mixed plexiform and cortical bone microstructure. Another consideration for future

71

studies is the use of pig femora and humeri. For example, the cortical bone of the pig humeri was thicker than observed in pig femora and human long bones. Additionally, femora of pigs have a more similar loading to that of human femora, when compared to the differences in locomotion and loading in humeri. These differences suggest pig femora are a better proxy for humans than pig humeri. However, the mixed long bone sample demonstrated the potential variation in diagenetic change between humeri and femora. Specifically, the femora demonstrated larger maximum diameter of MFD. Future iterations of this study should use femora and select similarly sized elements as it would be advantageous to have similar developmental ages.

Despite the accepted practice in the use of pig bone as an animal proxy for human (e.g., Komar and Beattie, 1998; Janjua and Rogers, 2008; Huculak and Rogers, 2009; Cunningham et al., 2011; White and Booth, 2014), the microstructure of pig bone differs significantly from that of human (Cuijpers, 2006; Martiniakova et al., 2006a; Hillier and Bell, 2007; Crescimanno and Stout, 2012; Junod and Pokines, 2014). Furthermore, a study on the use of animal proxies for medical research discovered that dog bone more closely resembled humans, however, pig was a close second (Aerssens et al., 1998). The plexiform structure of the bone inhibited smaller thick sections from being cut. Sections thinner than 1 mm would break halfway through cutting the bone, despite alterations in blade speed and arm weight. As demonstrated in Appendix A, Tables 1, 2, and 3, the microstructure of the entire control sample consisted of plexiform bone. While not unexpected, this inhibited some comparisons across time as some samples exhibited a mix of plexiform and cortical bone, while others exhibited only cortical bone. Plexiform bone also presents different patterns within the microstructure. For example, Haversian canals are not clearly delineated by concentric lamellae, making identification of MFD difficult in plexiform bone (Cuijpers, 2006; Martiniakova et al., 2006a; Hillier and Bell, 2007; Junod and Pokines,

2014). Analyses comparing the diagenetic changes to humans and pigs should be performed to understand the differences and create a standard upon which future studies can be compared to.

The microscope utilized to view the microscopic diagenetic changes also presented some challenges. The 10x lens was the only usable lens, as the focal length was not long enough to view the slide using the other three lenses. This more than likely complicated the identification of Wedl tunneling. The PAS stain was designed to stain the fungal spores in the bone, however, the microscope would not focus at a high enough magnification to see the spores. Therefore, many areas of possible Wedl tunneling could not be confidently identified as definitive.

A final limitation is the limited period of time in which this study was conducted. A period of time longer than 14 weeks would have provided conclusions of greater forensic significance. The decompositional phase presenting the greatest challenge for estimating time since death is skeletonization (Janjua and Rogers, 2008), however, the present study did not encompass that stage. Additionally, longer postmortem intervals should be examined in conjunction with the short collection intervals.

Despite these limitations, this study has generated several avenues for further research to create a direct correlation between diagenetic change and time since death. This research presents experimental data that demonstrates the early presence of diagenetic change. The results can be used as a pilot study for future analyses into diagenetic change and the correlation with time since death. The presence of diagenetic change beginning in Week 4 for both groups demonstrate the applicability of microscopic analysis for forensic research. A standardized protocol should be established to allow for comparisons across studies, such as the protocol that was presented in the current study adapted from Crowder et al. (2012). The trend in the increasing diameter of microscopical focal destruction presents the opportunity for the creation

of a regression equation to estimate time since death. A large sample size, different depositional contexts, and an extended time period could create a standard upon which estimation of time since death is more accurate without requiring gross taphonomic changes. Additionally, experimental data should be collected for regions outside of Central Florida.

Surprisingly, the archaeological literature is limited in the scope of diagenetic change. While many studies compare the preservation level between and within archaeological sites (Stout and Teitelbaum, 1976; Stout, 1978; Nielsen-Marsh and Hedges, 2000; Nielsen-Marsh et al., 2007; Smith et al., 2007; Maurer et al., 2014), the literature does not examine time as a variable. As Stout and Teitelbaum (1976) state that time is not a singular variable affecting diagenesis, but that it works in conjunction with other variables, such as environment. The present study and others in forensic anthropology (Yoshino et al., 1991; Bell et al., 1996; Turner-Walker, 2012; White and Booth, 2014; Jans, 2014) demonstrate the information that can be gleaned from further examination of diagenetic change, particularly the time interval upon which diagenetic changes occur and the variation that occurs between and within environments. Specifically, this can be used to interpret the taphonomic history of bone and, therefore, influence the interpretation of an archaeological site. Understanding the time interval in which diagenetic change occurs can be used to understand the original deposition of an archaeological burial. For example, since diagenetic change has been shown to occur in a relatively short time interval, especially when considering the antiquity of archaeological sites, good histological preservation could indicate a depositional environment free from chemical and biological diagenetic agents. Conversely, differential preservation levels within a site could represent multiple microenvironments within a site.

CHAPTER SIX: CONCLUSION

Estimating time since death continues to present difficulties when examining skeletonized remains (e.g., Janjua and Rogers, 2008). Microscopic analysis presents a new frontier to explore diagenetic changes as a corollary of time since death. The current study illustrates the early timing of diagenetic change in the Central Florida environment, with foci of non-Wedl microscopical focal destruction occurring within four weeks postmortem. Therefore, this pilot study demonstrates diagenetic changes before other comparative literature (Yoshino et al., 1991; Bell et al., 1996; Turner-Walker, 2012; White and Booth, 2014). The present research is of particular importance because it is the first experimental study to analyze the progression of diagenetic changes using a more frequent two week sampling increment. The results of the current study corroborate and refine other forensic research (Yoshino et al., 1991; Bell et al., 1996; Turner-Walker, 2012; White and Booth, 2014) and contrast with others (Jans, 2014). However, the unique Central Florida environment should be considered a causal agent for the early diagenetic change observed in the current study. Therefore, further experimental research is necessary to fully understand the relationship between diagenetic change and environment.

Additionally, Group A (sun) and Group B (shade) demonstrated different patterns in the size and occurrence of diagenetic change, indicating the importance of considering microenvironment, similar to Turner-Walker (2012). When examining the thin sections, it was clear that the diagenetic change occurred more often in Group A. Additionally, the measurements of the greatest diameter of MFD indicated that the foci of MFD in Group A were generally larger. This demonstrates the necessity of considering how microenvironment, in addition to overall environment, can alter the rate of diagenetic change. This means that analyses

of diagenetic change need to account for microenvironmental factors in order to fully sample the variation in a thin section.

These findings could not be directly correlated with time since death. This pilot study, however, demonstrated the early onset of diagenetic change in the sub-tropical environment of Central Florida. The most promising indicator of time since death appears to be the maximum diameter of MFD, and with additional research, the increasing trend if MFD diameter could be used to create a regression equation to estimate time since death. Therefore, this method deserves greater attention in the forensic literature to create microscopic analysis a viable option for estimating time since death. Additional research using a larger sample size, a longer experimental time period, different environments and depositional contexts, direct comparative research between pigs and humans, and a standardized protocol for analyzing histological features of bone for diagenetic change would make microscopic analysis of diagenetic change a useful tool in forensic investigations.

APPENDIX A: CONTROL ANALYSIS TABLES

Table 10: Thin section of cortical bone of the control from mid-diaphysis of a pig humerus. Not stained. Refer to three inset images for specific diagenetic changes in periosteal, middle cortical, and endosteal regions.

1: Periosteal region of the control.
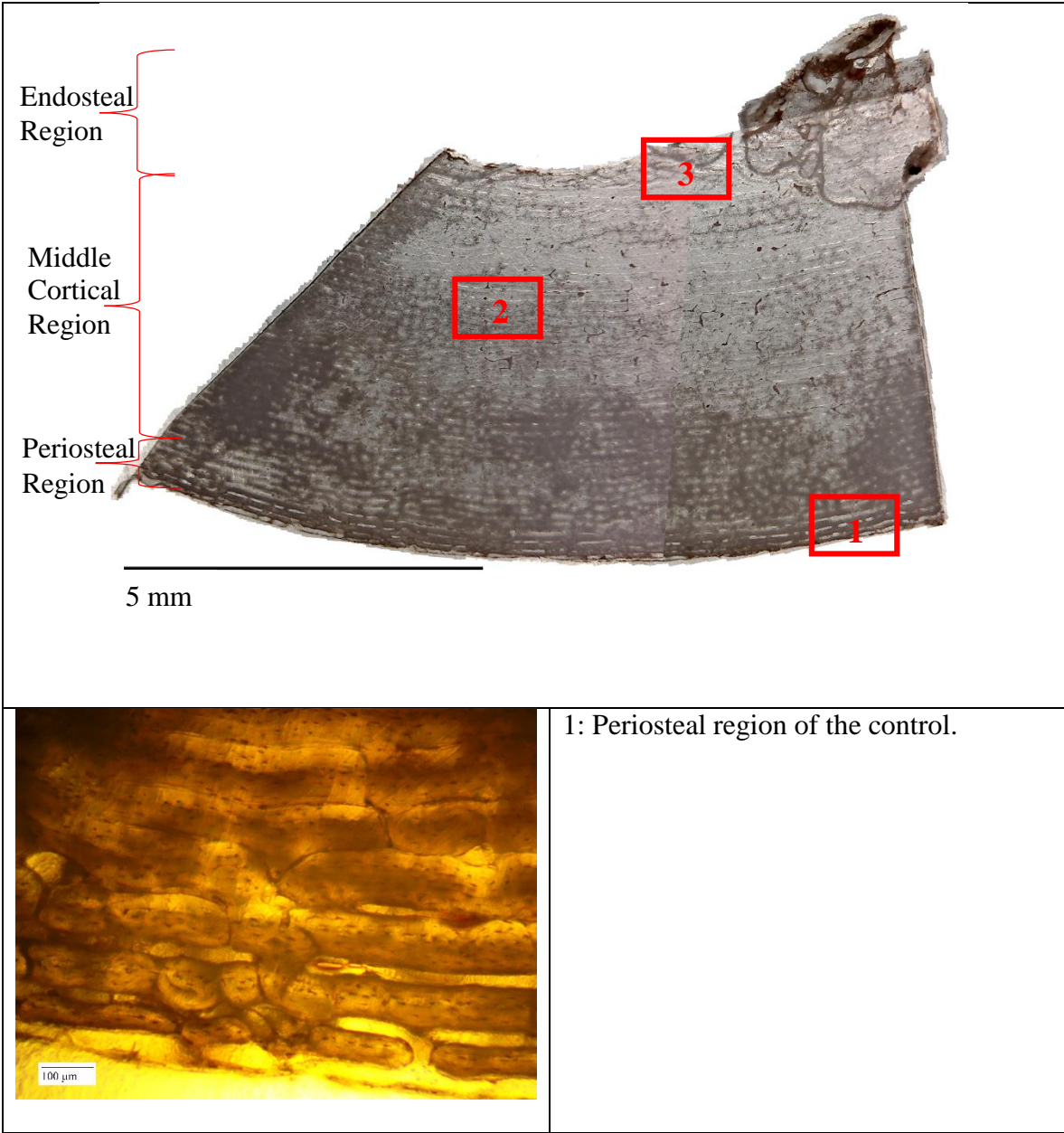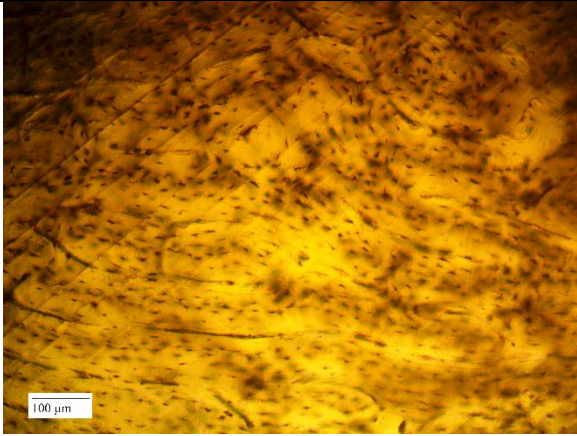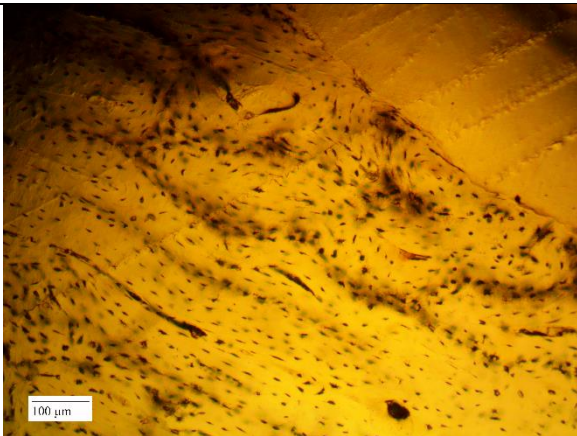
	2: Middle cortical region of the control.
	3: Endosteal region of the control.

Table 11: Thin section of cortical bone of the control from mid-diaphysis of a pig humerus. Stained with PAS. Refer to three inset images for specific diagenetic changes in periosteal, middle cortical, and endosteal regions.

1: Periosteal region of the control. Note the bacteria present (arrow).
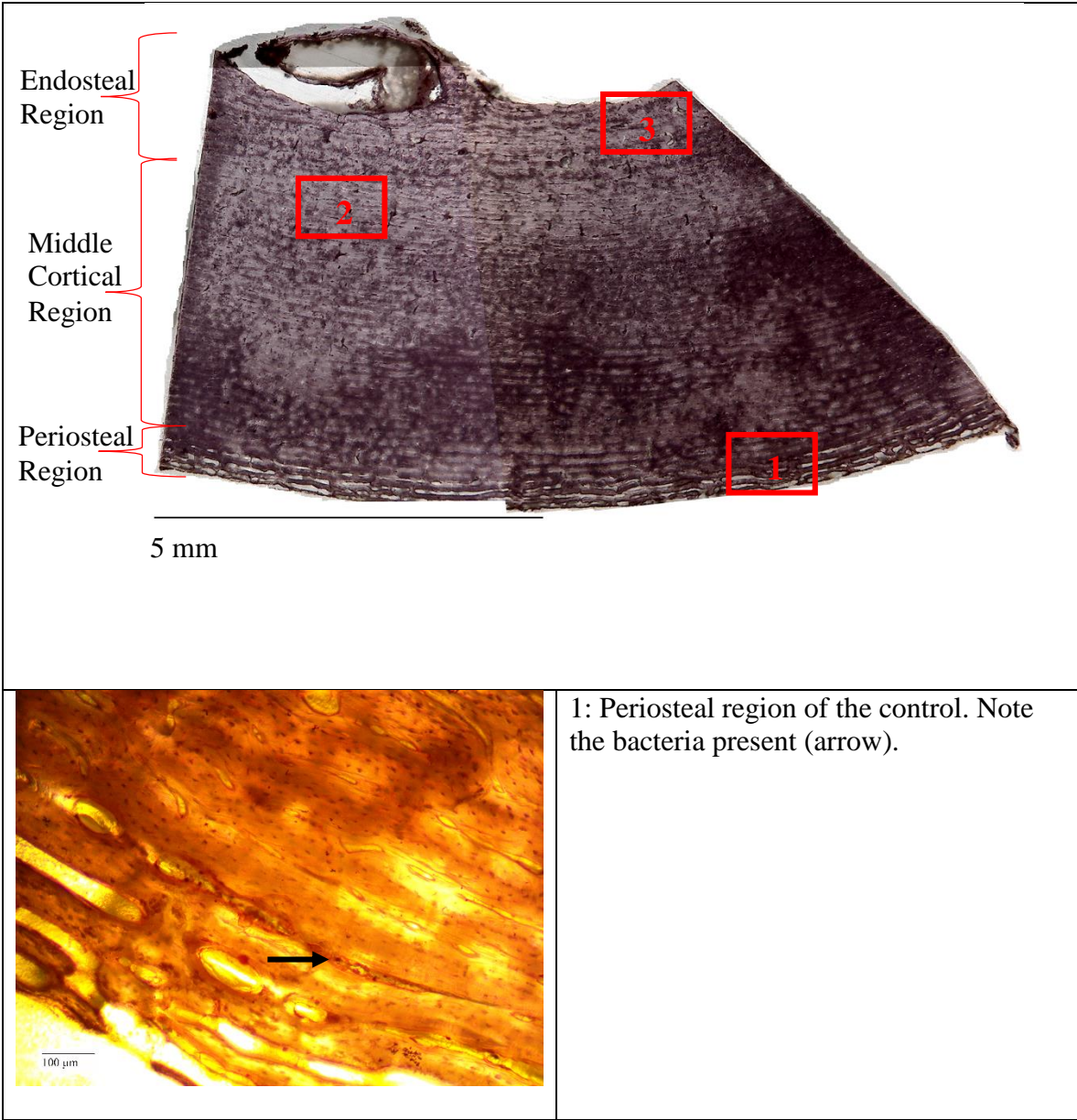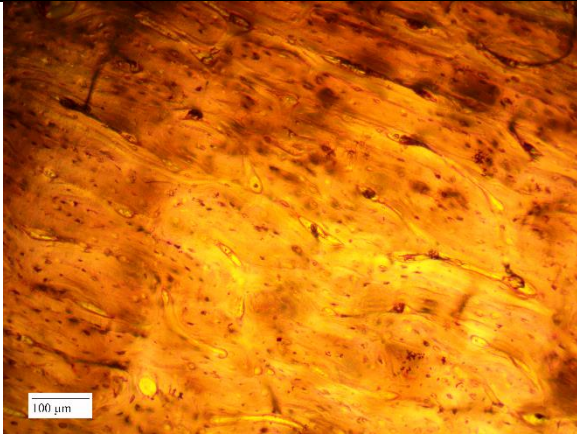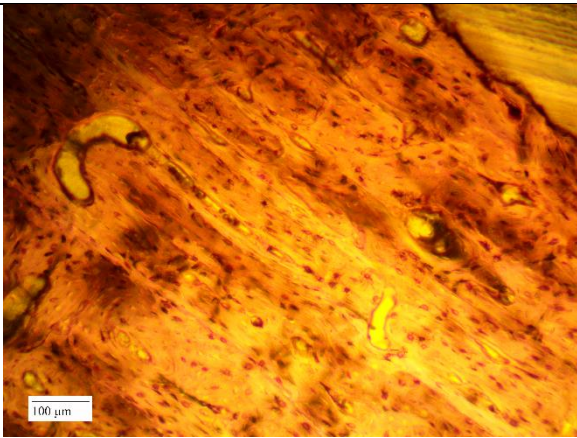
	2: Middle cortical region of the control.
	3: Endosteal region of the control.

Table 12: Thin section of cortical bone of the control from mid-diaphysis of a pig humerus. Stained with H and E. Refer to three inset images for specific diagenetic changes in periosteal, middle cortical, and endosteal regions.

1: Periosteal region of the control.
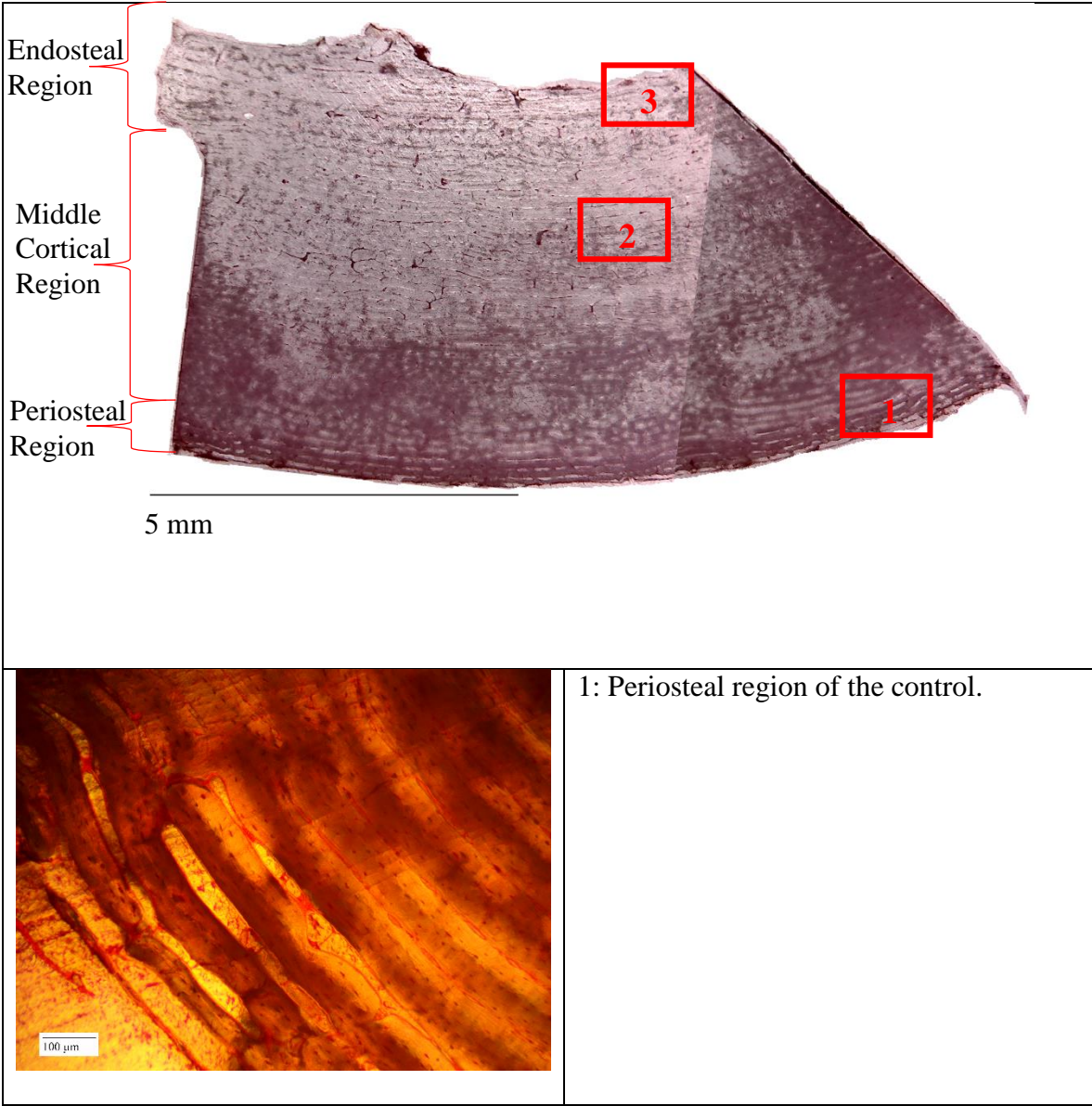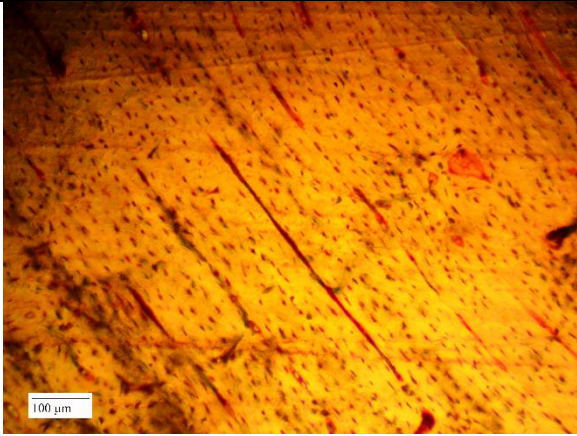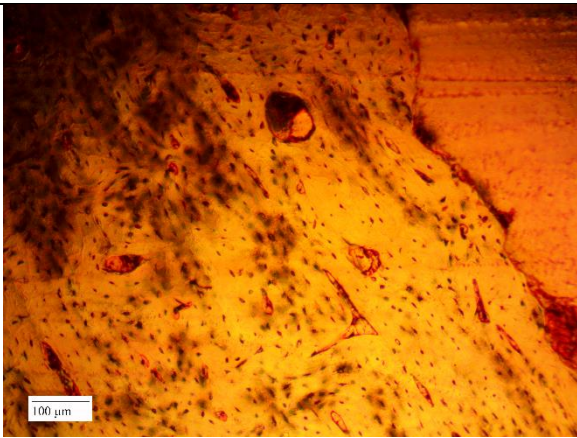
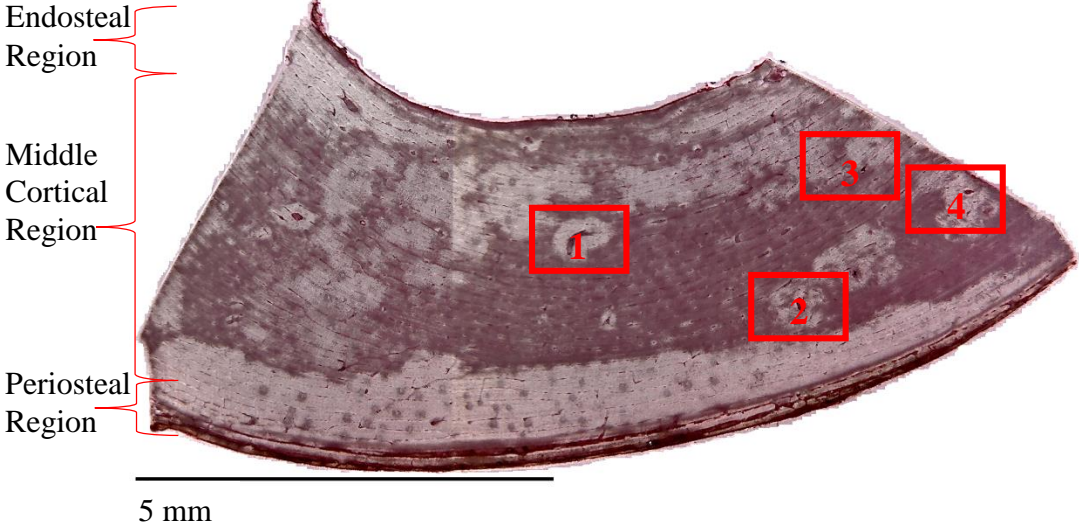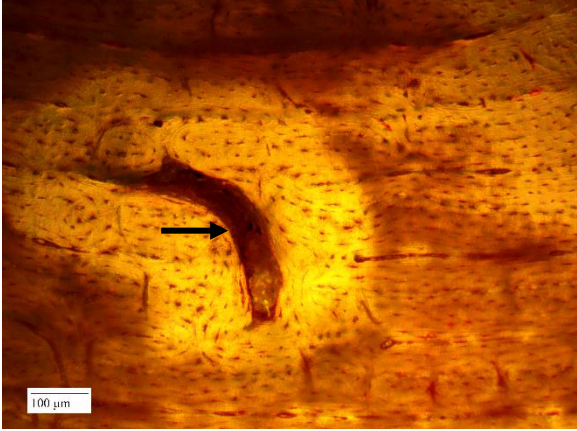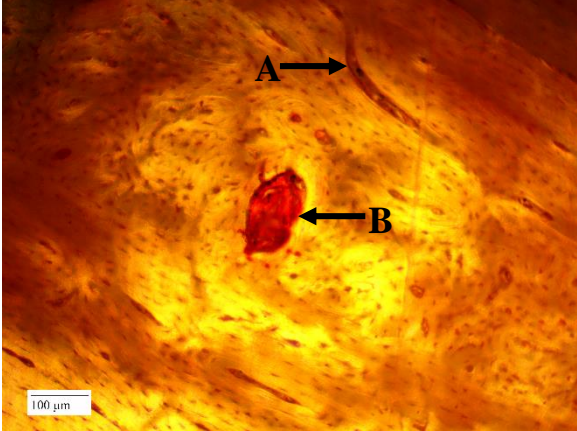|	2: Middle cortical region of the control.
	3: Endosteal region of the control.

APPENDIX B: GROUP A ANALYSIS TABLES

Table 13: Thin section of cortical bone of Group A, Week 2 from mid-diaphysis of a pig humerus. Stained with PAS. Refer to four inset images for specific diagenetic changes in periosteal, middle cortical, and endosteal regions.


	1: Plexiform bone tissue in the periosteal region. Note the slight presence of bacteria (arrow).
	2: Presence of bacterial inclusions in Haversian canals in the middle cortical region (arrows).
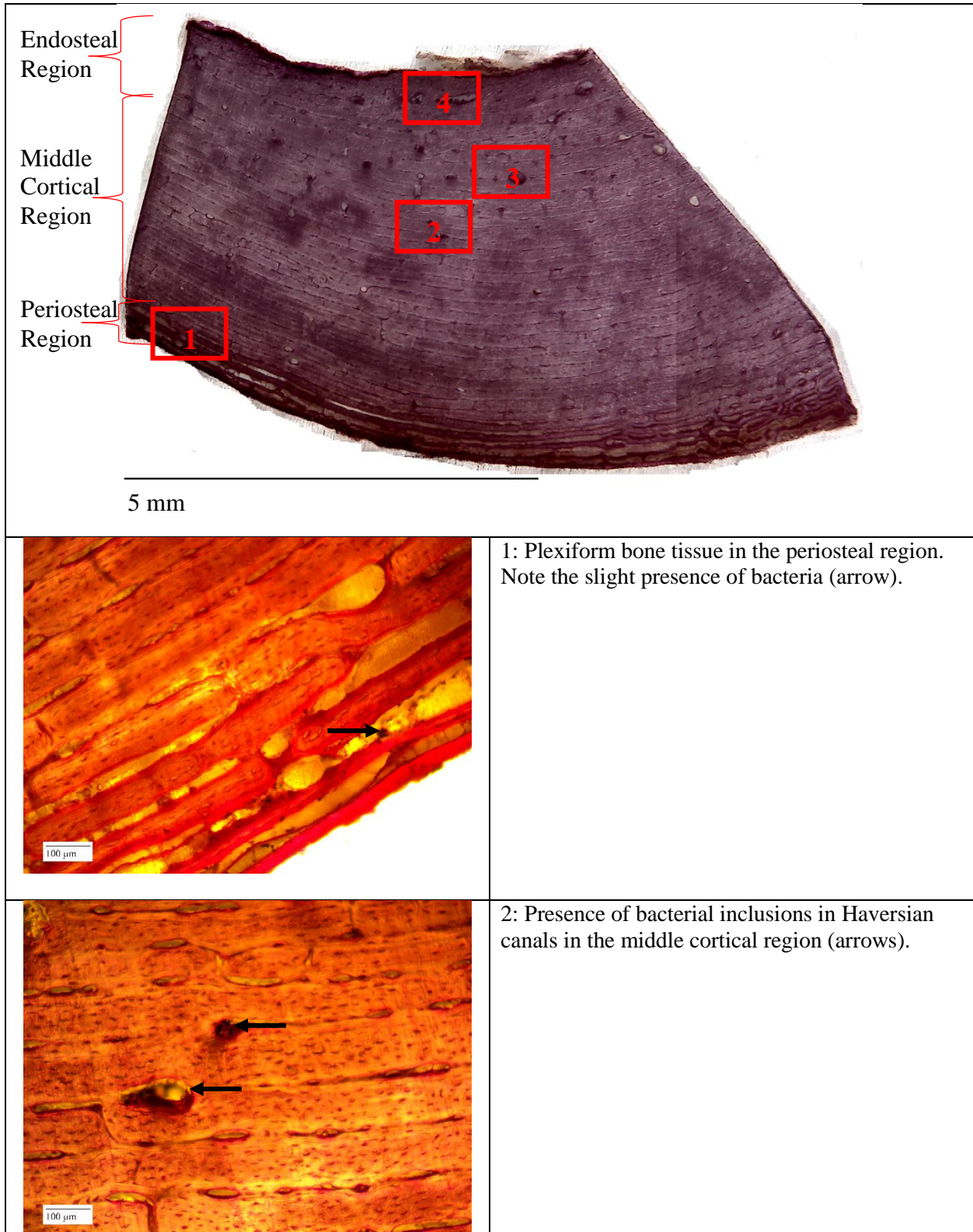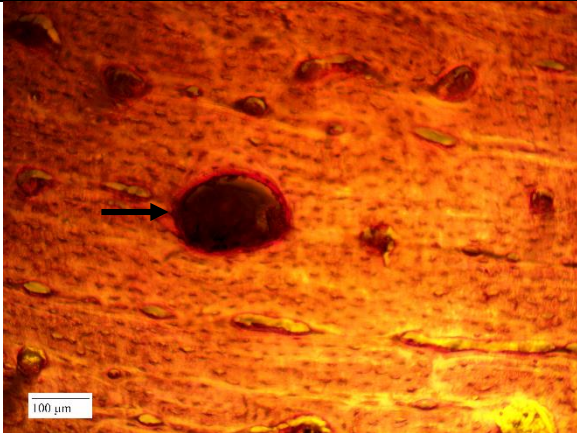
	3: Possible microscopical focal destruction caused by bacteria in the middle cortical region (arrow). However, this structure was aligned with other large circular structures, suggesting large Haversian canals with bacterial inclusions.
	4: Presence of bacteria in the endosteal region (arrows).
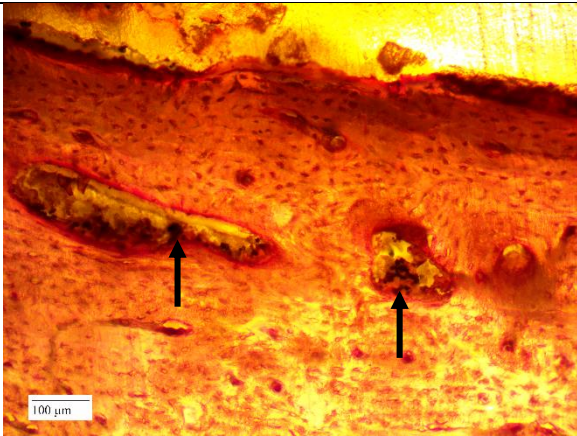
Table 14: Thin section of cortical bone of Group A, Week 2 from mid-diaphysis of a pig humerus. Stained with H and E. Refer to three inset images for specific diagenetic changes in periosteal, middle cortical, and endosteal regions.

1: Plexiform bone tissue in the endosteal region. Note the slight presence of bacteria (arrow).

2: Plexiform bone tissue in the middle cortical region, creating horizontal lines. Haversian canals indicated by arrows.
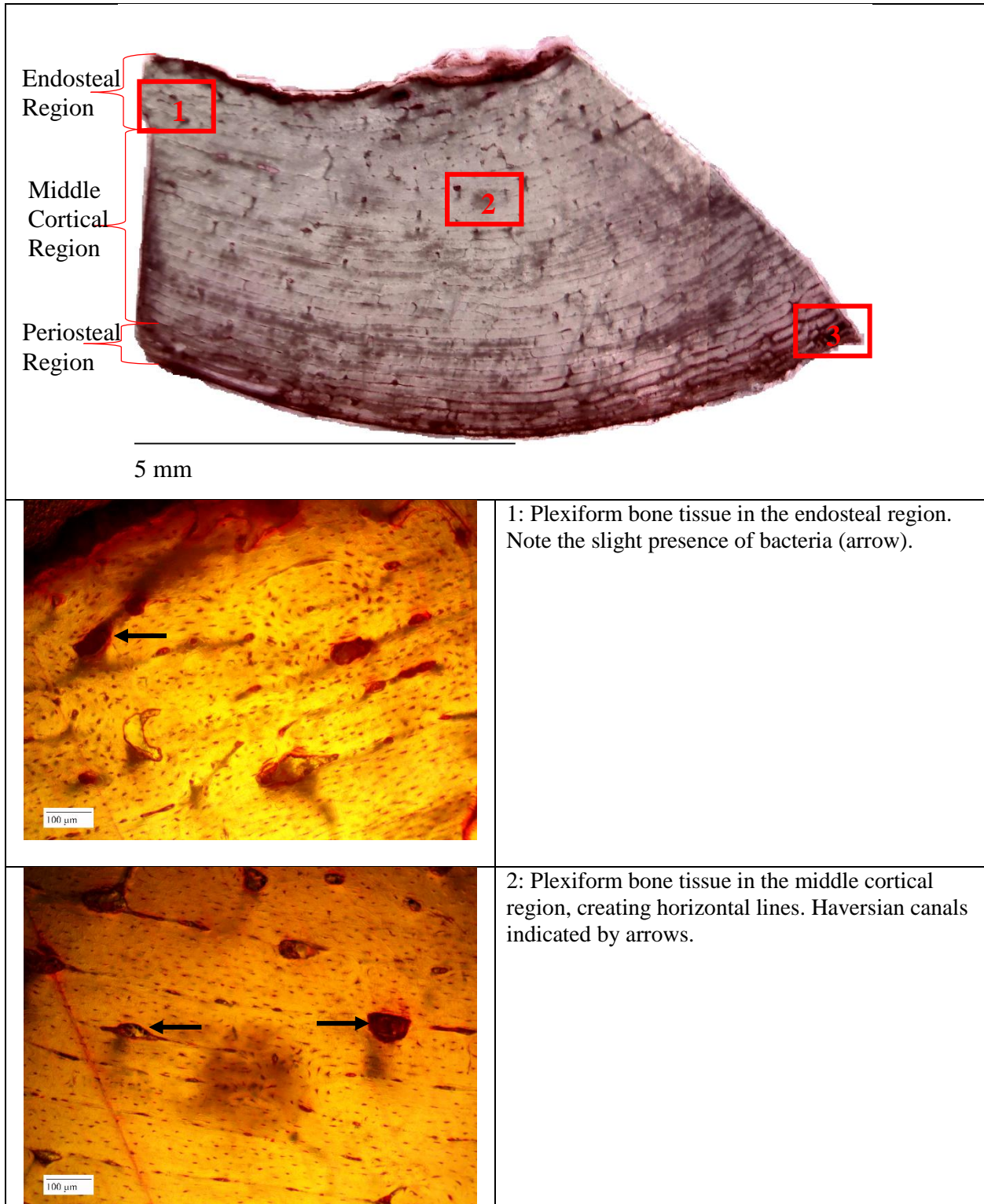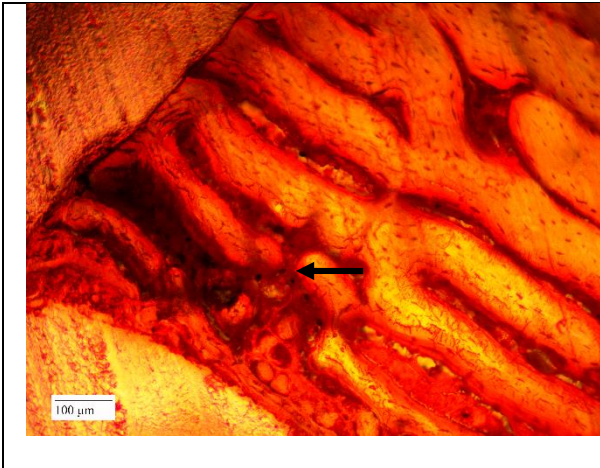
3: Plexiform bone tissue in the periosteal region. Note the slight presence of bacteria (arrow).

Table 15: Thin section of cortical bone of Group A, Week 4 from mid-diaphysis of a pig humerus. Stained with PAS. Refer to five inset images for specific diagenetic changes in periosteal, middle cortical, and endosteal regions.

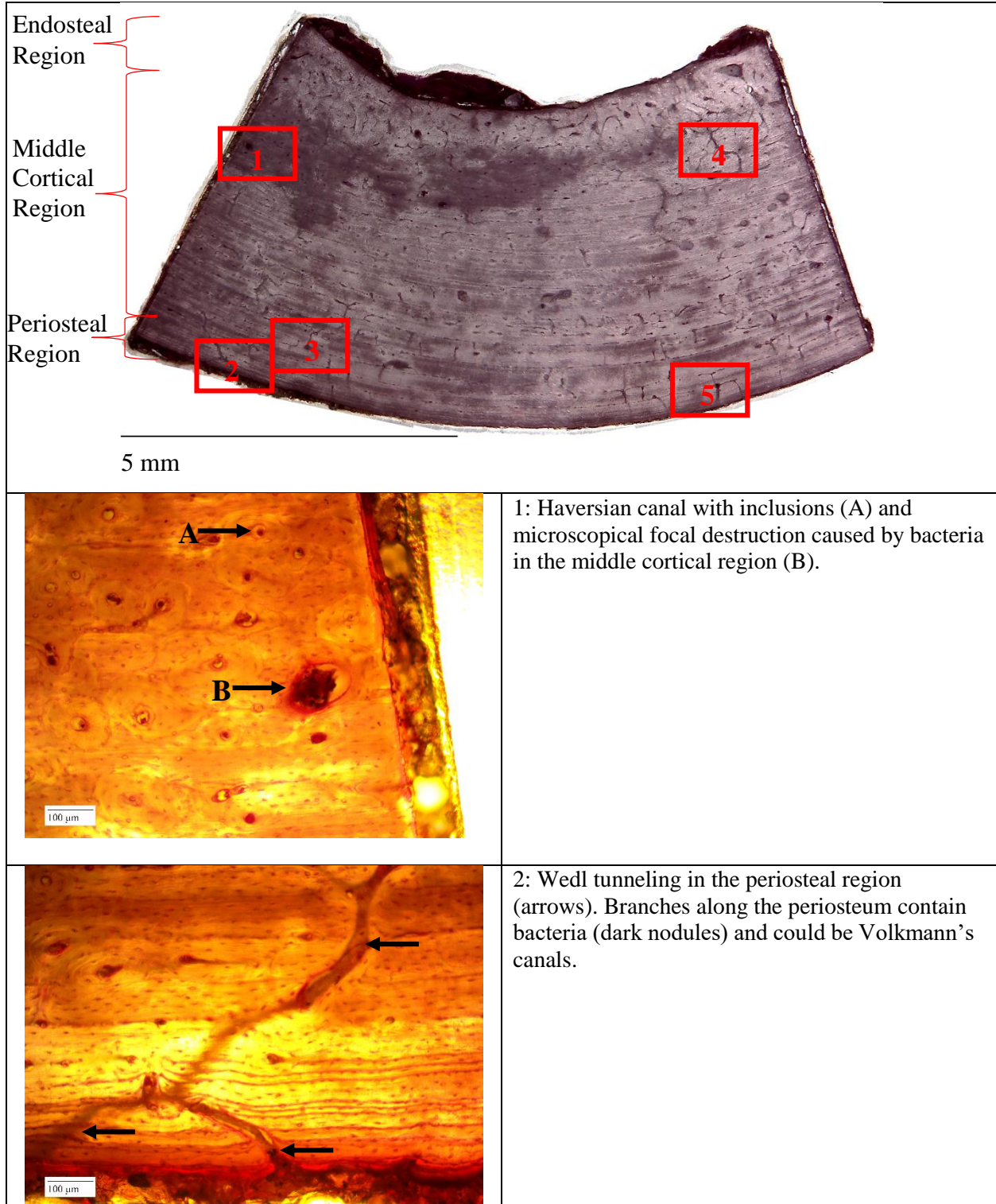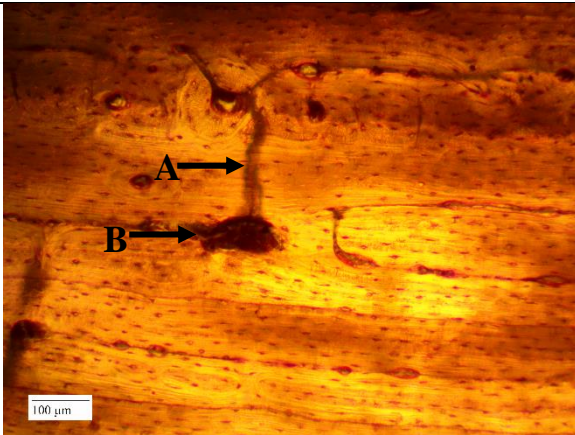|	
	1: Haversian canal with inclusions, darkened area within the canal (A) Haversian canal without inclusions (B) and osteoclastic activity (C). Note the scalloped edges of the area of osteoclastic activity.
	2: Probable microscopical focal destruction caused by bacteria in the middle cortical region (arrow). Note the presence of bacteria within the structure.
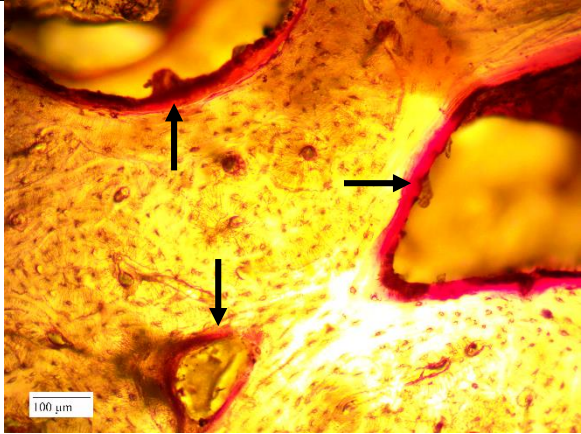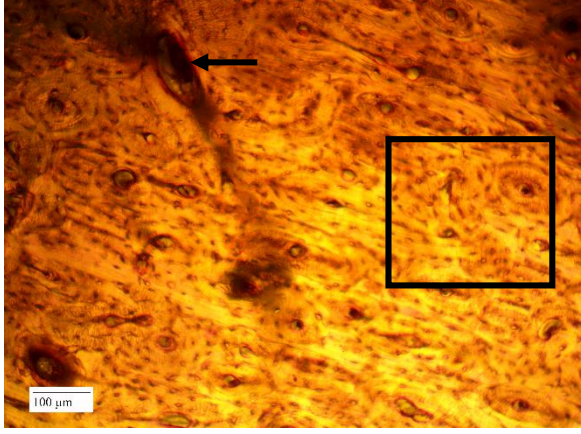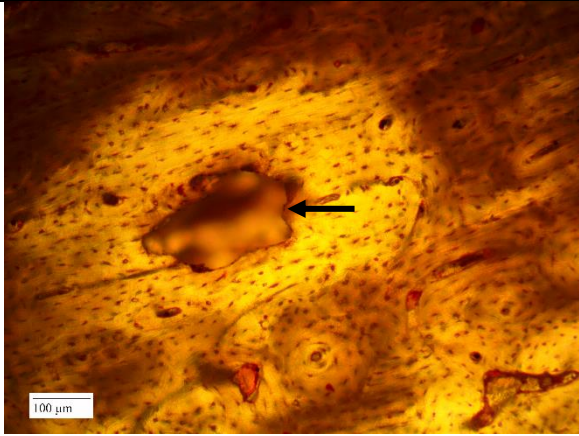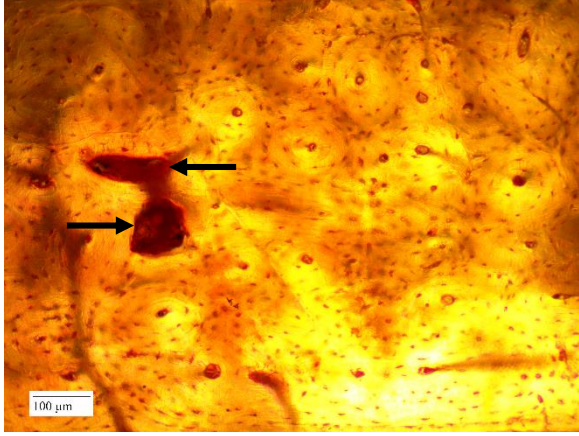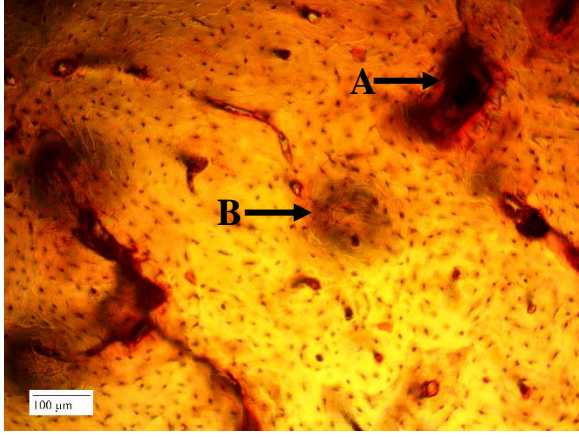
	3: Trabecularized cortical bone demonstrating the transition from cortical bone to trabecular bone (arrows).
	4: Microscopical focal destruction caused by bacteria in the periosteal region (arrow) and regular osteons (square).
	5: Microscopical focal destruction caused by bacteria in the middle cortical region (arrow) and regular osteons (square).

Table 16: Thin section of cortical bone of Group A, Week 4 from mid-diaphysis of a pig humerus. Stained with H and E. Refer to five inset images for specific diagenetic changes in periosteal and middle cortical regions.


1: Area of regular osteons. Note the presence of Volkmann's canals connecting Haversian canals (A). Additionaly, the resence of Haversian canals with inclusions (B)
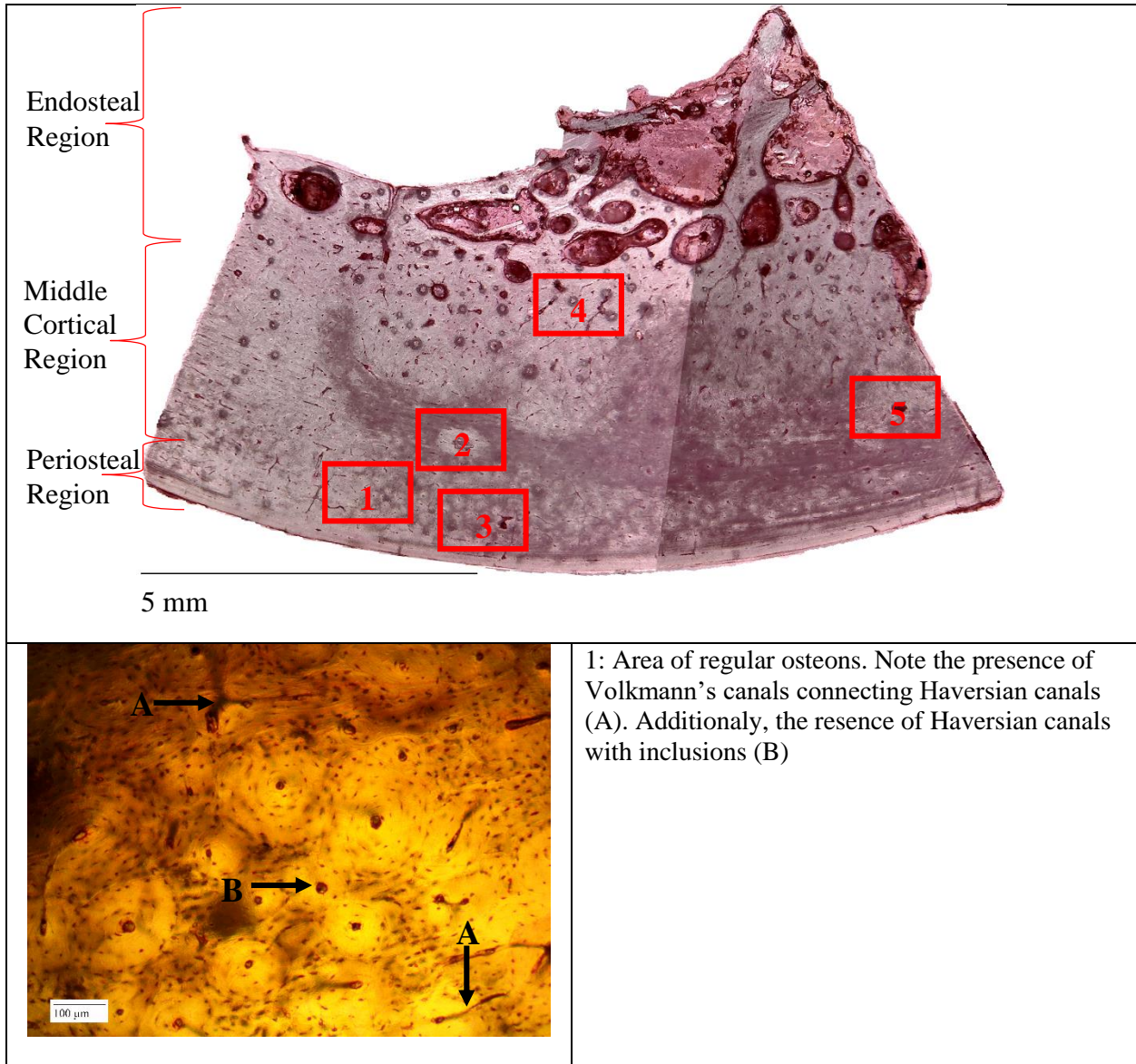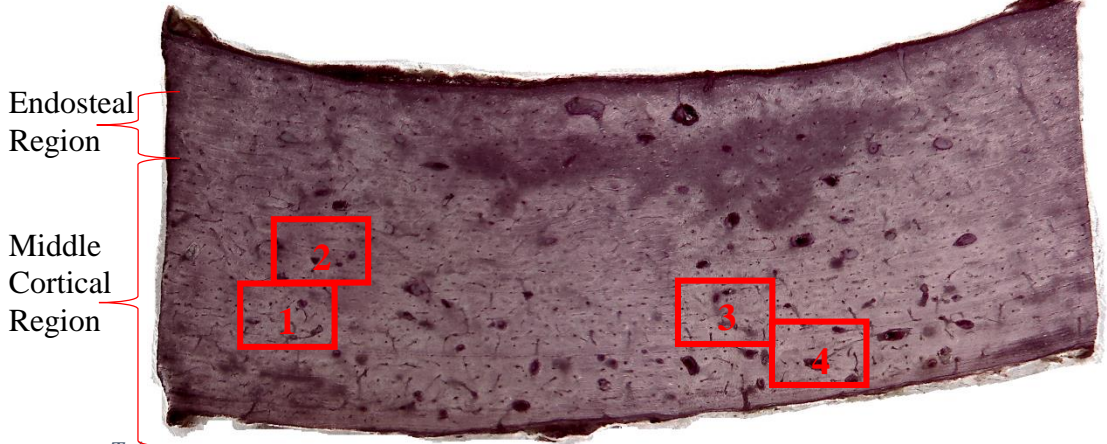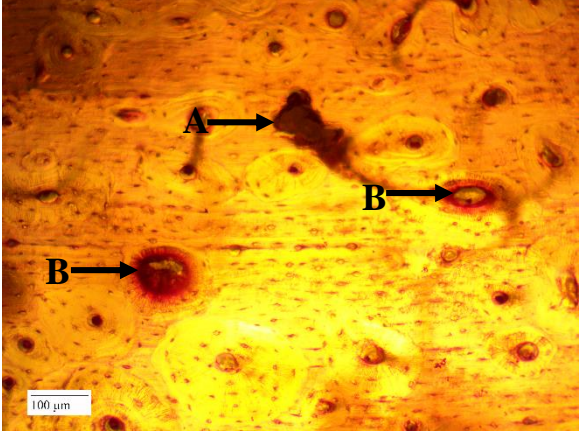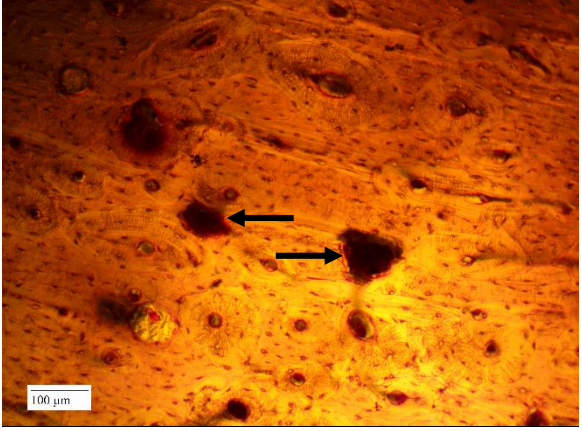
	2: Osteoclastic activity in the middle cortical region. Note the scalloped edges (arrow).
	3: Microscopical focal destruction caused by bacteria in the middle cortical region (arrows).
	4: Probable microscopical focal destruction caused by bacteria, but presence in endosteal region excludes structure from analysis (A). Note the bubble in the mounting medium (B).

5: Microscopical focal destruction caused by bacteria in the middle cortical region (A) and the presence of bacteria (B).

Table 17: Thin section of cortical bone of Group A, Week 6 from mid-diaphysis of a pig femur. Stained with PAS. Refer to four inset images for specific diagenetic changes in periosteal and middle cortical regions.

Endosteal Region

Middle Cortical Region

Periosteal Region

5 mm

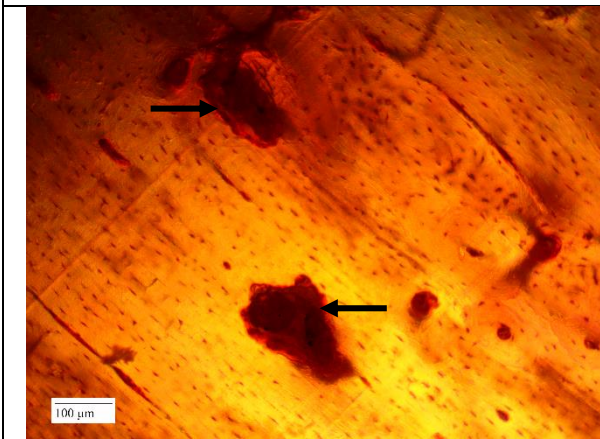|	
	1: Microscopical focal destruction caused by bacteria in the middle cortical region (A) and possible microscopical focal destruction (B).
	2: Microscopical focal destruction caused by bacteria in the middle cortical region (arrows).
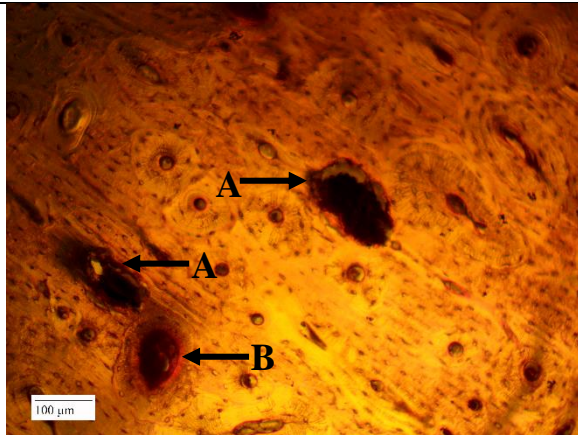
3: Microscopical focal destruction caused by bacteria in the middle cortical region (A) and a large osteon with inclusions (B). Note the presence of concentric lamellae around the Haversian canal labelled B, which distinguishes the Haversian canal from microscopical focal destruction.
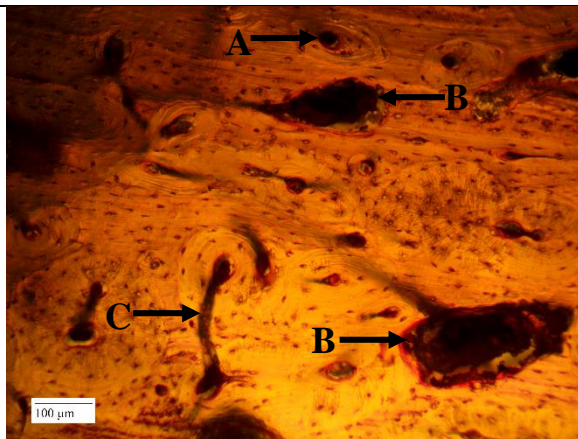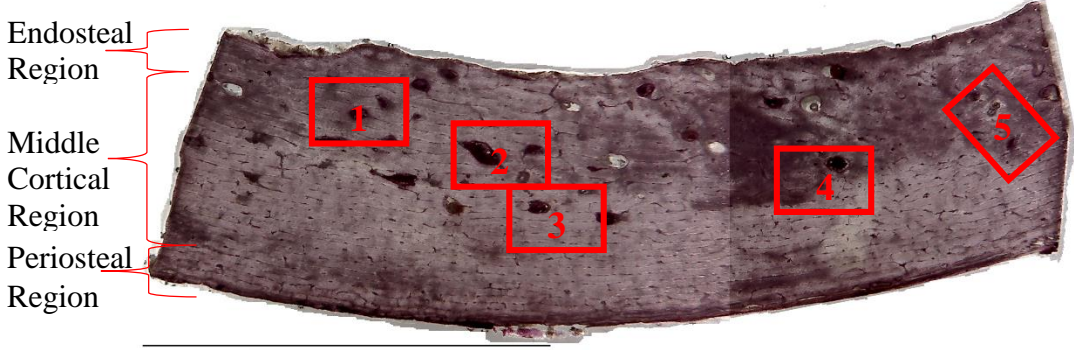

4: A regular osteon (A), microscopical focal destruction caused by bacteria in the middle cortical region (B), and a Volkmann's canal connecting two Haversian canals (C).

Table 18: Thin section of cortical bone of Group A, Week 6 from mid-diaphysis of a pig femur. Stained with H and E. Refer to five inset images for specific diagenetic changes in periosteal and middle cortical regions.

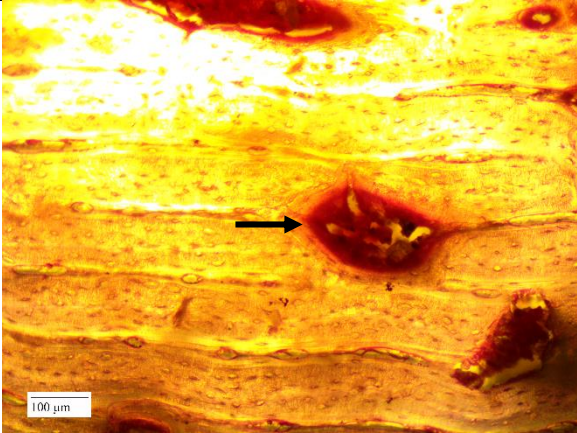|	
	1: Microscopical focal destruction caused by bacteria in the periosteal region (arrows).
	2: Microscopical focal destruction caused by bacteria in the middle cortical region (arrow).
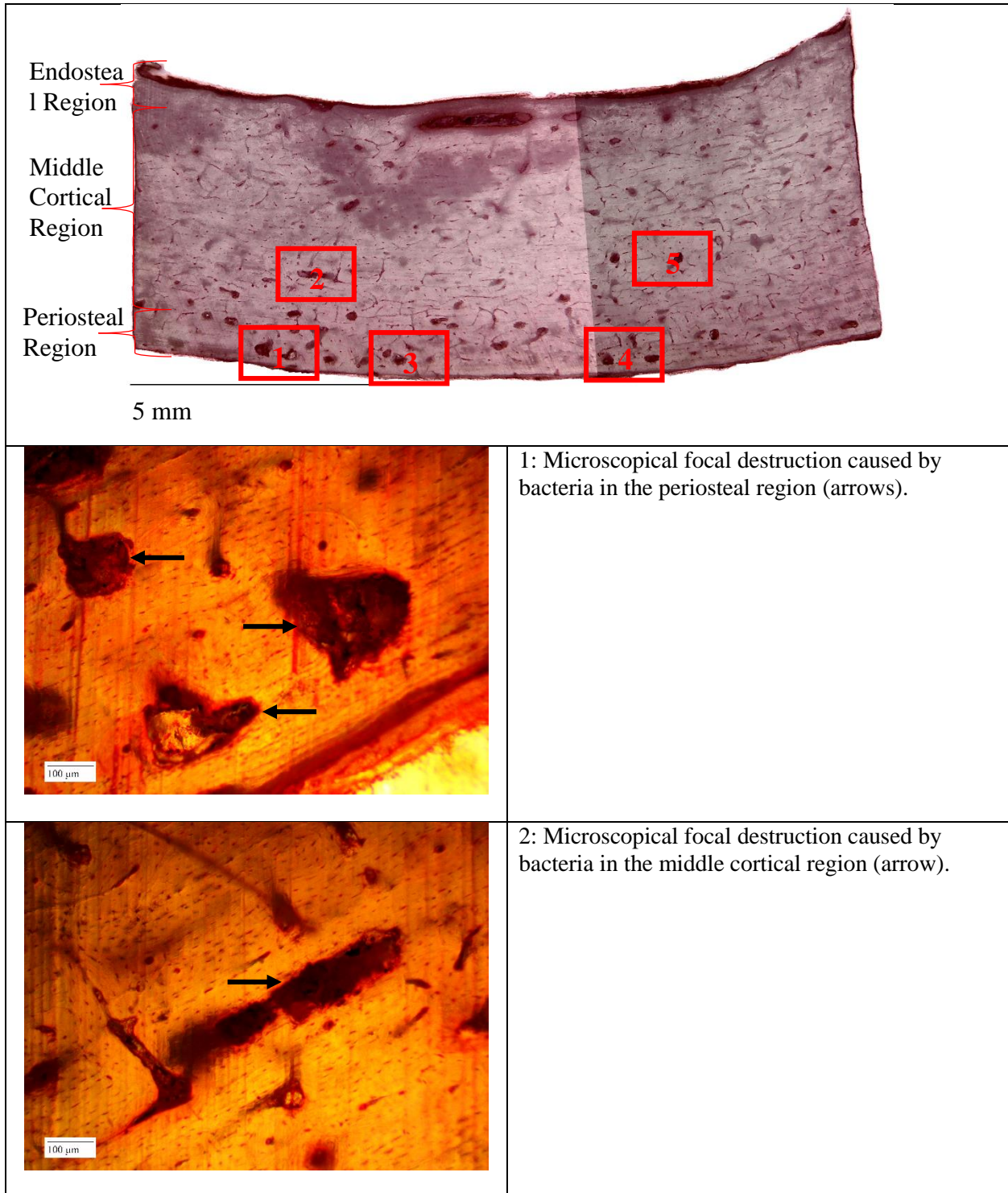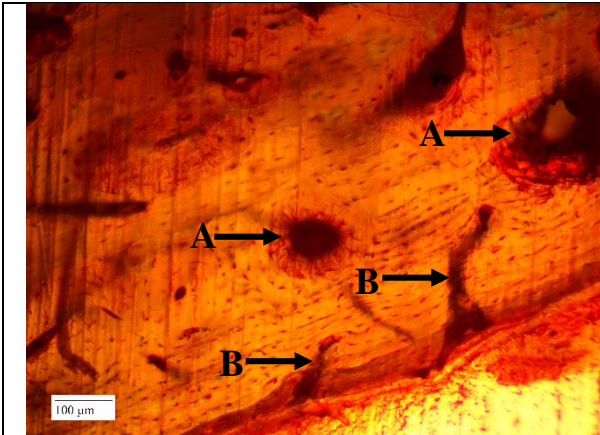
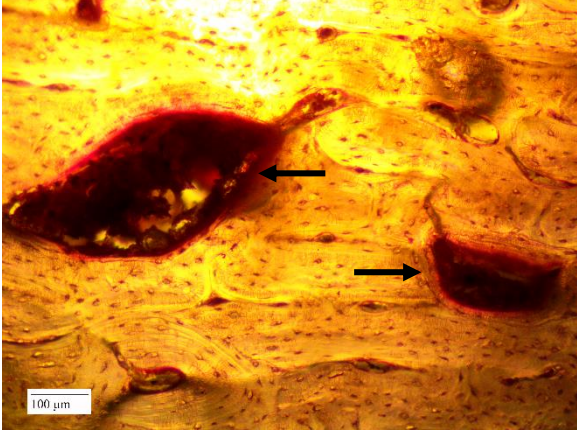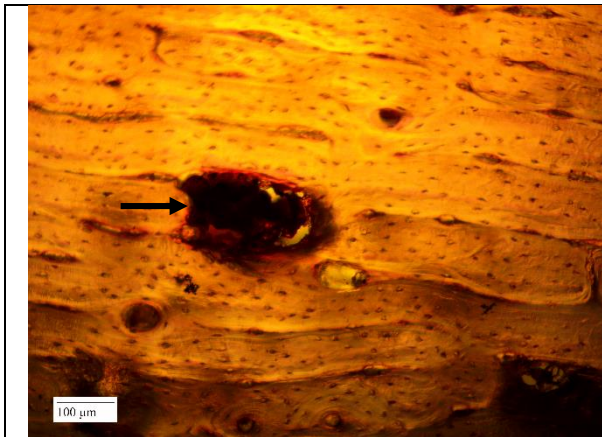3: Microscopical focal destruction caused by bacteria in the periosteal region (A) and Wedl tunneling (B).
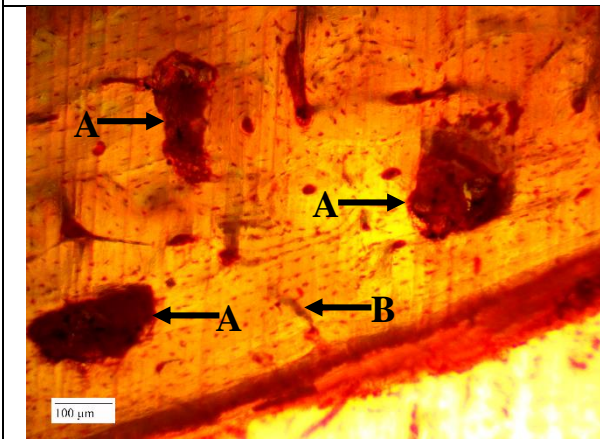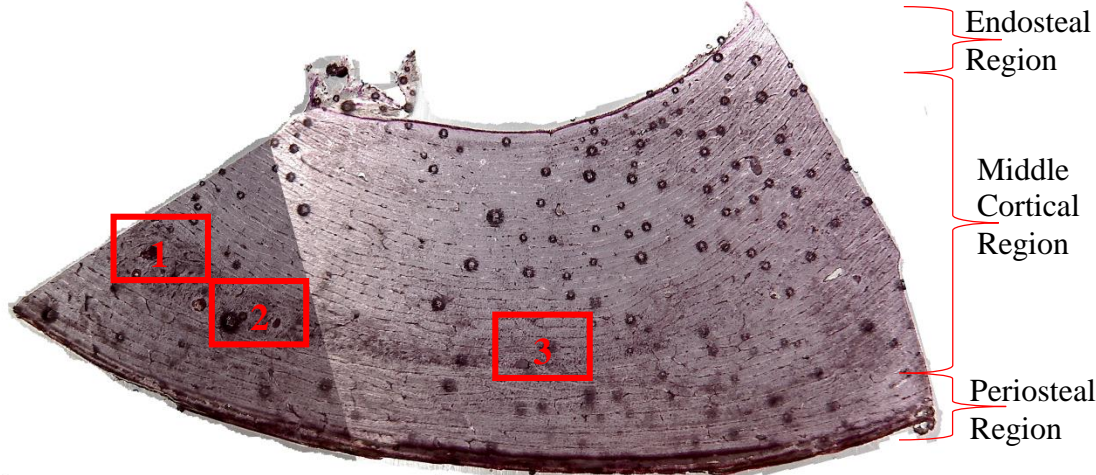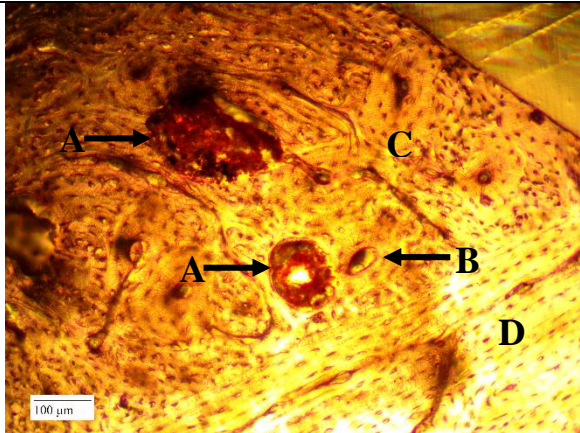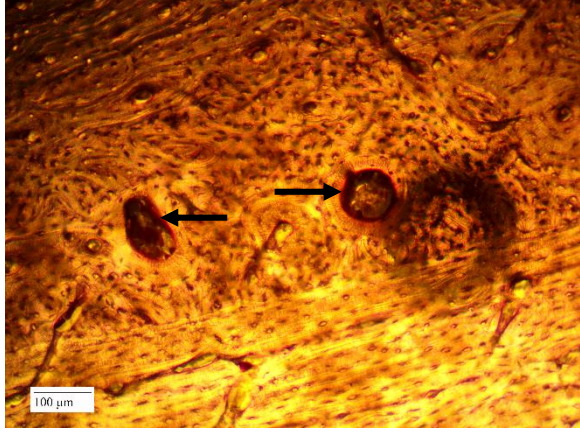
4: Microscopical focal destruction caused by bacteria in the periosteal region (A). Note the large presence of bacteria (dark nodules). Also, possible Wedl tunneling from the periosteum into the bone tissue (B)

5: Microscopical focal destruction caused by bacteria in the middle cortical region (arrow).

Table 19: Thin section of cortical bone of Group A, Week 8 from mid-diaphysis of a pig humerus. Stained with PAS. Refer to three inset images for specific diagenetic changes in periosteal and middle cortical regions.
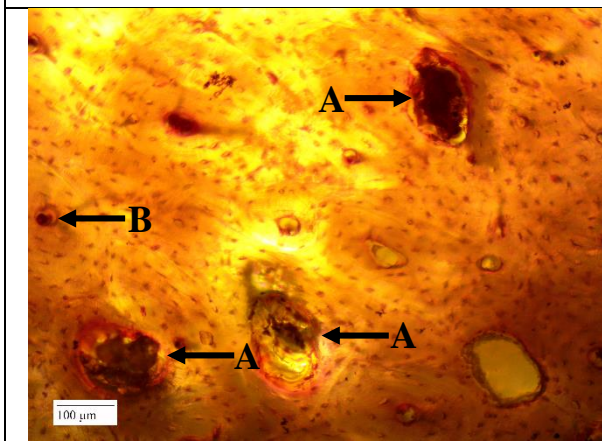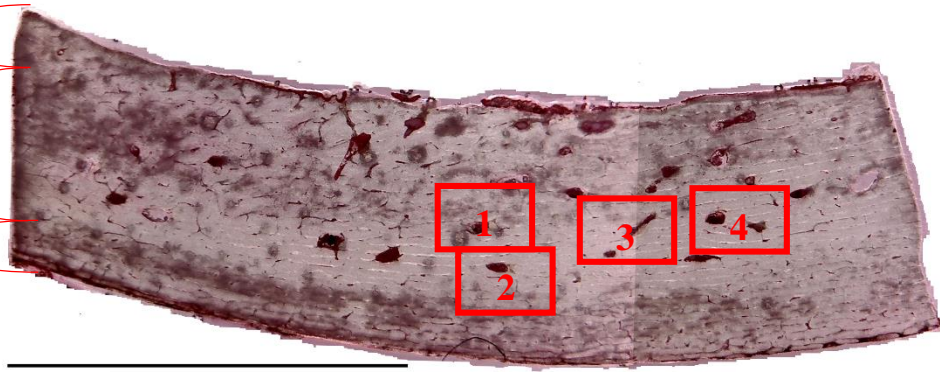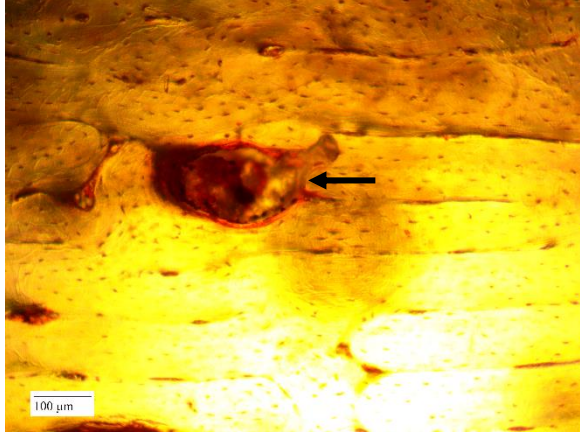

	1: Microscopical focal destruction caused by bacteria in the middle cortical region (A) and a Haversian canal with inclusions (B). Note the layers of cortical bone (C) and plexiform bone (D).
	2: Probable microscopical focal destruction caused by bacteria in the middle cortical region (arrows). Possible concentric lamellae, however, presence is not distinct enough to classify as a Haversian canal.
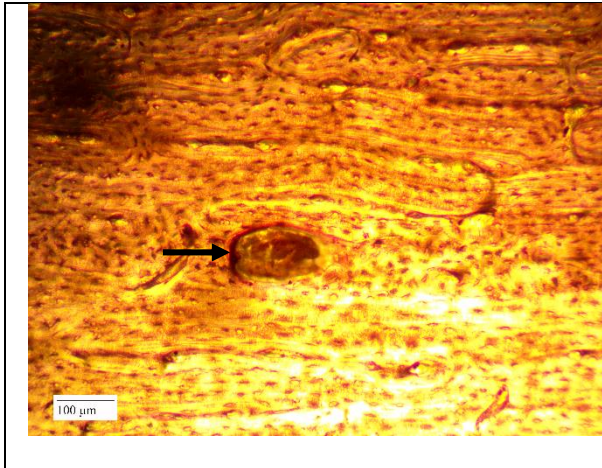
3: Microscopical focal destruction caused by bacteria in the middle cortical region (arrow).

Table 20: Thin section of cortical bone of Group A, Week 8 from mid-diaphysis of a pig humerus. Stained with H and E. Refer to four inset images for specific diagenetic changes in periosteal and middle cortical regions.
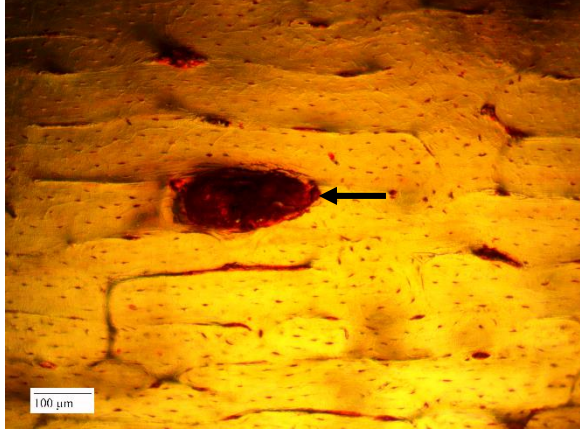

|	
	1: Microscopical focal destruction caused by bacteria in the middle cortical region (arrow). Note the presence of bacteria (dark nodules).
	2: Likely a Volkmann's canal in the plexiform bone tissue (A) and microscopical focal destruction caused by bacteria in the middle cortical region in the cortical bone (B).
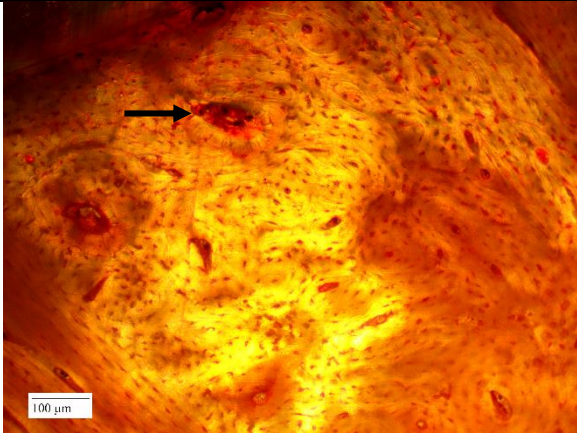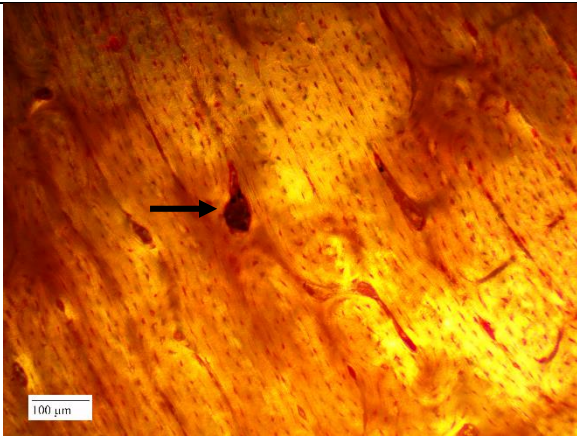
	3: Microscopical focal destruction caused by bacteria in the middle cortical region (arrow). Note the presence of bacteria (dark nodules).
	4: Microscopical focal destruction caused by bacteria in the middle cortical region in plexiform bone tissue (arrow). Note the large presence of bacteria (dark nodules).

Table 21: Thin section of cortical bone of Group A, Week 10 from mid-diaphysis of a pig humerus. Stained with PAS. Refer to five inset images for specific diagenetic changes in periosteal and middle cortical regions.

Endosteal Region

Middle Cortical Region

Periosteal Region

5 mm

1: Haversian canal with inclusions (A) and microscopical focal destruction caused by bacteria in the middle cortical region (B).

2: Wedl tunneling in the periosteal region (arrows). Branches along the periosteum contain bacteria (dark nodules) and could be Volkmann's canals.

3: Probable Volkmann's canal (A) and microscopical focal destruction caused by bacteria in the middle cortical region (B).
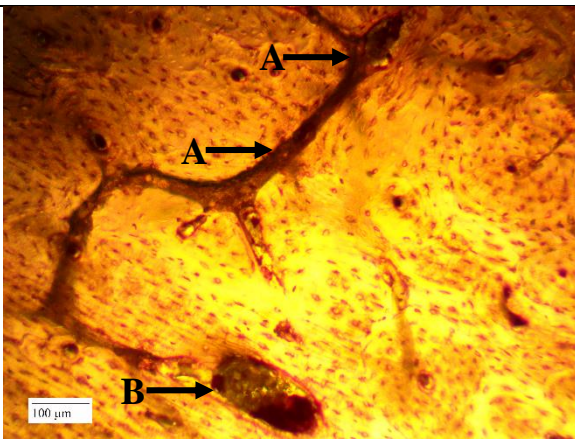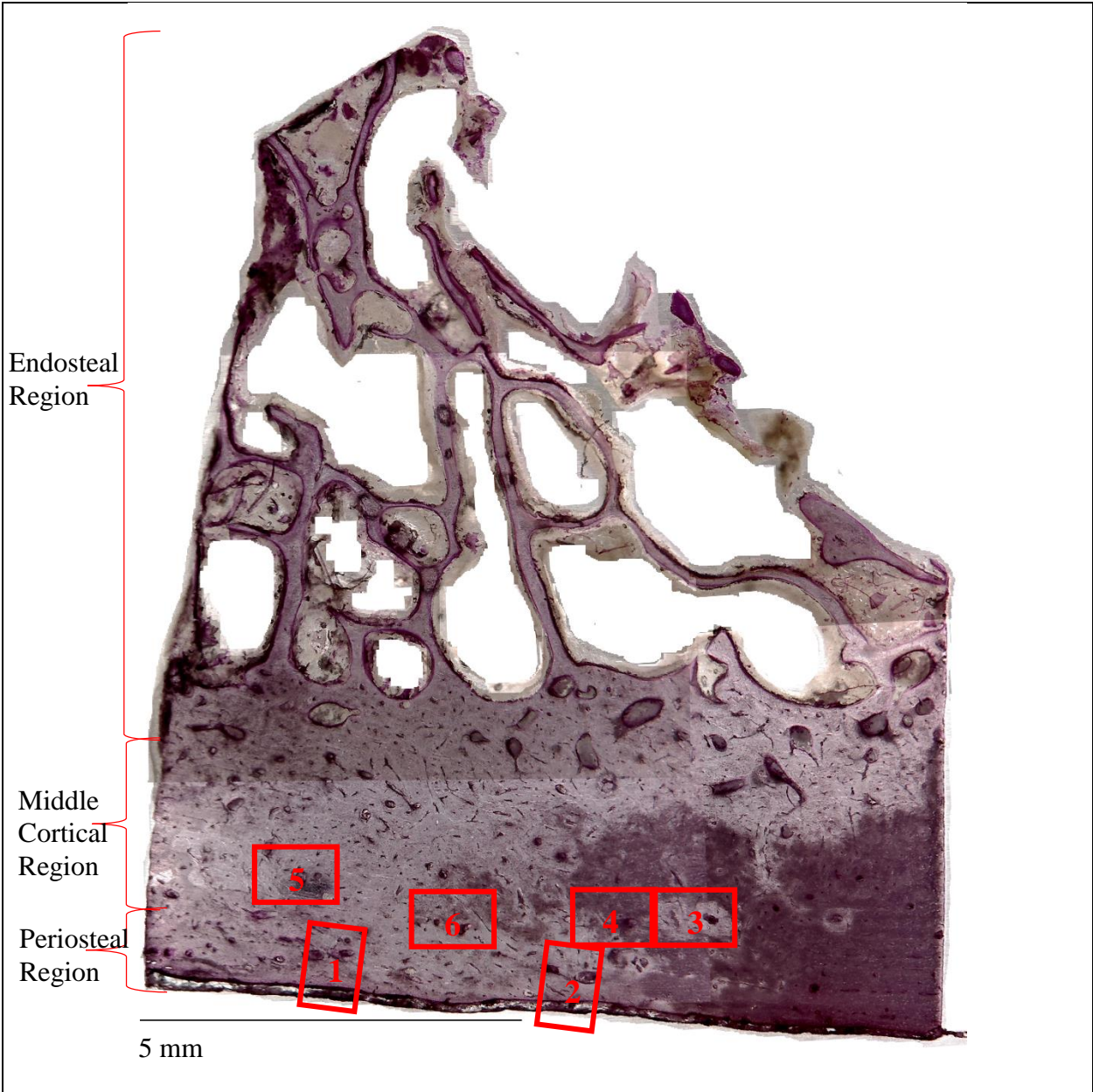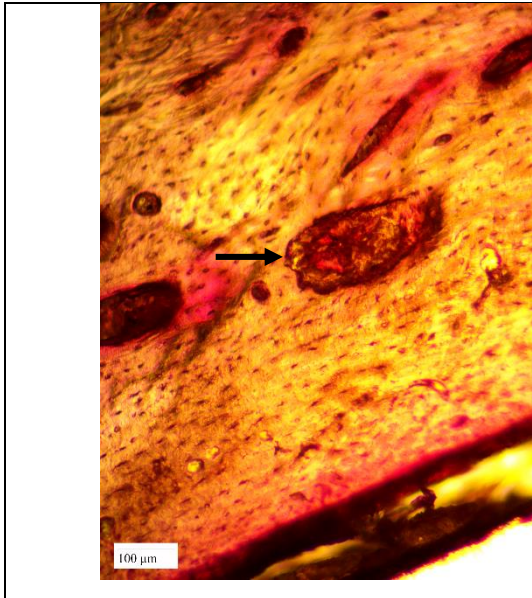

4: Possible Wedl tunneling (A) and microscopical focal destruction caused by bacteria in the middle cortical region (B).
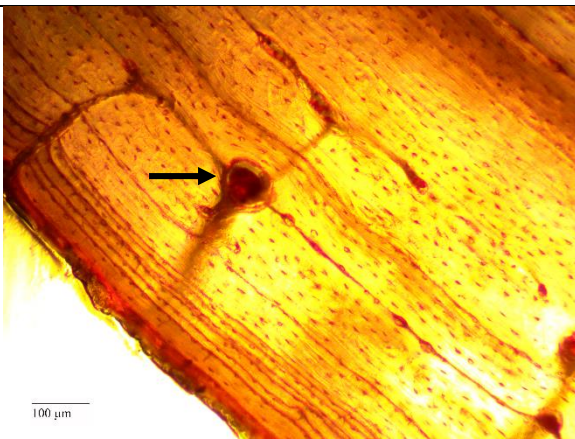
5: Microscopical focal destruction caused by bacteria in the periosteal region (arrow).

Table 22: Thin section of cortical bone of Group A, Week 10 from mid-diaphysis of a pig humerus. Stained with H and E. Refer to six inset images for specific diagenetic changes in periosteal and middle cortical regions.
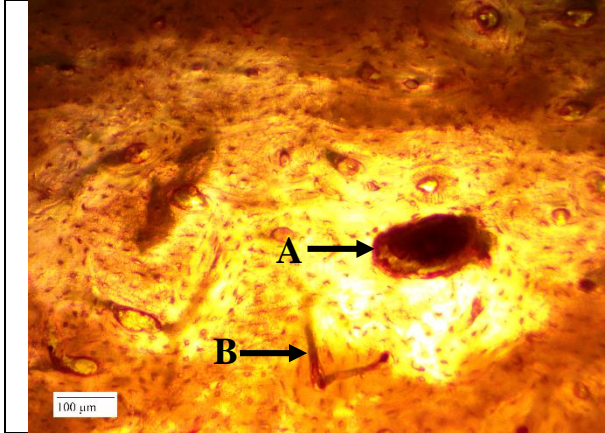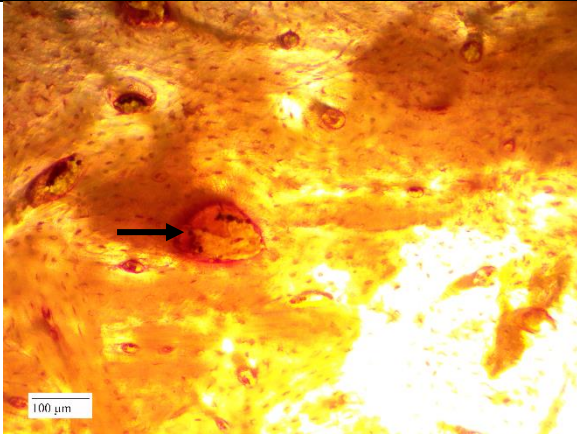

	1: Microscopical focal destruction caused by bacteria in the middle cortical region (arrows).
	2: Microscopical focal destruction caused by bacteria in the periosteal region (arrow).
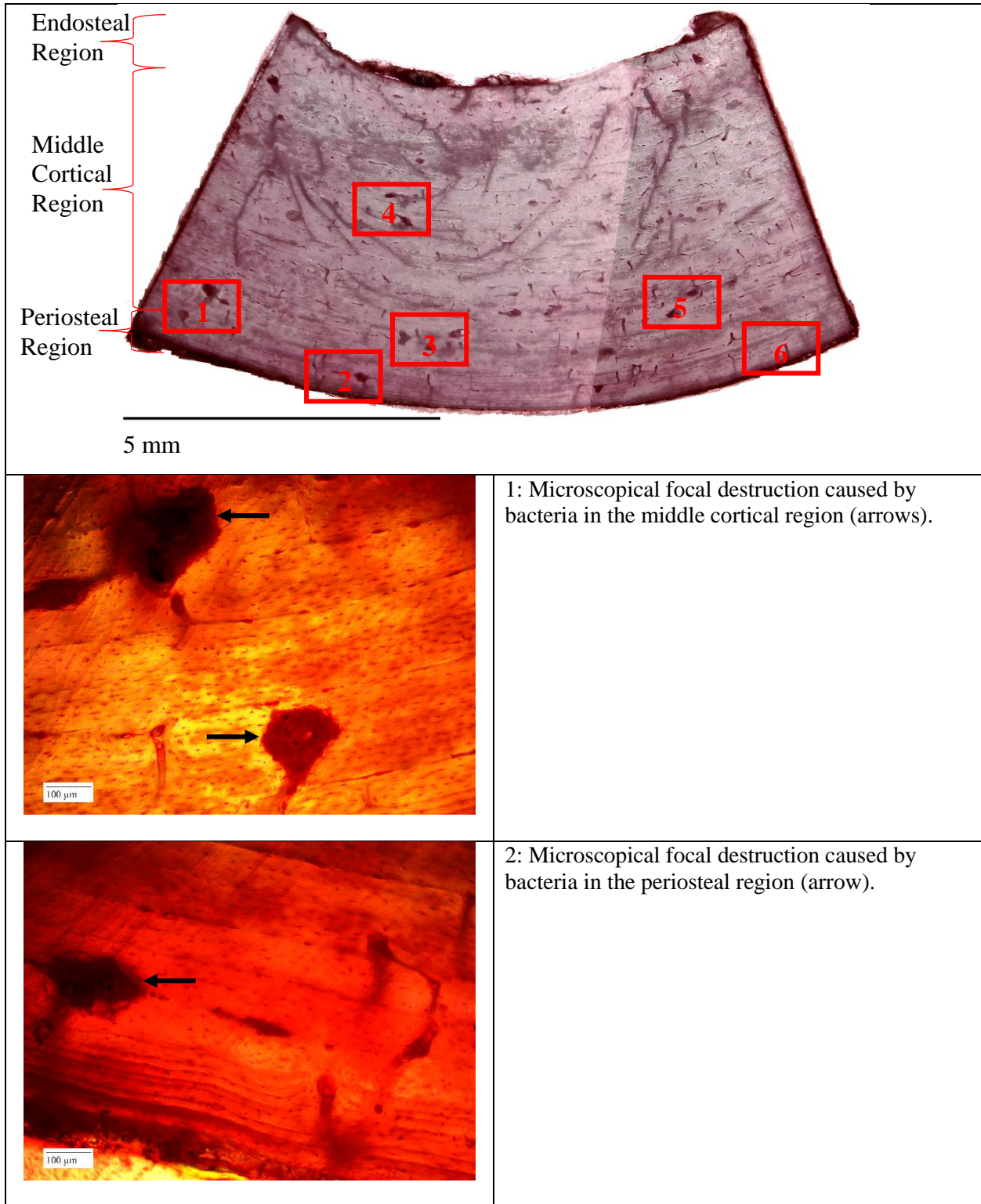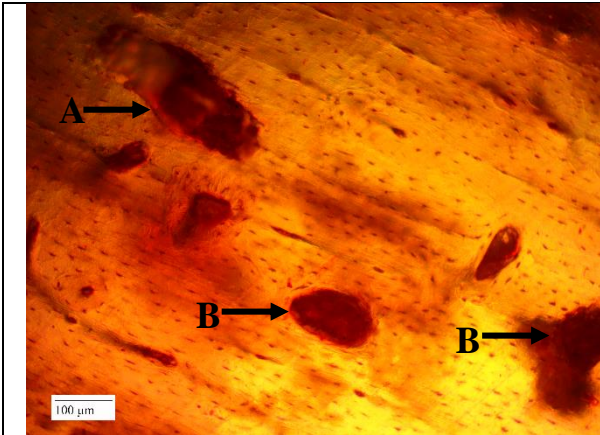
3: Probable osteoclastic activity (A) and microscopical focal destruction caused by bacteria in the middle cortical region (B).
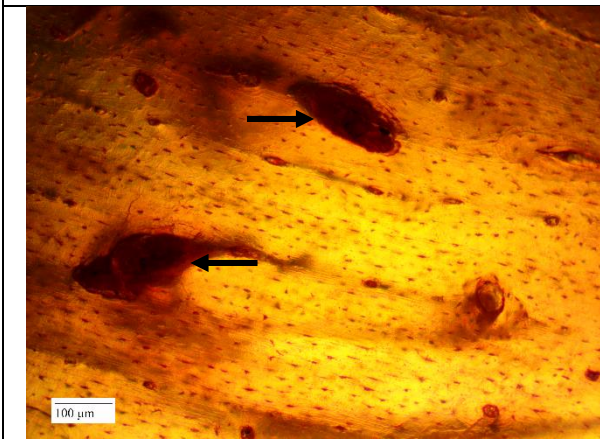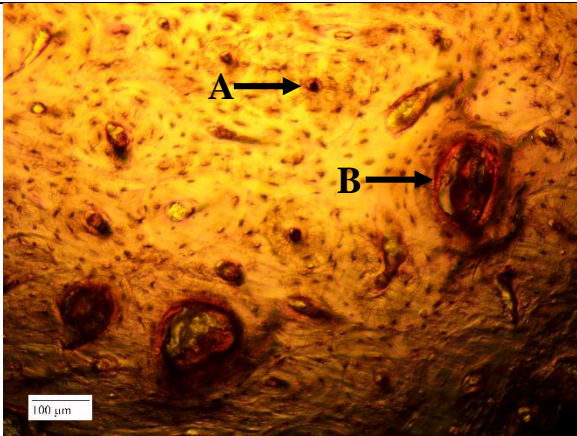

4: Microscopical focal destruction caused by bacteria in the middle cortical region (arrow).

5: Microscopical focal destruction caused by bacteria in the middle cortical region (arrows).
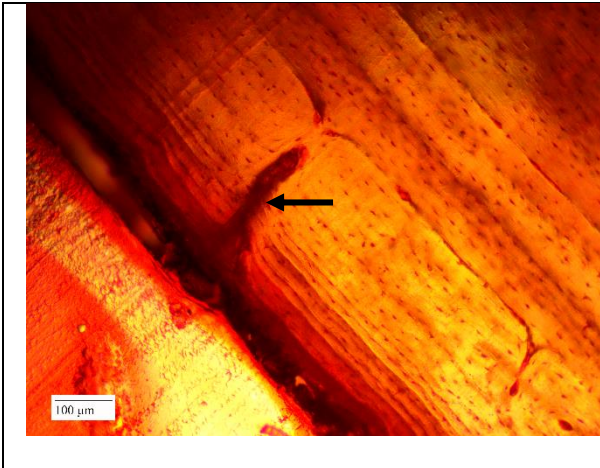
6: Wedl tunneling in the periosteal region (arrow).

Table 23: Thin section of cortical bone of Group A, Week 12 from mid-diaphysis of a pig femur. Stained with PAS. Refer to five inset images for specific diagenetic changes in periosteal and middle cortical regions.

1: Microscopical focal destruction caused by bacteria in the middle cortical region (arrow). Note the horizontal lines created by plexiform bone structure.

2: Microscopical focal destruction caused by bacteria in the middle cortical region (arrows).

3: Microscopical focal destruction caused by bacteria in the middle cortical region (arrow).
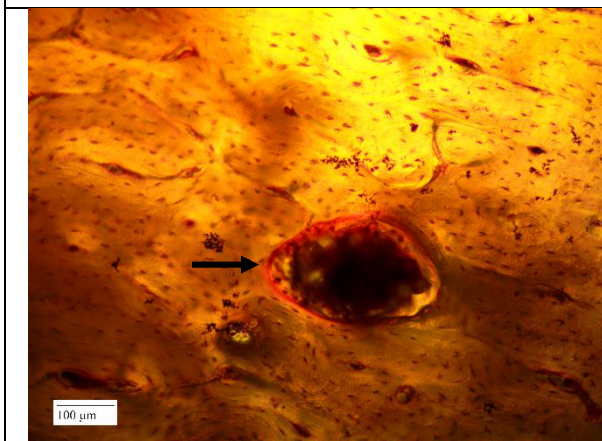
4: Microscopical focal destruction caused by bacteria in the middle cortical region (arrow). Note the large presence of bacteria (dark nodules).

5: Microscopical focal destruction caused by bacteria in the middle cortical region (A) and a Haversian canal with inclusions.
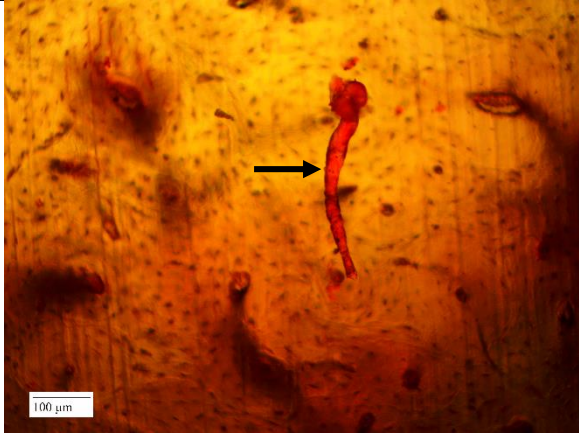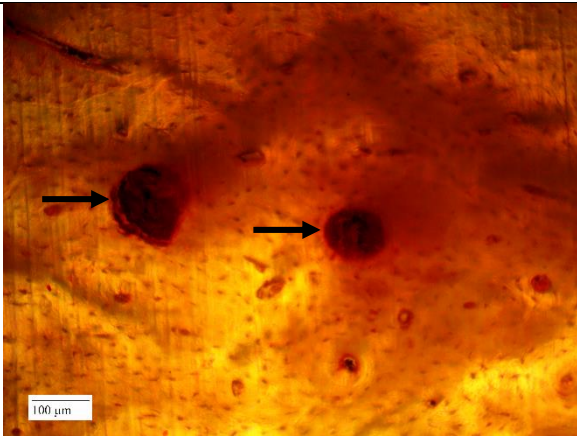
Table 24: Thin section of cortical bone of Group A, Week 12 from mid-diaphysis of a pig femur. Stained with H and E. Refer to five inset images for specific diagenetic changes in periosteal and middle cortical regions.

5 mm

	1: Microscopical focal destruction caused by bacteria in the middle cortical region (arrow). Note the presence of bacteria (dark nodules).
	2: Microscopical focal destruction caused by bacteria in the middle cortical region (arrow). Note the horizontal lines created by the plexiform bone tissue.

3: Microscopical focal destruction caused by bacteria in the middle cortical region (arrows).
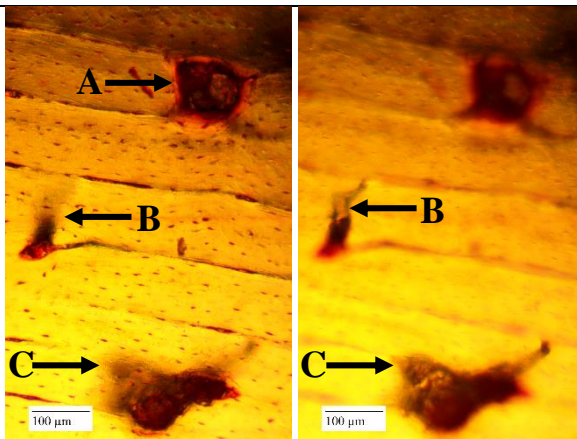
4: Microscopical focal destruction caused by bacteria in the middle cortical region (A) and tunneling caused by fungal diagenesis (B and C).

Table 25: Thin section of cortical bone of Group A, Week 14 from mid-diaphysis of a pig humerus. Stained with PAS. Refer to six inset images for specific diagenetic changes in periosteal and middle cortical regions.

1: Microscopical focal destruction caused by bacteria along the periosteal margin (arrow).
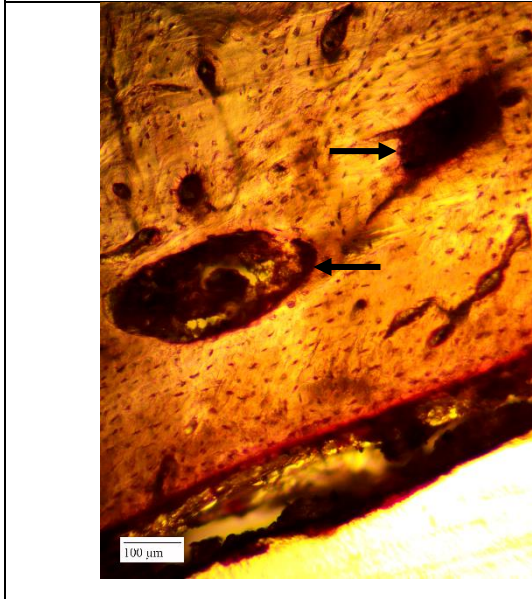
2: Microscopical focal destruction caused by bacteria along the periosteal margin (arrows).

3: Microscopical focal destruction caused by bacteria in the middle cortical region (A) and probable Volkmann's canal (B).

4: Bacteria (small dark nodules) within an area of microscopical focal destruction caused by bacteria in the middle cortical region.
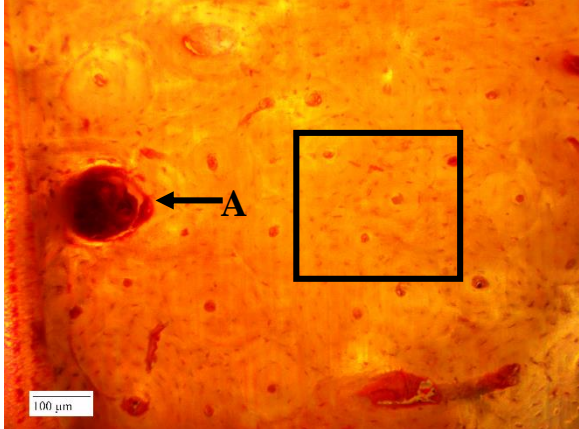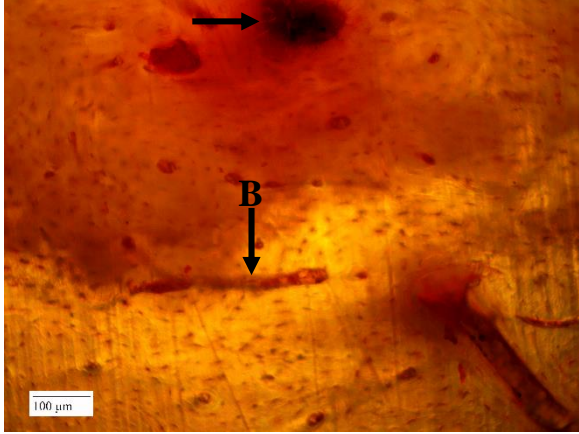
5: Regular Haversian canal with inclusions (A) and microscopical focal destruction caused by bacteria in the middle cortical region (B).
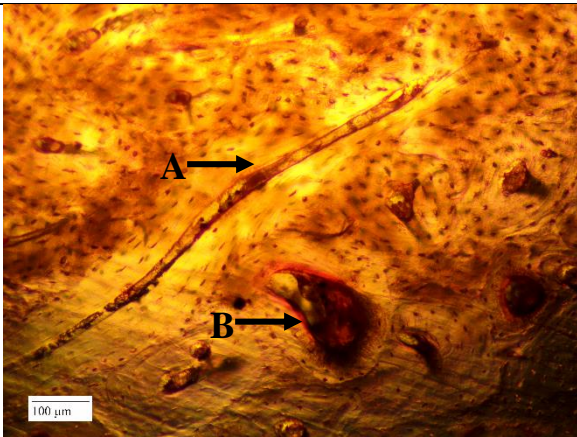
6: Wedl tunneling caused by fungal diagenesis (A) and microscopical focal destruction caused by bacteria in the middle cortical region (B).
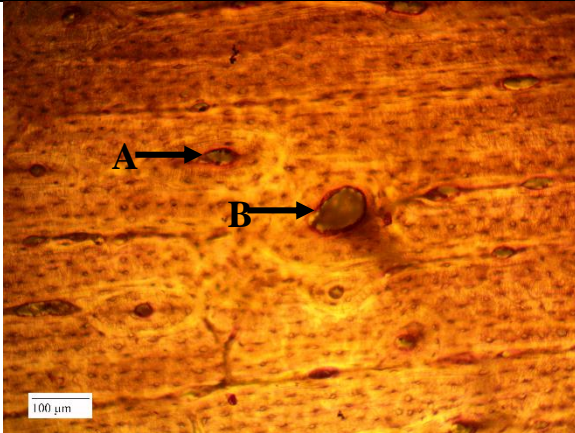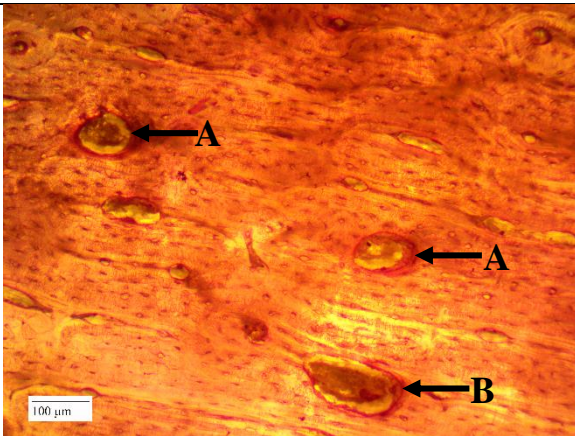
Table 26: Thin section of cortical bone of Group A, Week 14 from mid-diaphysis of a pig humerus. Stained with H and E. Refer to five inset images for specific diagenetic changes in periosteal and middle cortical regions.
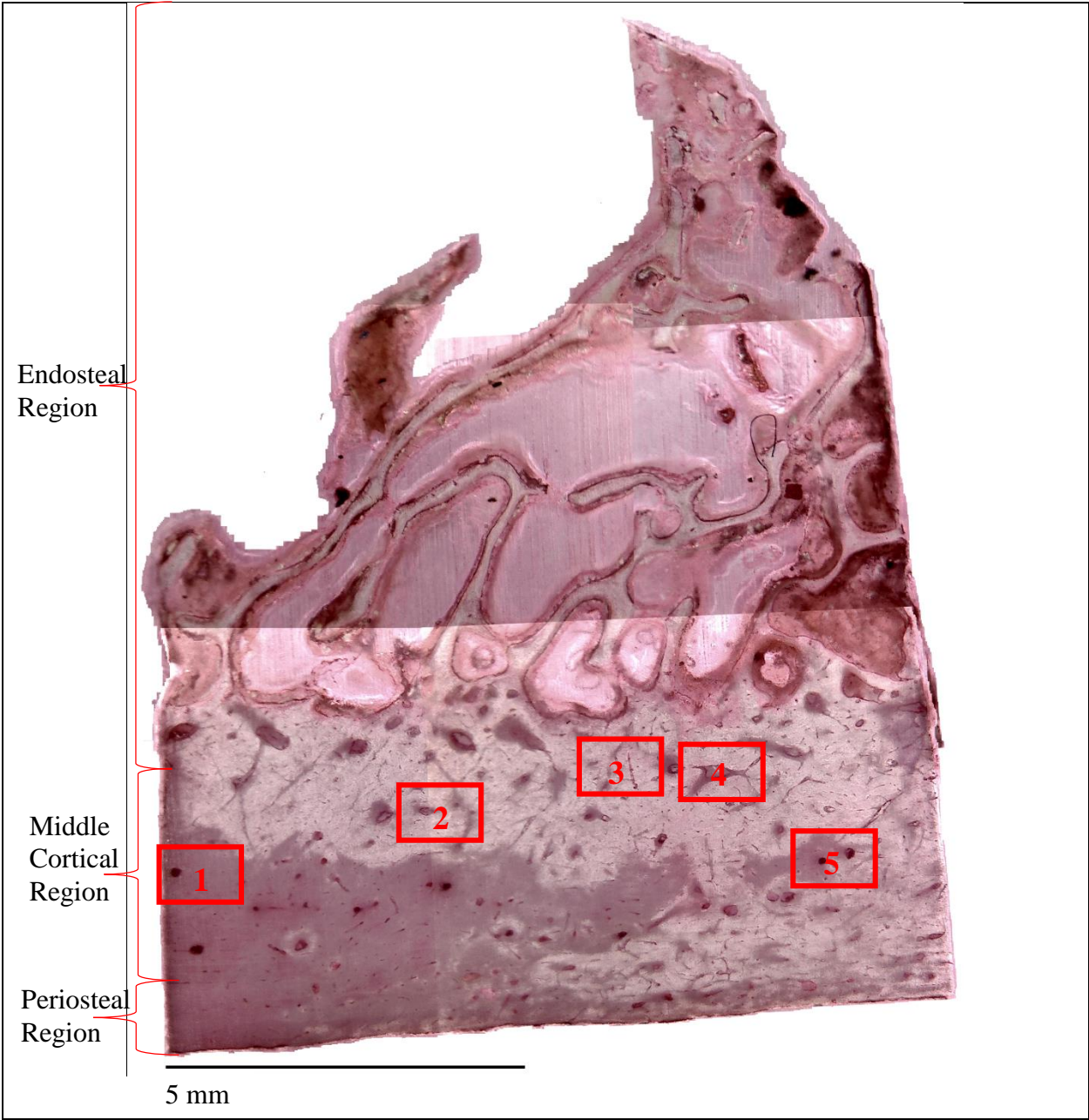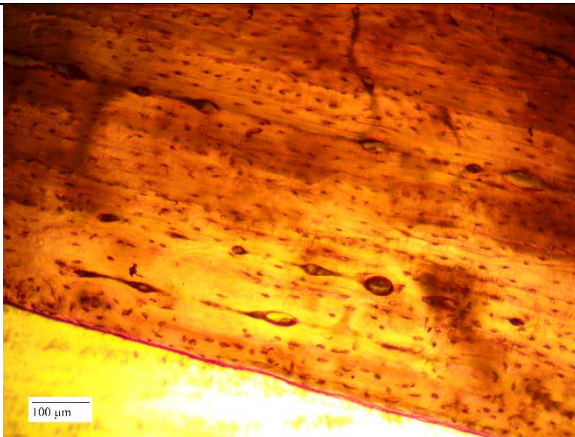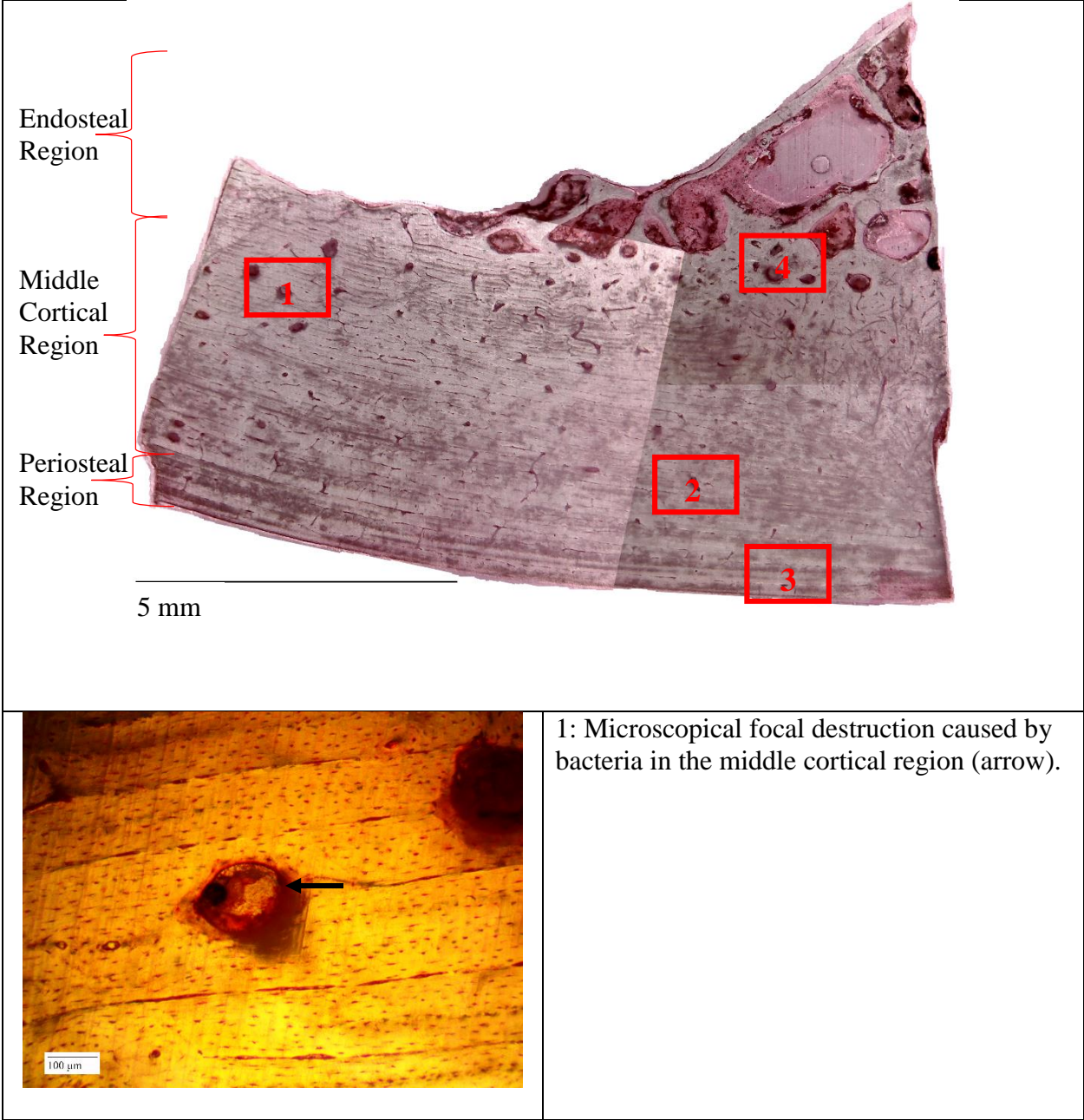
	1: Microscopical focal destruction caused by bacteria in the middle cortical region (arrow) and regular osteons (square).
	2: Microscopical focal destruction caused by bacteria (A) and possible tunneling (B) in the middle cortical region.
	3: Possible tunneling caused by fungal diagenesis in the endosteal region (arrow).
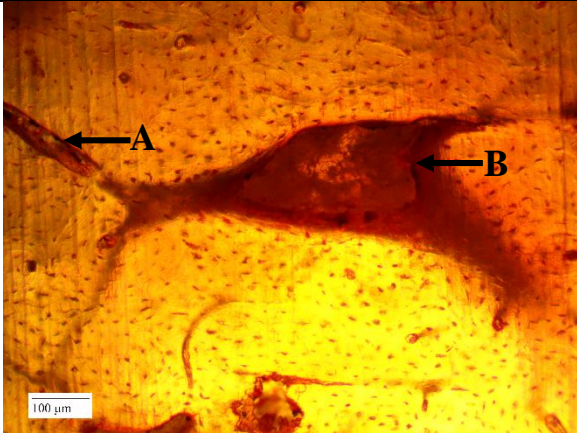
4: Possible tunneling caused by fungal diagenesis (A) and probable microscopical focal destruction caused by bacteria in the middle cortical region (B).

5: Microscopical focal destruction caused by bacteria in the middle cortical region (arrows).

APPENDIX C: GROUP B ANALYSIS TABLES

Table 27: Thin section of cortical bone of Group B, Week 2 from mid-diaphysis of a pig humerus. Stained with PAS. Refer to four inset images for specific diagenetic changes in periosteal and middle cortical regions.
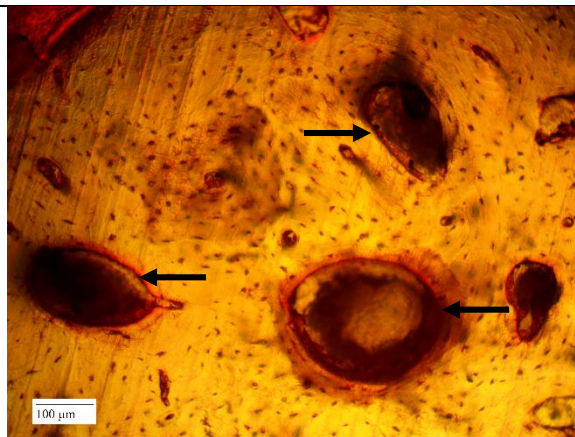

Endosteal Region

Middle Cortical Region

Periosteal Region

5 mm

1: Probable microscopical focal destruction caused by bacteria in the periosteal region (arrow).

100 μm
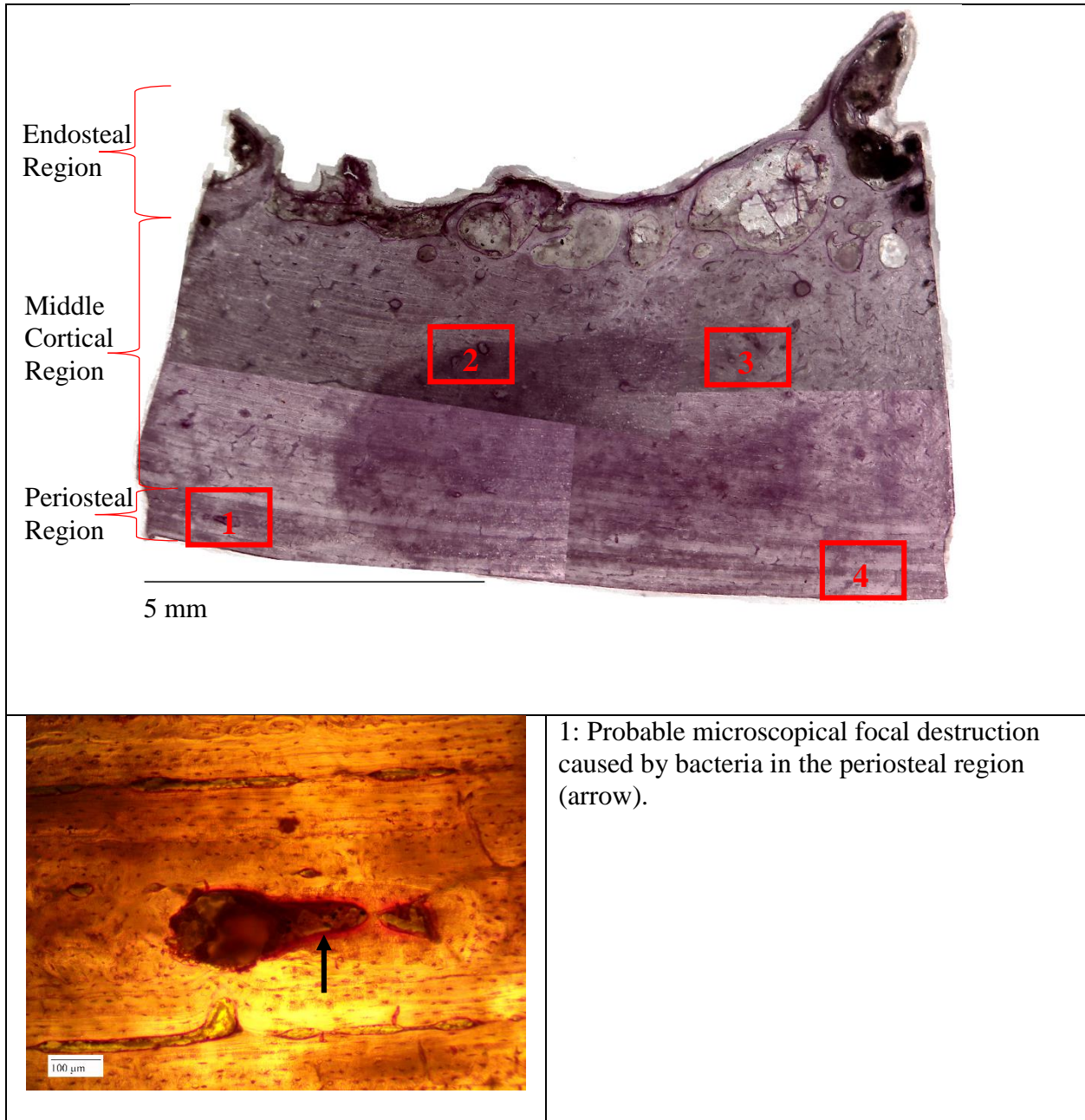
	2: Bacteria inclusion in a Haversian canal (A) and a large Haversian canal (B) in the middle cortical region.
	3: Large Haversian canals with inclusions (A) and likely microscopical focal destruction caused by bacteria in the middle cortical region consisting of plexiform bone (B).
	4: Plexiform bone structure in the periosteal region.

Table 28: Thin section of cortical bone of Group B, Week 2 from mid-diaphysis of a pig humerus. Stained with H and E. Refer to four inset images for specific diagenetic changes in periosteal, middle cortical, and endosteal regions.

1: Microscopical focal destruction caused by bacteria in the middle cortical region (arrow).
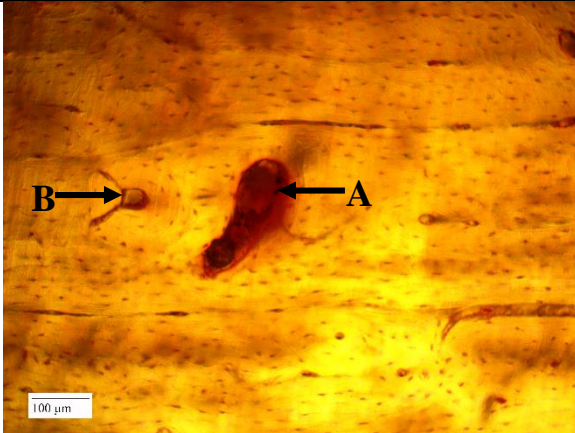
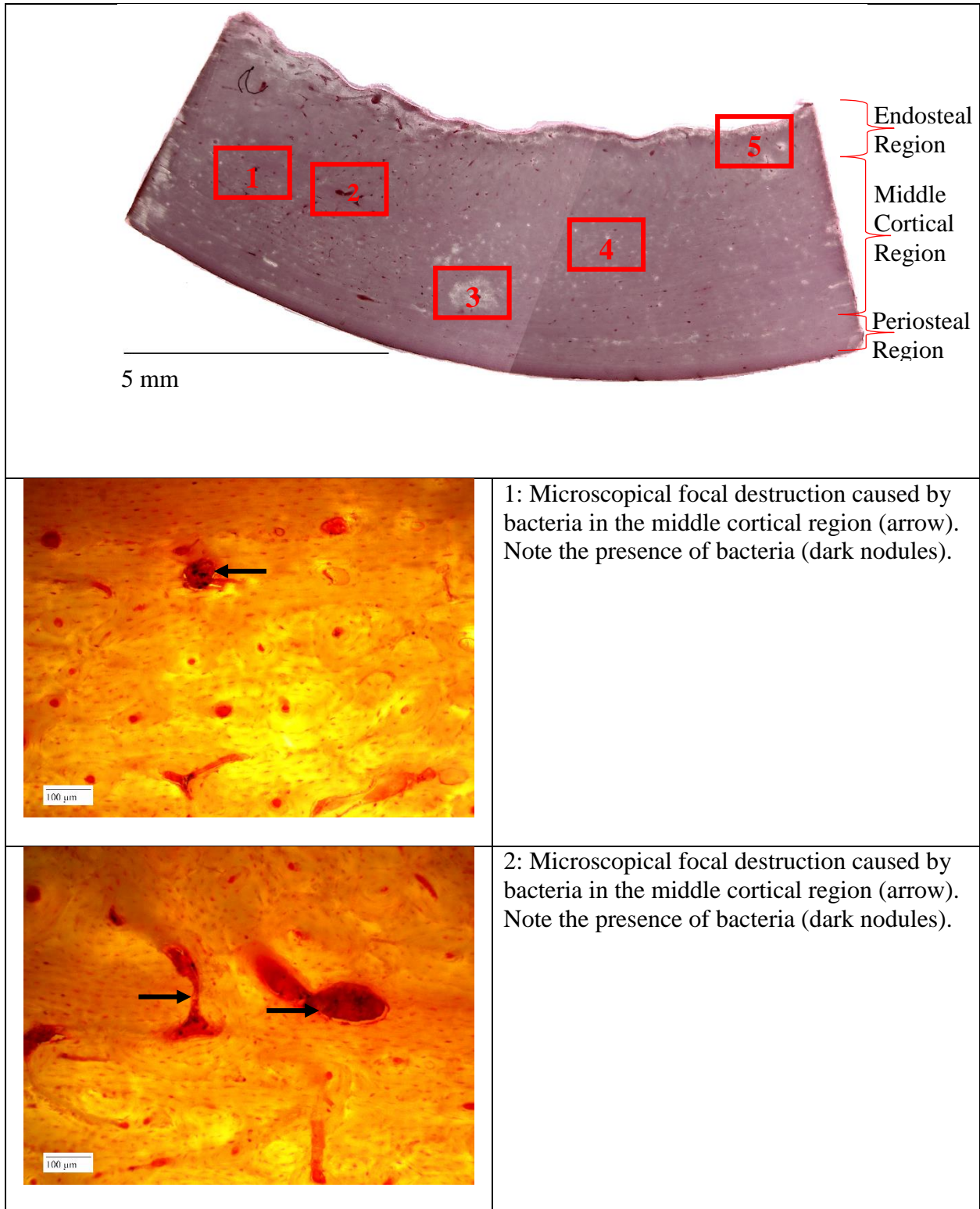|	
	2: Probable microscopical focal destruction caused by bacteria (A) and a regular osteon (B) in the middle cortical region.
	3: Plexiform bone tissue in the periosteal region and a Haversian canal with a bacterial inclusion (arrow).
	4: Large structures in the transition from cortical bone to trabecular bone in the endosteal region, called "trabecularized" cortical bone (arrows). Note the bacteria in the structures (dark nodules).
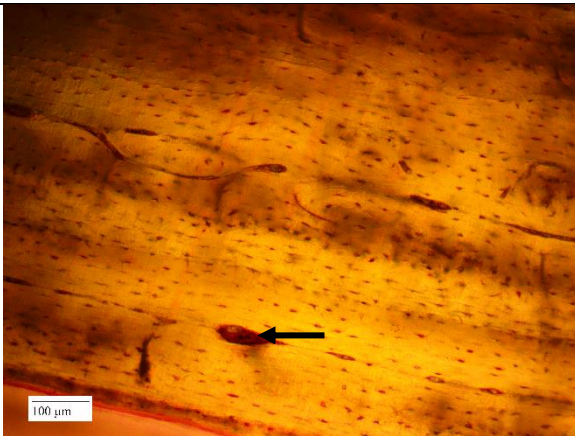
121

Table 29: Thin section of cortical bone of Group B, Week 4 from mid-diaphysis of a pig humerus. Stained with PAS. Refer to three inset images for specific diagenetic changes in periosteal, middle cortical, and endosteal regions.
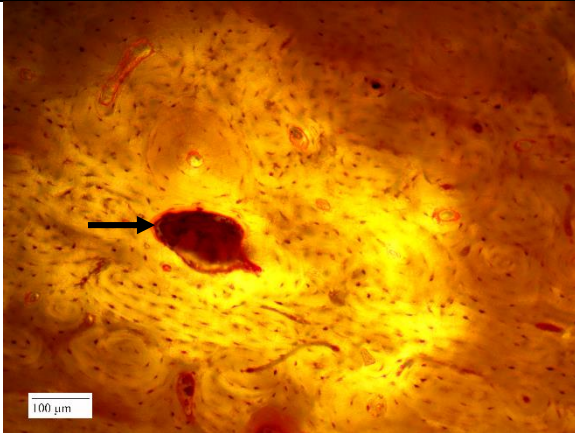

	1: Haversian canal with a bacterial inclusion (A) and microscopical focal destruction caused by bacteria in the middle cortical region (B).
	2: Haversian canal with inclusion (A) and osteon banding (B) in the middle cortical region.
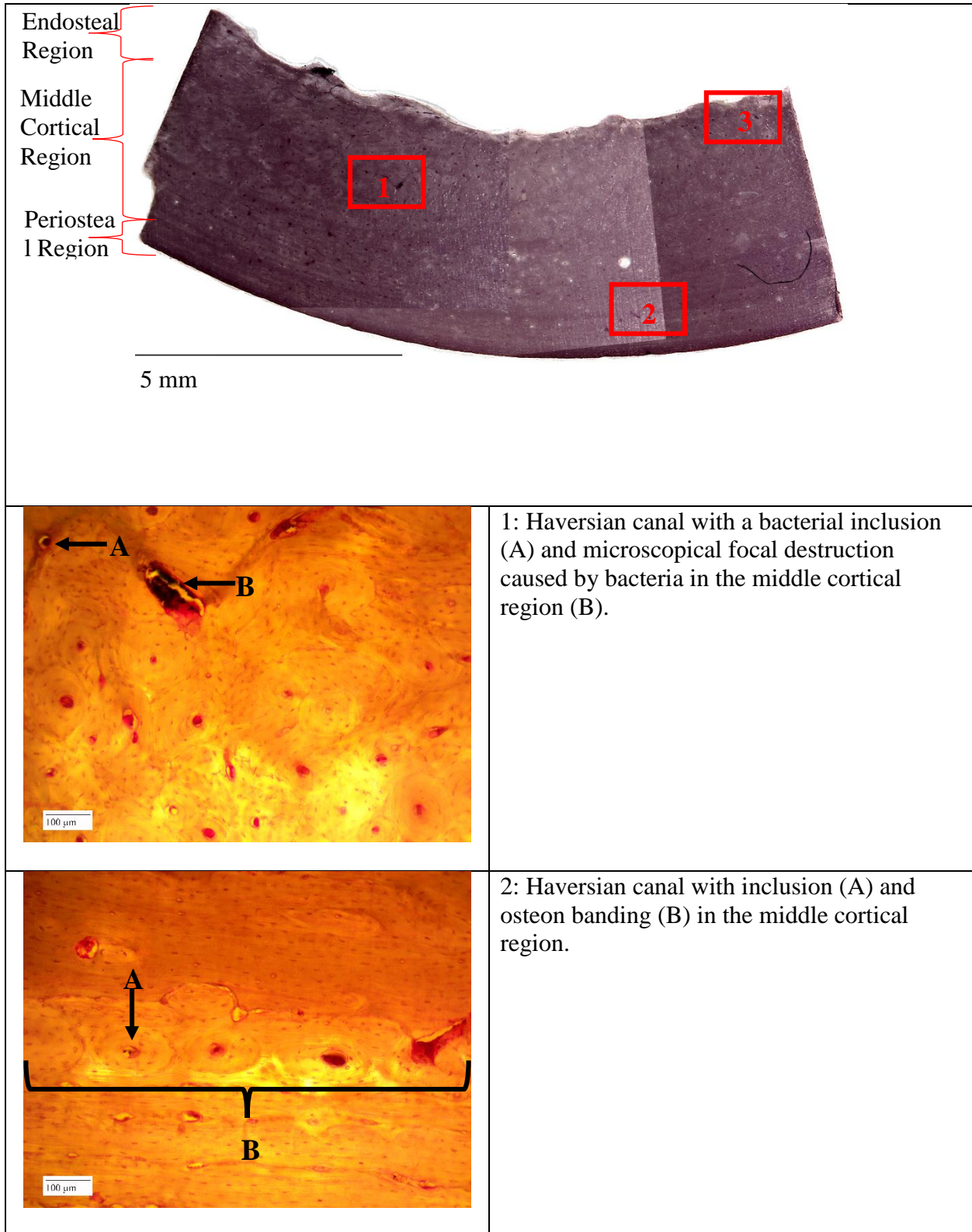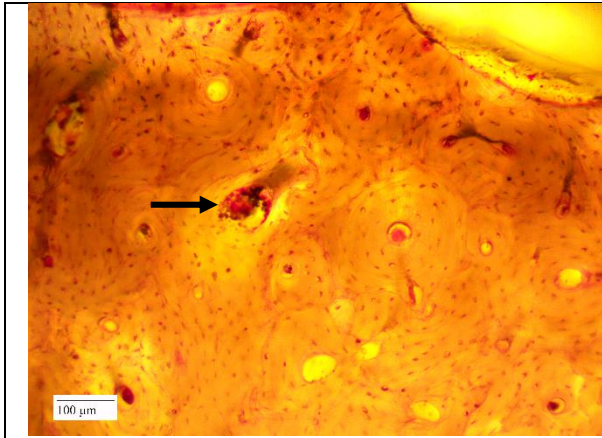
3: Likely microscopical focal destruction caused by bacteria in the endosteal region, but excluded from analysis due to location (arrow). Note the presence of bacteria (dark nodules).

Table 30: Thin section of cortical bone of Group B, Week 4 from mid-diaphysis of a pig humerus. Stained with H and E. Refer to five inset images for specific diagenetic changes in periosteal, middle cortical, and endosteal regions.
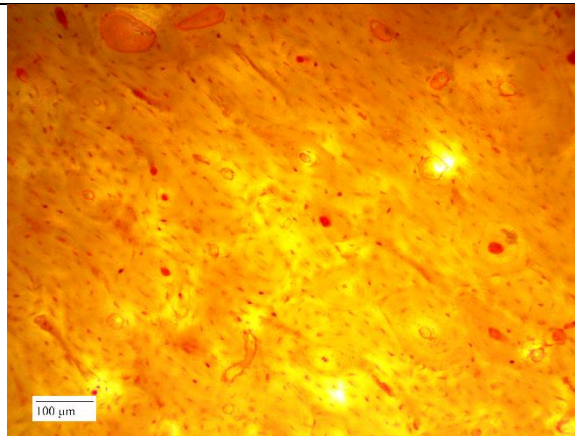

	1: Microscopical focal destruction caused by bacteria in the middle cortical region (arrow). Note the presence of bacteria (dark nodules).
	2: Microscopical focal destruction caused by bacteria in the middle cortical region (arrow). Note the presence of bacteria (dark nodules).

3: Microscopical focal destruction caused by bacteria in the middle cortical region (arrow).


4: Area of cortical bone with regular osteons.
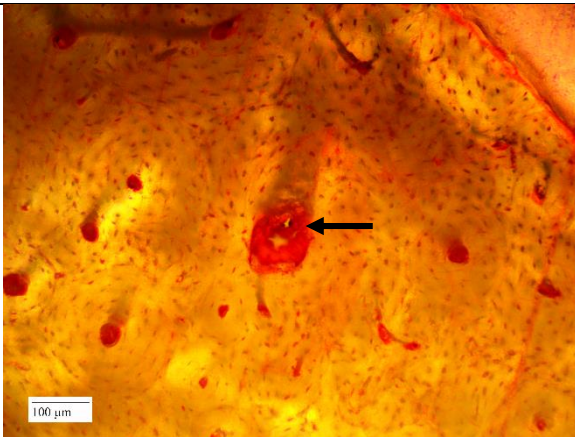
5: Likely microscopical focal destruction (arrow), but location in endosteal region excludes structure from analysis. Note the presence of bacteria (dark nodules).

Table 31: Thin section of cortical bone of Group B, Week 6 from mid-diaphysis of a pig humerus. Stained with PAS. Refer to three inset images for specific diagenetic changes in periosteal and middle cortical regions.

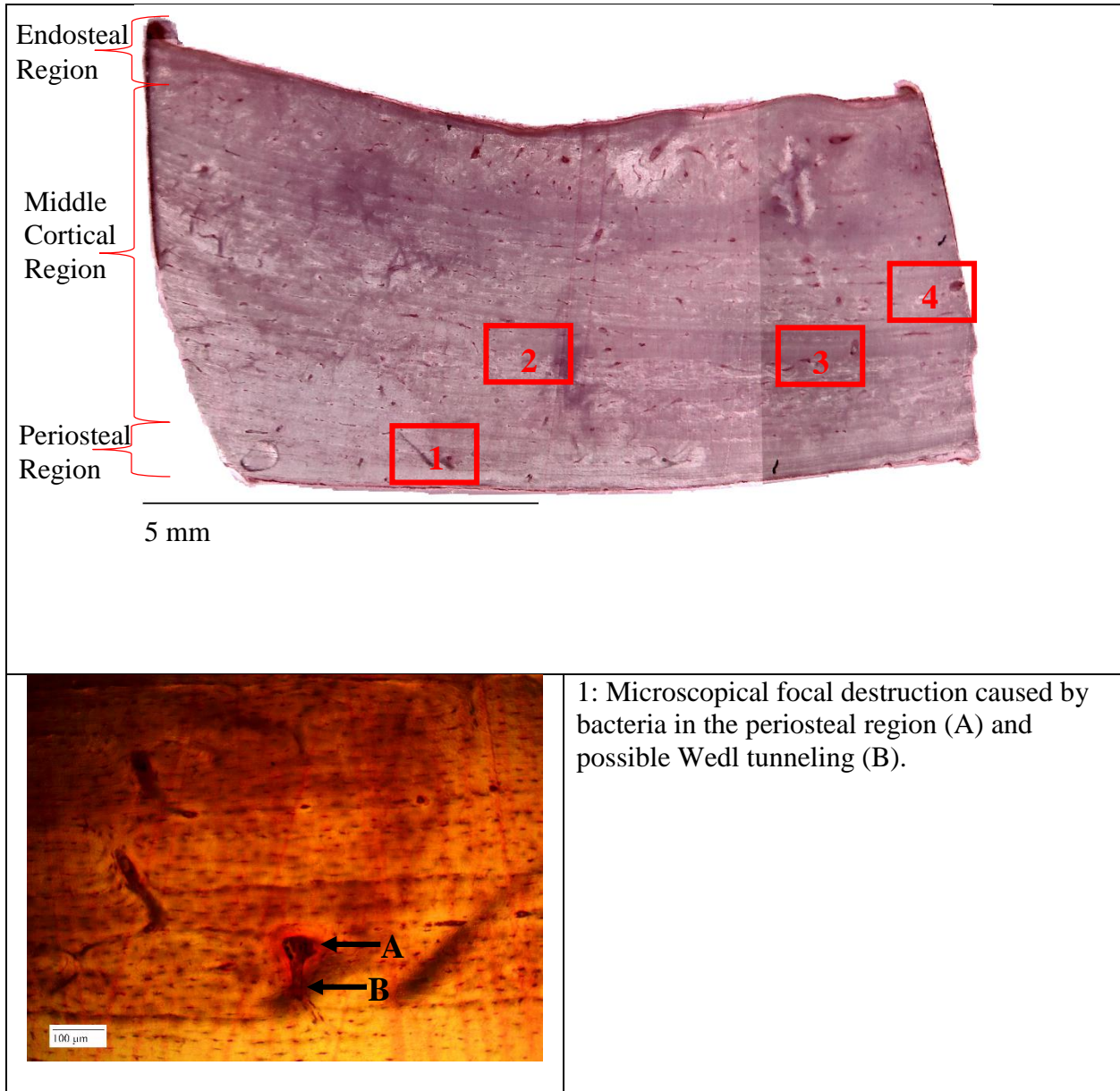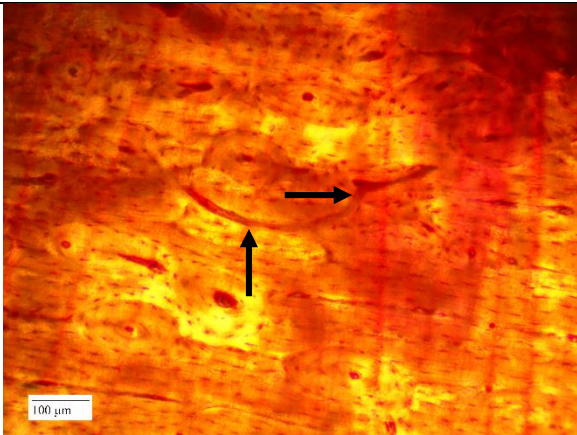1: Microscopical focal destruction caused by bacteria in the middle cortical region (arrows).
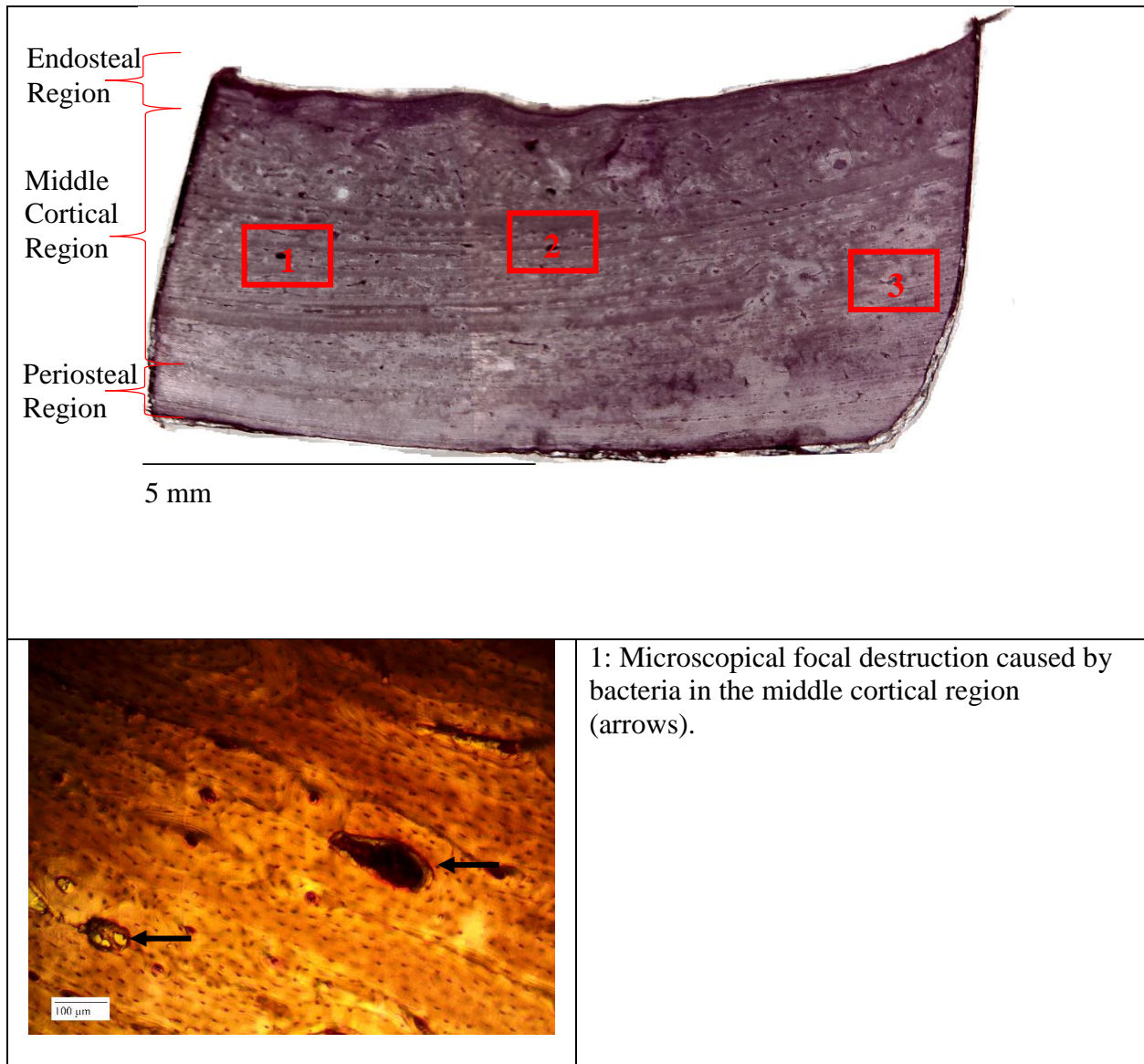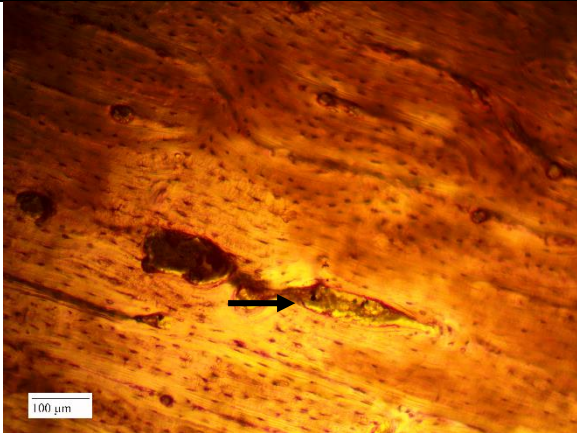
2: Microscopical focal destruction caused by bacteria in the middle cortical region (arrow). Note the presence of bacteria (dark nodules).
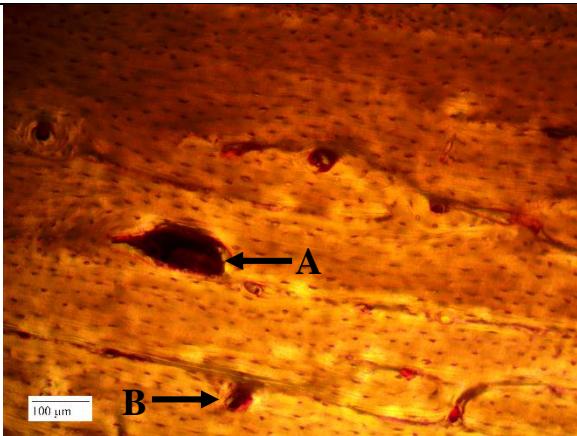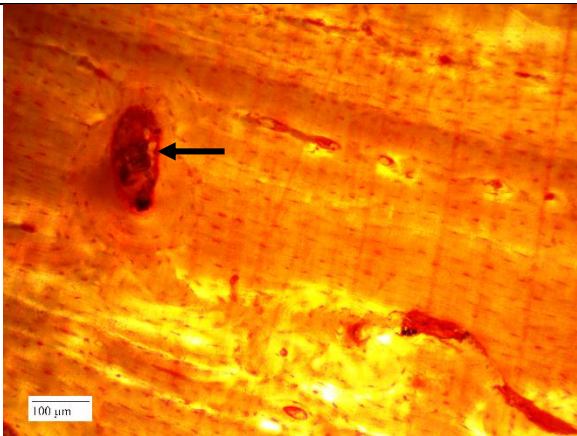

3: Microscopical focal destruction caused by bacteria in the middle cortical region (A) and a Haversian canal with an inclusion (B).

Table 32: Thin section of cortical bone of Group B, Week 6 from mid-diaphysis of a pig humerus. Stained with H and E. Refer to four inset images for specific diagenetic changes in periosteal and middle cortical regions.

Endosteal Region

Middle Cortical Region

Periosteal Region

5 mm

1: Microscopical focal destruction caused by bacteria in the periosteal region (A) and possible Wedl tunneling (B).
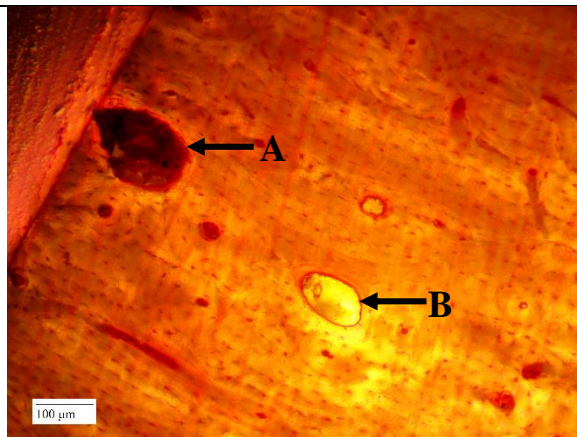
2: Possible Wedl tunneling in the middle cortical region (arrows). However, the path from Haversian canal to Haversian canal suggests a Volkmann's canal.
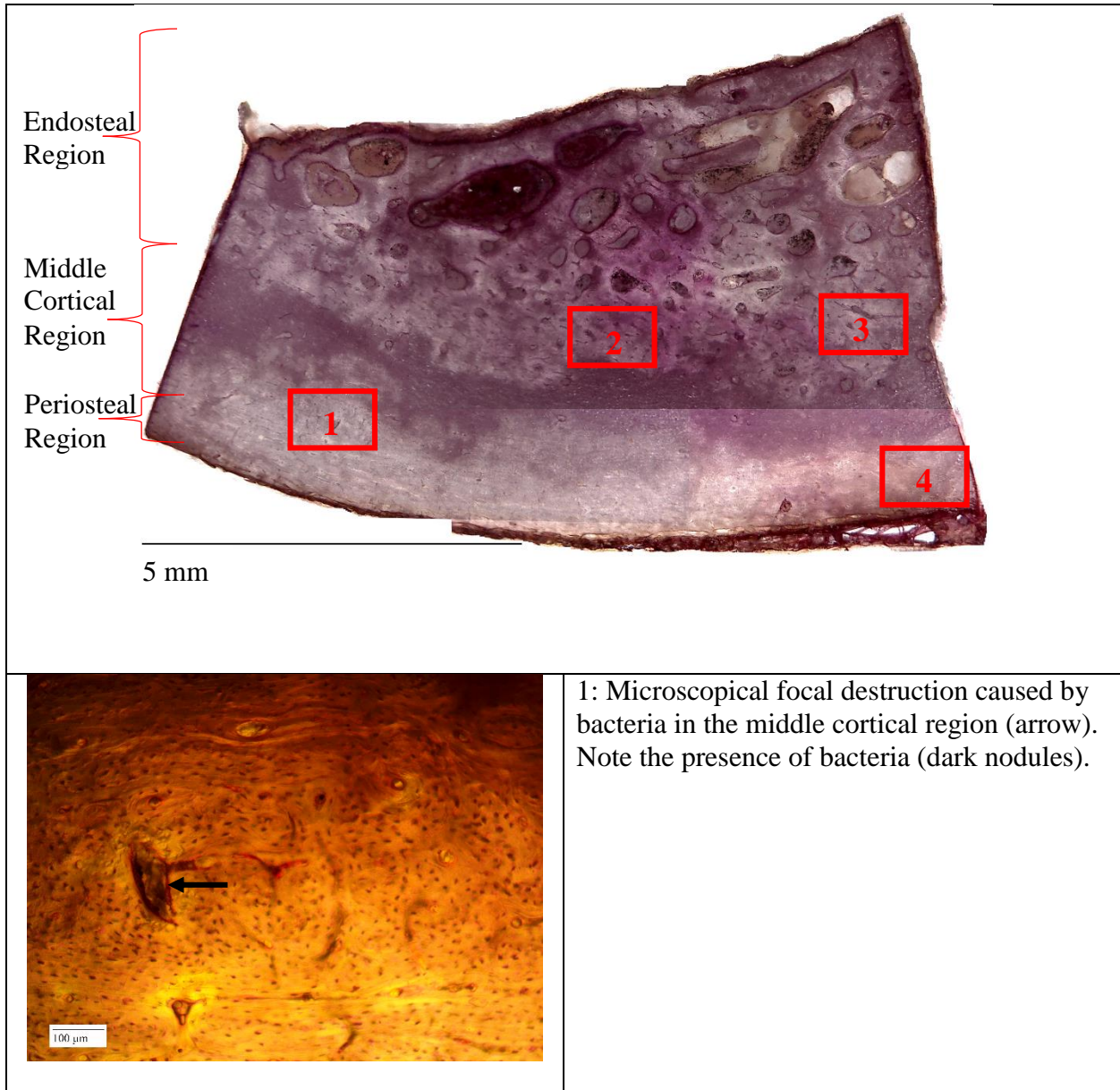

3: Microscopical focal destruction caused by bacteria in the middle cortical region (arrow).

4: Microscopical focal destruction caused by bacteria in the middle cortical region (A) and a structure most consistent with osteoclastic activity (B).

Table 33: Thin section of cortical bone of Group B, Week 8 from mid-diaphysis of a pig femur. Stained with PAS. Refer to four inset images for specific diagenetic changes in periosteal and middle cortical regions.

5 mm

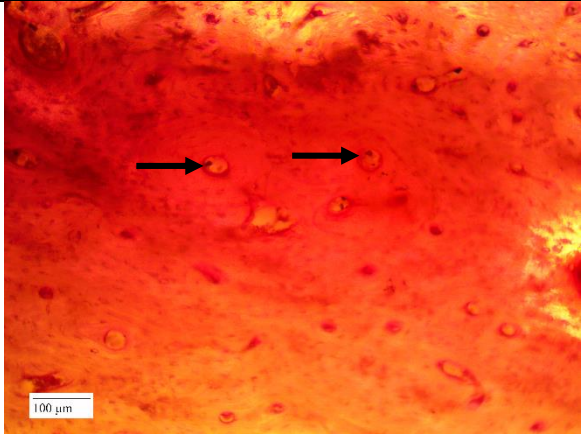1: Microscopical focal destruction caused by bacteria in the middle cortical region (arrow). Note the presence of bacteria (dark nodules).
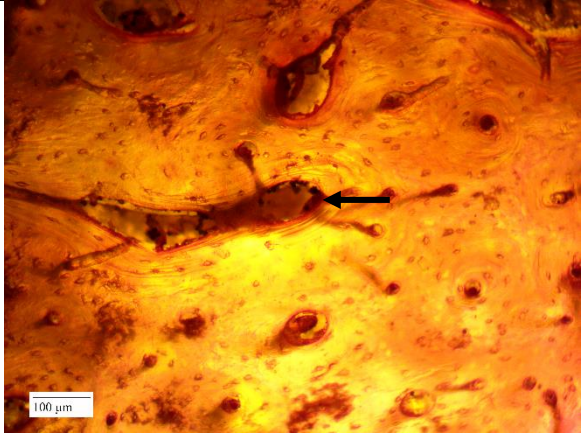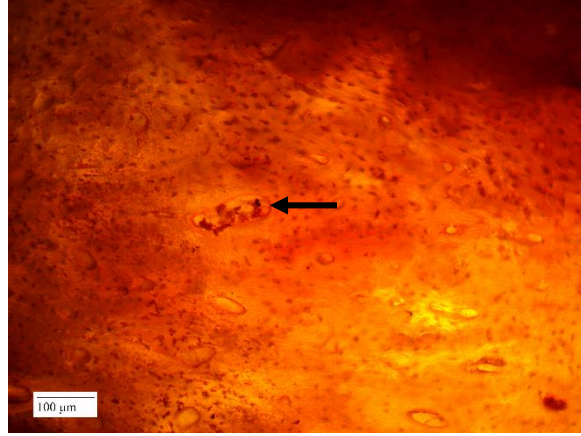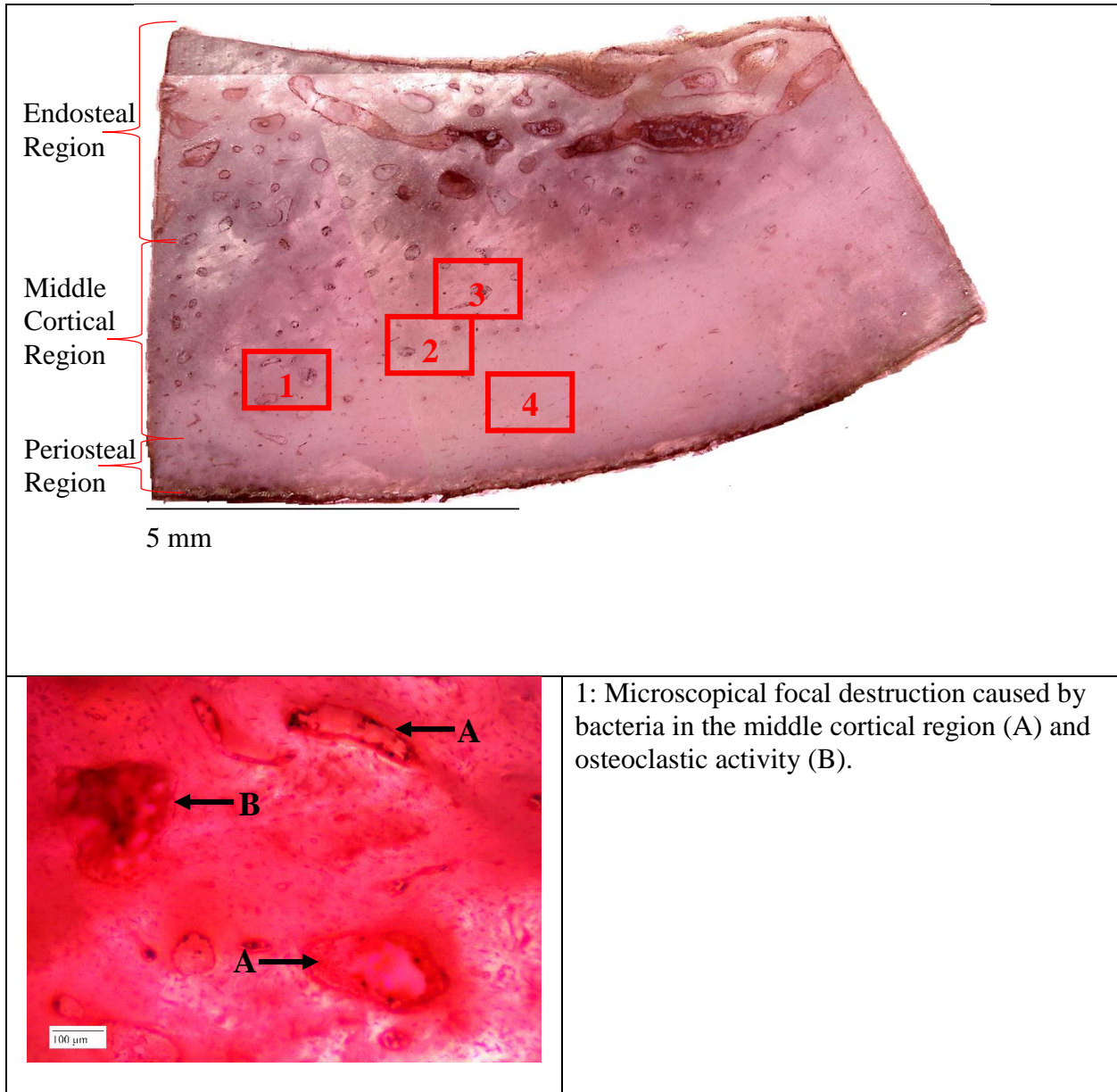
2: Bacteria inclusions in a Haversian canals (arrows)

3: Microscopical focal destruction caused by bacteria in the middle cortical region (arrow). Note the presence of bacteria (dark nodules).

4: Microscopical focal destruction caused by bacteria in the periosteal region (arrow).

Table 34: Thin section of cortical bone of Group B, Week 8 from mid-diaphysis of a pig femur. Stained with H and E. Refer to four inset images for specific diagenetic changes in periosteal and middle cortical regions.
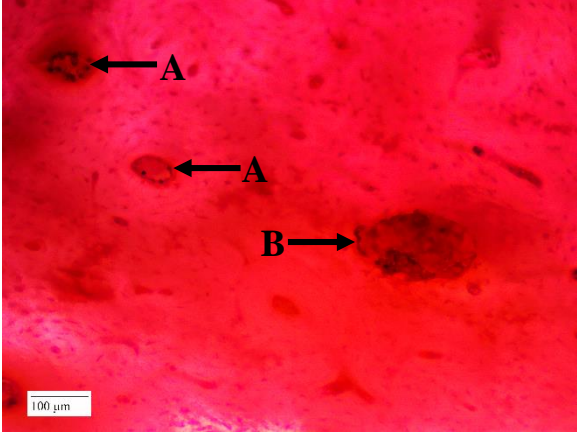

1: Microscopical focal destruction caused by bacteria in the middle cortical region (A) and osteoclastic activity (B).

	2: Bacterial inclusions in Haversian canals (A) and osteoclastic activity (B).
	3: Microscopical focal destruction caused by bacteria in the middle cortical region (arrow).
	4: Possible Wedl tunneling caused by fungal diagenesis (arrows). However, areas marked could also represent Volkmann's canals.

Table 35: Thin section of cortical bone of Group B, Week 10 from mid-diaphysis of a pig femur. Stained with PAS. Refer to three inset images for specific diagenetic changes in periosteal and middle cortical regions.
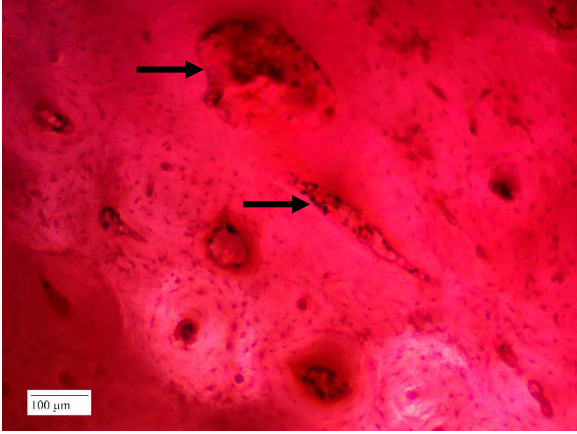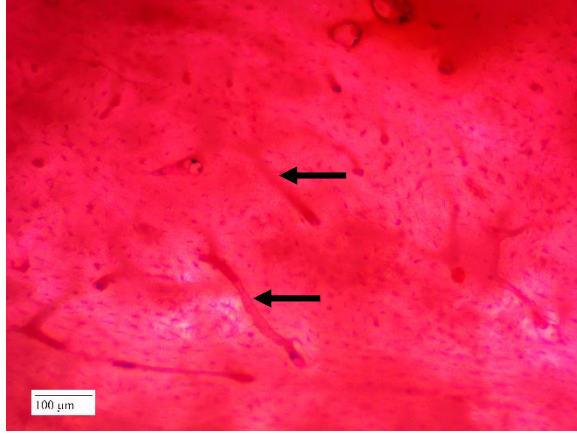

1: Large Haversian canal with inclusion (A) and osteoclastic activity (B) in the middle cortical region.
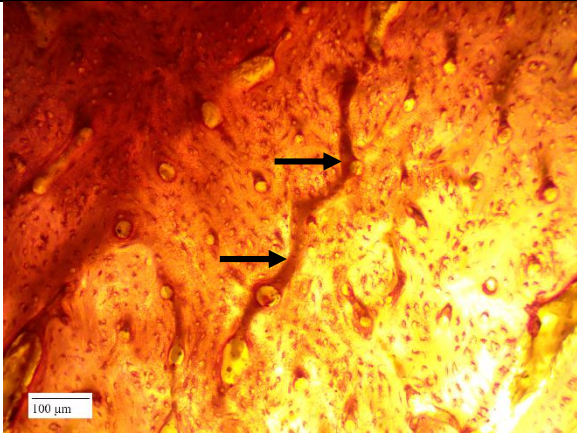
2: Probable Volkmann's canal in the middle cortical region (arrows).
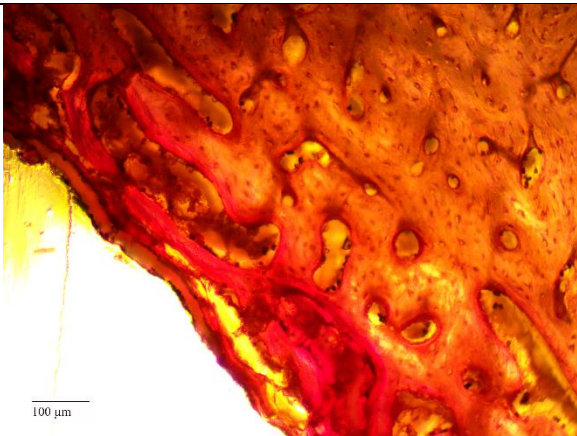
3: Heavy presence of bacteria in the periosteal region (dark nodules).

Table 36: Thin section of cortical bone of Group B, Week 10 from mid-diaphysis of a pig femur. Stained with H and E. Refer to three inset images for specific diagenetic changes in periosteal and middle cortical regions.
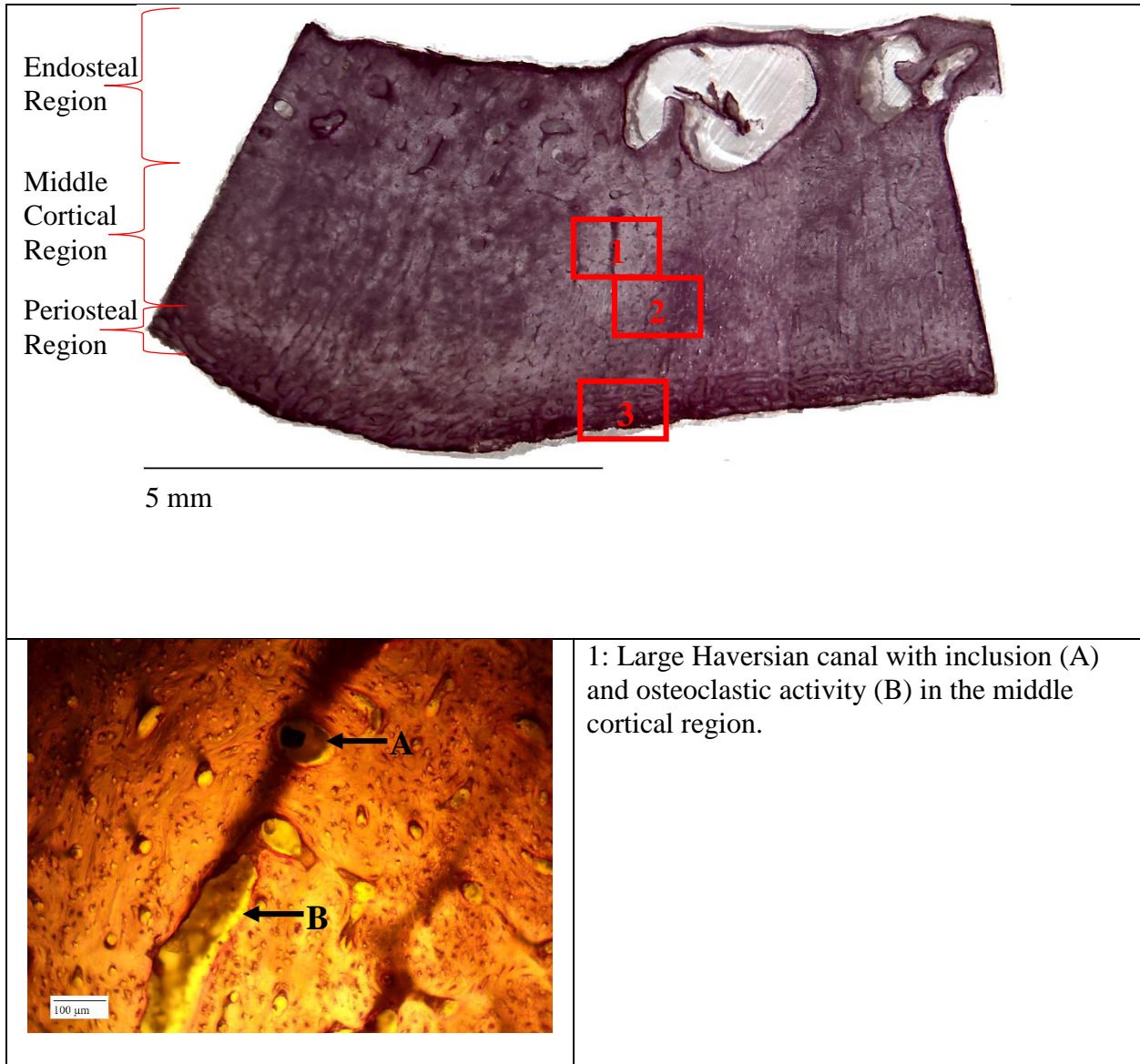

Endosteal Region

Middle Cortical Region

Periosteal Region

5 mm

100 μm

1: Possible Wedl tunneling in the middle cortical region (arrow).

2: Microscopical focal destruction caused by bacteria in the middle cortical region (arrow)
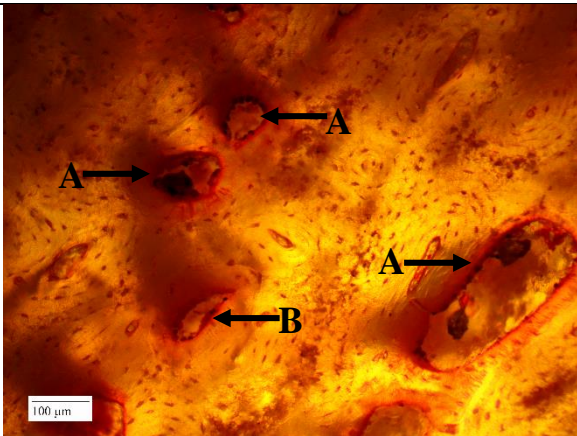
3: Microscopical focal destruction caused by bacteria in the middle cortical region (A) and a Haversian canal with bacterial inclusions (B).

Table 37: Thin section of cortical bone of Group B, Week 12 from mid-diaphysis of a pig humerus. Stained with PAS. Refer to four inset images for specific diagenetic changes in periosteal and middle cortical regions.

1: Microscopical focal destruction caused by bacteria in the middle cortical region (arrow).

2: Large structure most consistent with osteoclastic activity (A) and a bacteria inclusion in a Haversian canal (B).

3: Microscopical focal destruction caused by bacteria in the middle cortical region (arrow).

4: Wedl tunneling caused by fungal diagenesis in the middle cortical region (arrows).

139

Table 38: Thin section of cortical bone of Group B, Week 12 from mid-diaphysis of a pig humerus. Stained with H and E. Refer to four inset images for specific diagenetic changes in periosteal and middle cortical regions.

	1: Presence of bacteria (dark nodules) withing the structure of the bone in the middle cortical region (arrows).
	2: Possible tunneling (A) and likely microscopical focal destruction caused by bacteria in the middle cortical region (B). Note the bacteria (dark nodules) present in the structure.
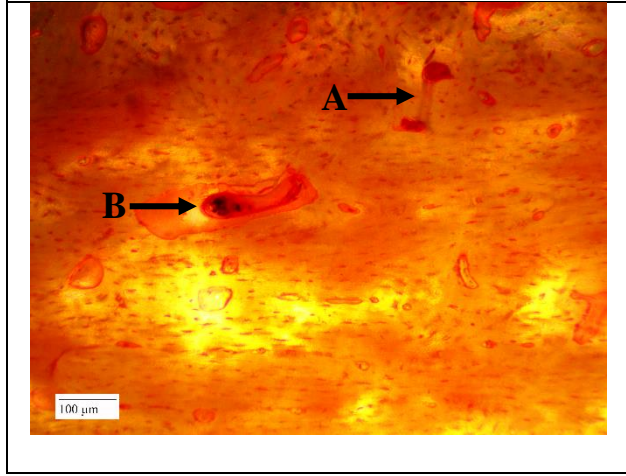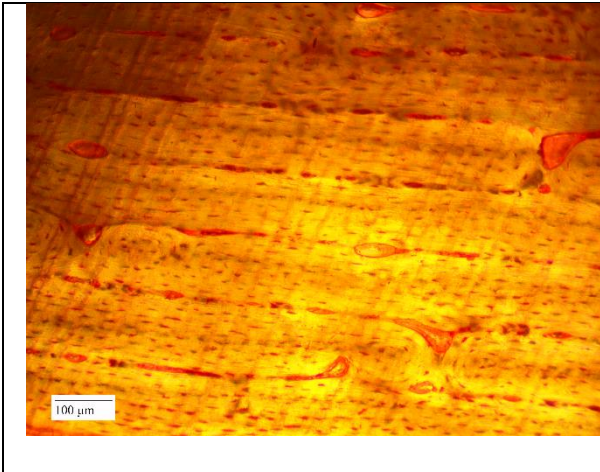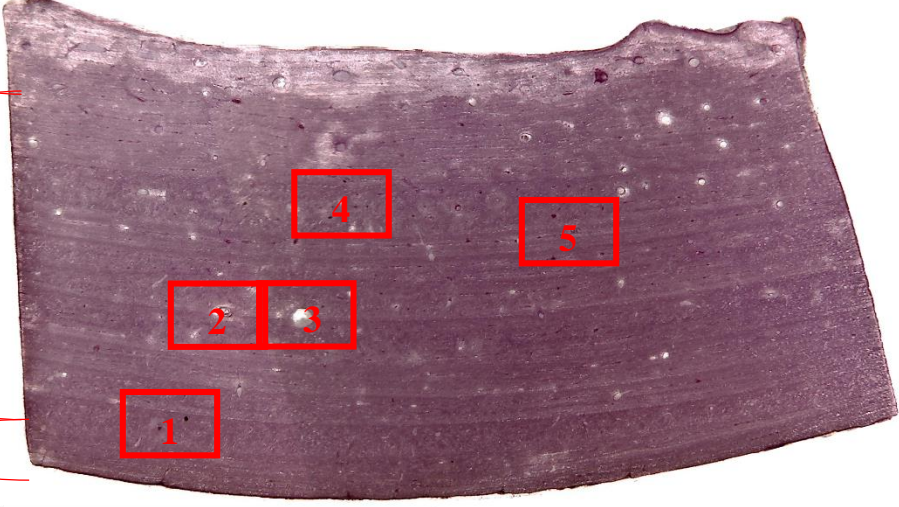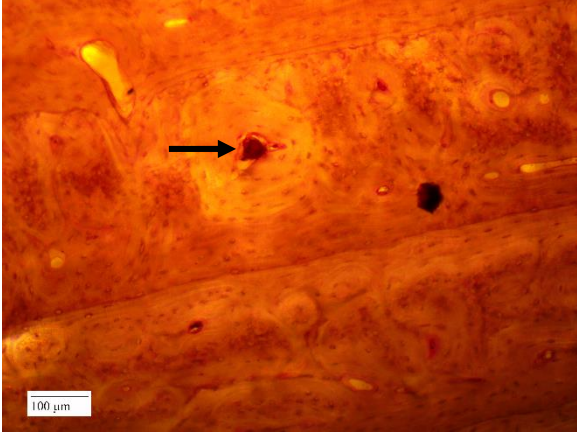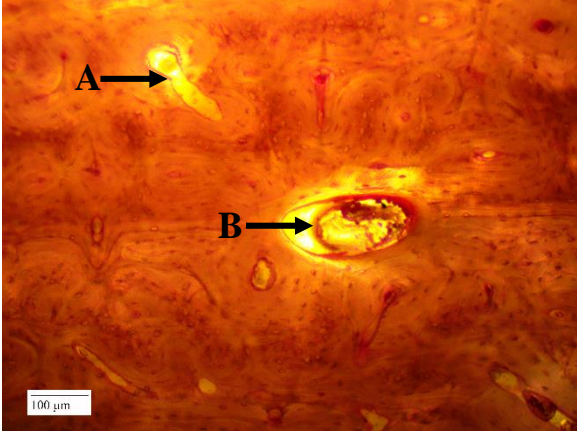
3: Plexiform bone tissue in the periosteal region.

Table 39: Thin section of cortical bone of Group B, Week 14 from mid-diaphysis of a pig humerus. Stained with PAS. Refer to five inset images for specific diagenetic changes in periosteal and middle cortical regions.
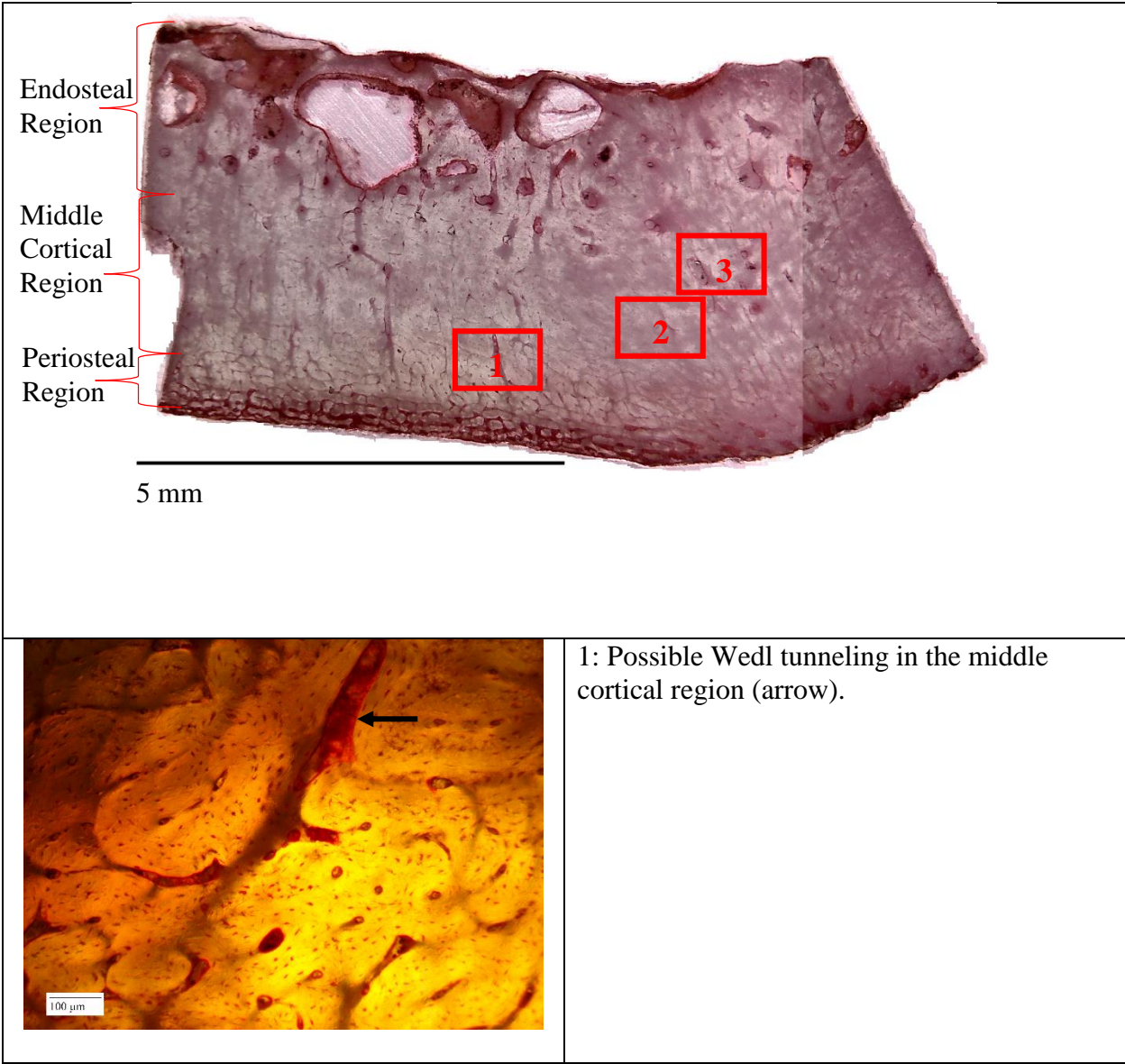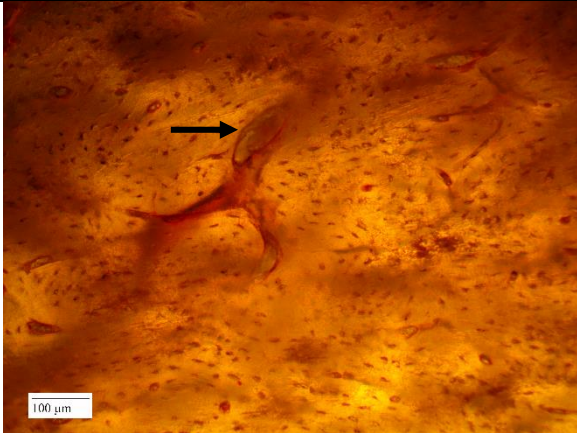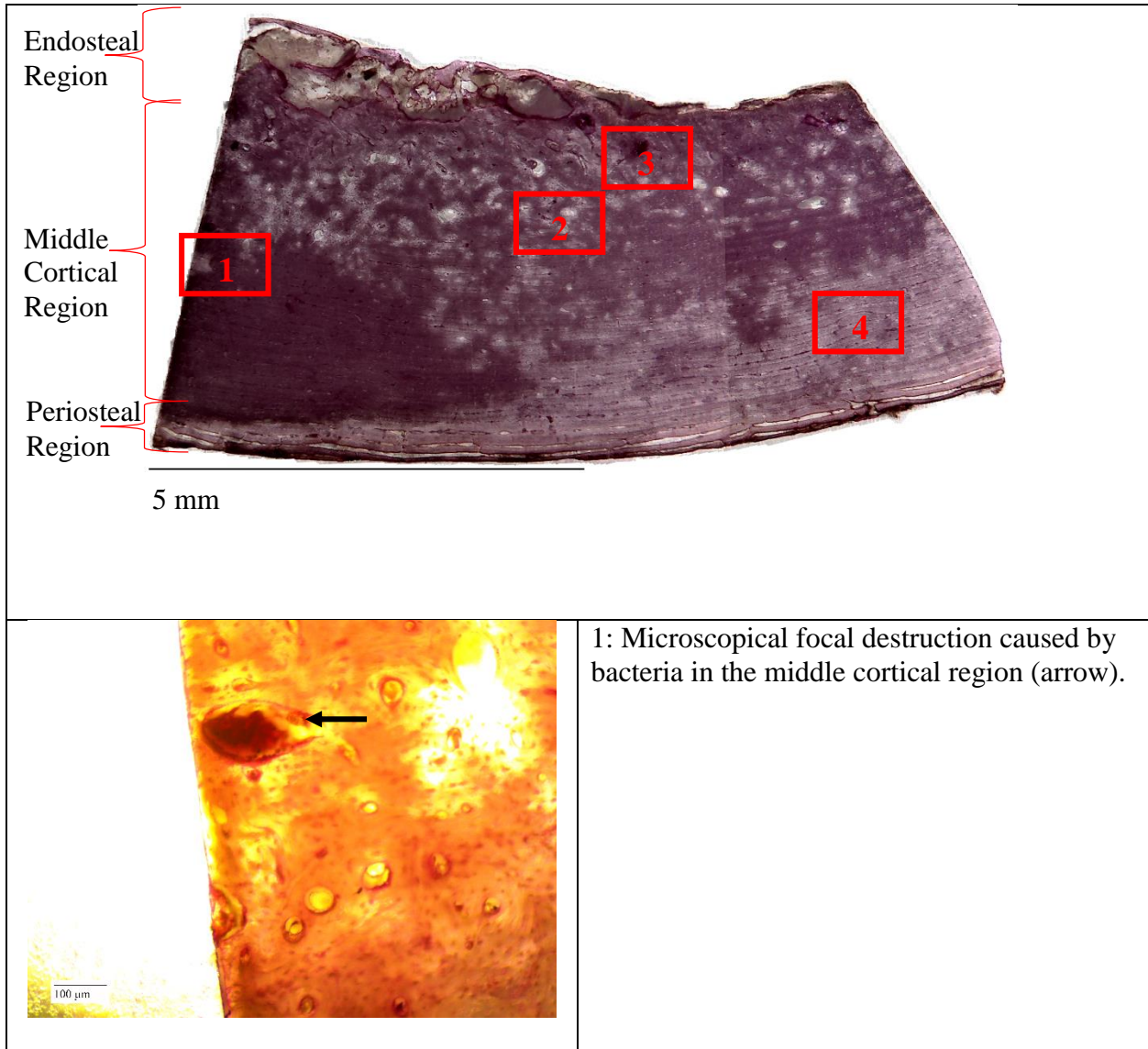

	1: Haversian canal with inclusions in the middle cortical region (arrow)
	2: Possible osteoclastic activity (A) and microscopical focal destruction caused by bacteria in the middle cortical region (B).
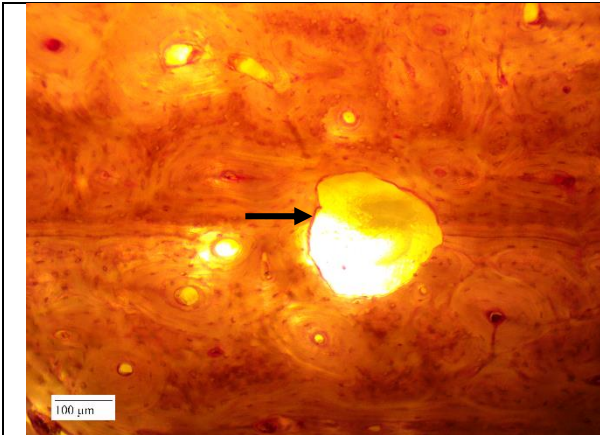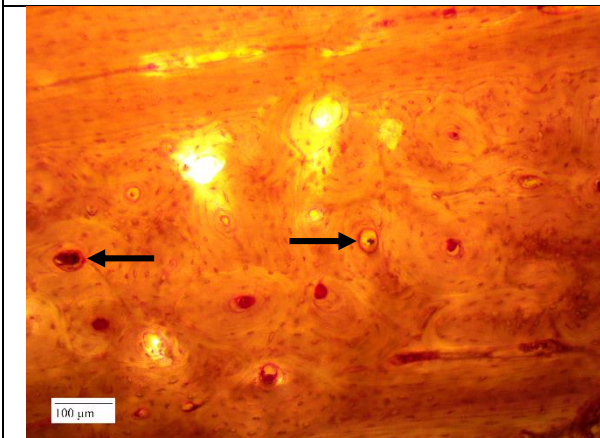
	3: Large structure most consistent with osteoclastic activity in the middle cortical region (arrow).
	4: Osteons with inclusions in the middle cortical region (arrows)
	5: Microscopical focal destruction caused by bacteria in the middle cortical region (arrow), and a plexiform bone layer (A) followed by disorganized primary and secondary osteons (B).
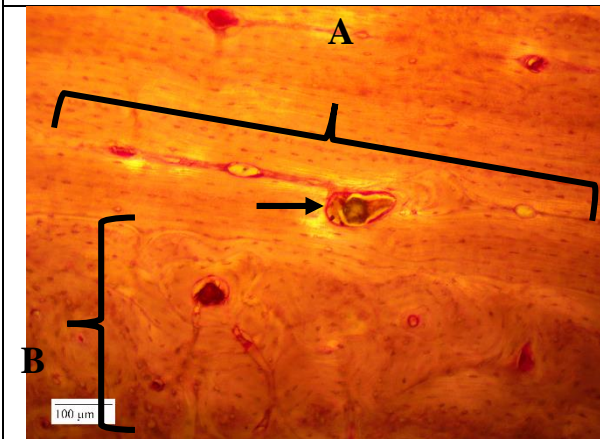
Table 40: Thin section of cortical bone of Group B, Week 14 from mid-diaphysis of a pig humerus. Stained with H and E. Refer to five inset images for specific diagenetic changes in periosteal and middle cortical regions.
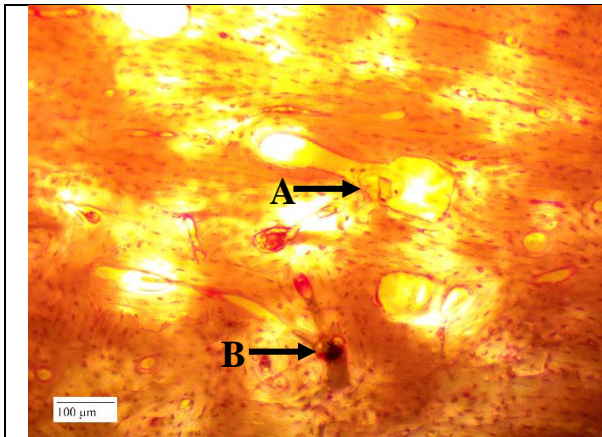

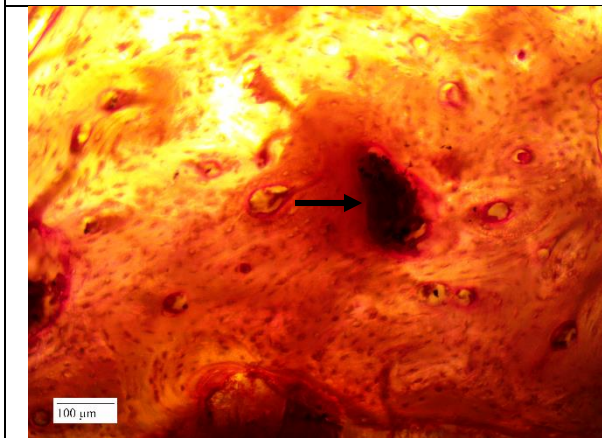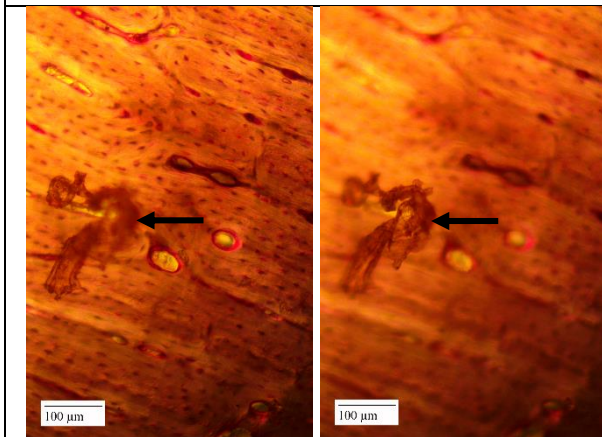1: Microscopical focal destruction caused by bacteria in the middle cortical region (arrow).
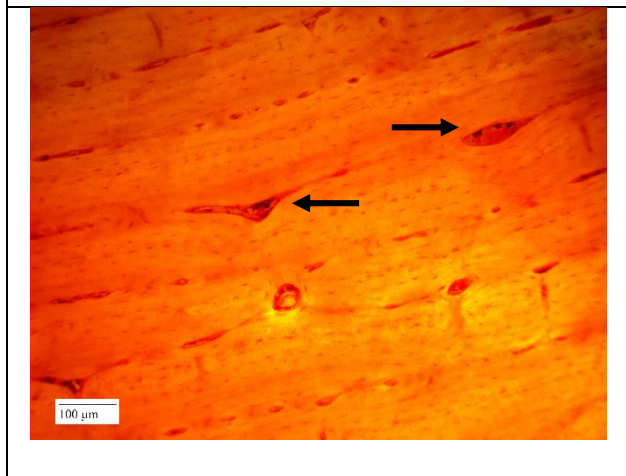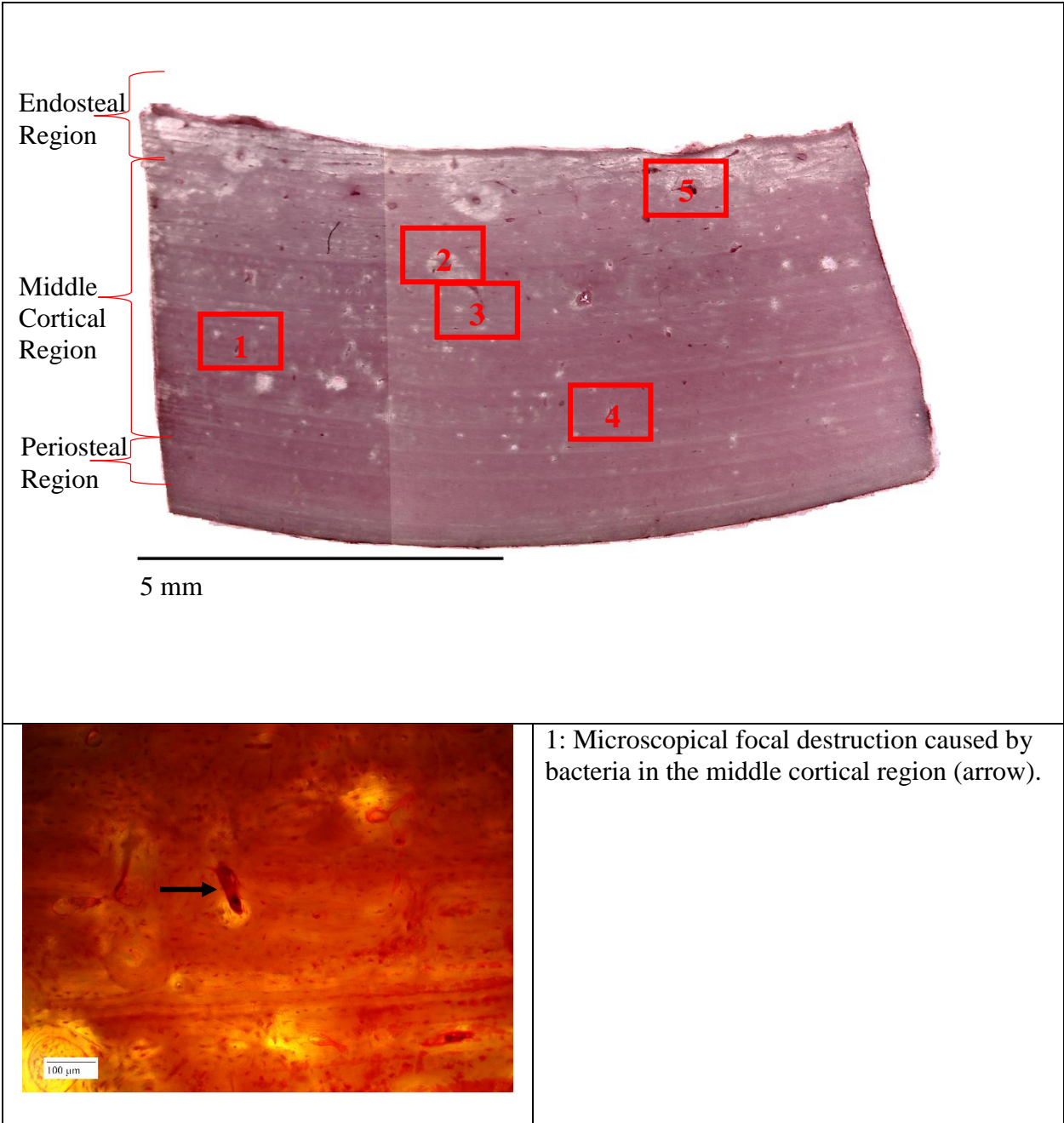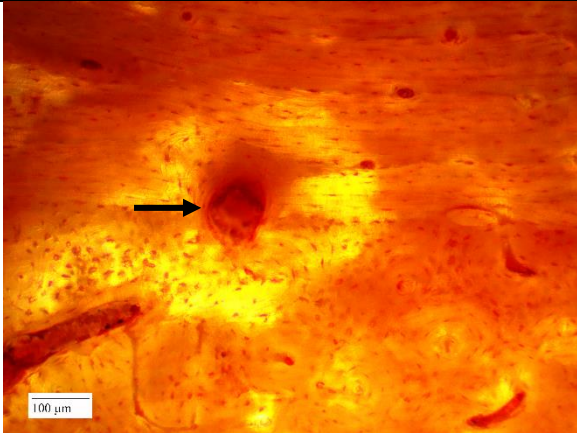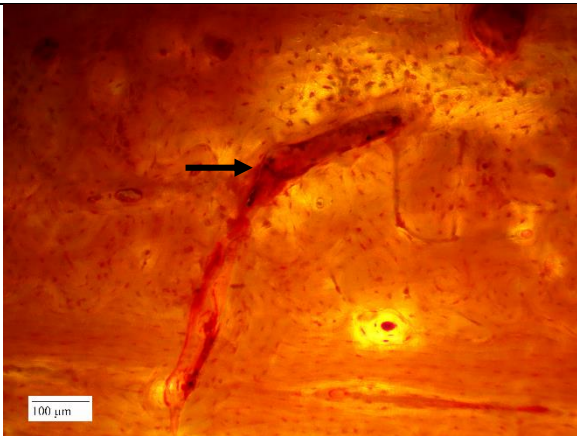
	2: Microscopical focal destruction caused by bacteria in the middle cortical region (arrow).
	3: Possible tunneling caused by fungal diagenesis in the middle cortical region (arrow).
	4: Microscopical focal destruction caused by bacteria in the middle cortical region (arrow).
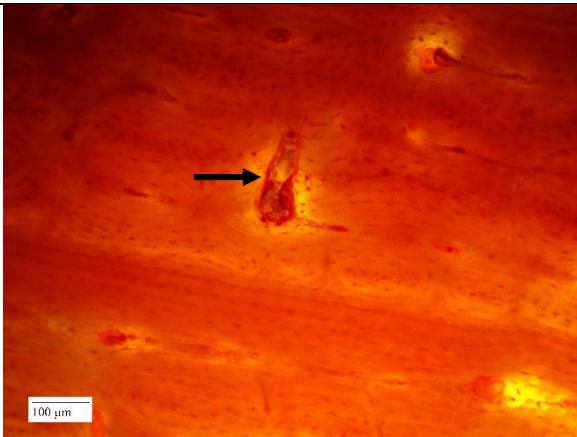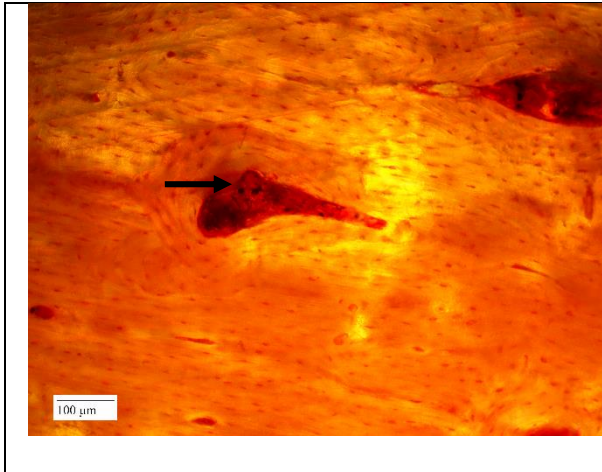
5: Presence of bacteria on the endosteal margin (arrow). Note the concentric lamellae around the structure, suggesting presence of a Haversian canal.

REFERENCES

Aerssens J, Boonen S, Lowet G, Dequeker J. 1998. Interspecies differences in bone composition, density, and quality: Potential implications for *in Vivo* bone research. Endocrinology 139(2):663-670.

Alkass K, Buchholz BA, Ohtani S, Yamamoto T, Druid H, Spalding KL. 2010. Age estimation in forensic sciences: Application of combined aspartic acid racemization and radiocarbon analysis. Molecular and Cellular Proteomics 9.5: 1022-1030.

Amednt J, Campobasso CP, Gaudry E, Reiter C, LeBlanc HN, Hall MJR. 2007. Best practice in forensic entomology – standards and guidelines. International Journal of Legal Medicine 121:90-104.

Anderson GS. 1995. The use of insects in death investigations: An analysis of cases in British Colombia over a five year period. Canadian Society of Forensic Science Journal 28(4):277-292.

Anderson GS. 2001. Insect succession on carrion and its relationship to determining time of death. In: Byrd JH, Castner JL eds. Forensic Entomology: The Utility of Arthropods in Legal Investigations. Boca Raton: CRC Press. P. 143-176.

Anderson GS, VanLaerhoven SL. 1996. Initial studies on insect succession on carrion in Southwestern British Columbia. Journal of Forensic Science 41(4):617–625.

Andrews P, Cook J. 1985. Natural modifications to bones in a temperate setting. Man, New Series 20(4):675-691.

Andrews P, Whybrow P. 2005. Taphonomic observations on a camel skeleton in a desert environment in Abu Dhabi. Paleontologica Electronica 8(23A):1-17.

Bass WM. 2006. Outdoor decomposition rates in Tennessee. In: Sorg MH and Haglund WD eds. Forensic Taphonomy: The Postmortem Fate of Human Remains. Boca Raton: CRC Press. P181-186.

Beauchesne P, Saunders S. 2006. A test of the revised Frost's 'Rapid Manual Method' for the preparation of bone thin sections. International Journal of Osteoarchaeology 16:82-87.

Beary MO, Lyman RL. 2012. The use of taphonomy in forensic anthropology: past trends and future prospects. In: Dirkmaat D editor. A Companion to Forensic Anthropology. West Sussex:Wiley-Blackwell P.499-527.

Behrensmeyer AK. 1978. Taphonomic and ecologic information from bone weathering. Paleobiology 4(2):150-162.

Bell LS. 1990. Palaeopathology and diagenesis: An SEM evaluation of structural changes using backscattered electron imaging. Journal of Archaeological Science 17(1):85-102.

Bell LS, Skinner MF, Jones SJ. 1996. The speed of post mortem change to the human skeleton and its taphonomic significance. Forensic Science International 82:129-140.

Boaks A, Siwek D, Mortazavi F. 2014. The temporal degradation of bone collagen: A histochemical approach. Forensic Science International 240:104-110.

Buchan MJ, Anderson GS. 2001. Time since death: A review of the current status of methods used in the later postmortem interval. Canadian Society of Forensic Science Journal 34(1):1-22.

Byrd JH, Castner JL. 2001. Insects of forensic importance. In: Byrd JH, Castner JL eds. Forensic Entomology: The Utility of Arthropods in Legal Investigations. Boca Raton: CRC Press. P. 43-80.

Cardoso HFV, Santos A, Dias R, Garcia C, Pinto M, Sérgio C, Magalhães T. 2010. Establishing a minimum postmortem interval of human remains in an advanced state of skeletonization using the growth rate of bryophytes and plant roots. International Journal of Legal Medicine 124:451-456.

Caropreso S, Bondioli L, Capannolo D, Cerroni L, Macchiarelli R, Condo SG. 2000. Thin sections for hard tissue histology: A new procedure. Journal of Microscopy 199(3):244-247.

Carter DO, Yellowlees D, Tibbett M. 2010. Moisture can be the dominant environmental parameter governing cadaver decomposition in soil. Forensic Science International 200:60-66.

Cattaneo C. 2007. Forensic anthropology: Developments of a classical discipline in the new millennium. Forensic Science International 165:185-193.

Charabidze D, Depeme A, Devigne C, Hedouin V. 2015. Do necrophagous blowflies (Diptera: Calliphoridae) lay their eggs in wounds? Experimental data and implications for forensic entomology. Forensic Science International 253:71-75

Child AM. 1995. Towards an understanding of the microbial decomposition of archaeological bone in the burial environment. Journal of Archaeological Science 22:165-174.

Christensen AM, Passalaqua NV, Bartelink EJ. 2014. Forensic anthropology: Current methods and practice. Cambridge: Academic Press

Coe M. 1978. The decomposition of elephant carcasses in the Tsavo (East) National Park, Kenya. Journal of Arid Envrionments 1:71-86.

Coelho L, Cardoso HFV. 2013. Timing of blunt force injuries in long bones: The effects of the environment, PMI length, and human surrogate model. Forensic Science International 233:230-237.

Collins MJ, Nielsen-Marsh CM, Hiller J, Smith CI, Roberts JP, Prigodich RV, Wess TJ, Csapo J, Millard AR, Turner-Walker G. 2002. The survival of organic matter in bone: A review. Archaeometry 44(3):383-394.

Courtin GM, Fairgrieve SI. 2004. Estimation of postmortem interval (PMI) as revealed throught the analysis of annual growth in woody tissue. Journal of Forensic Sciences 49(4):1-3.

Crescimanno A, Stout SD. 2012. Differentiating fragmented human and nonhuman long bone using osteon circularity. Journal of Forensic Sciences 57(2):267-294.

Crowder C, Heinrich J, Stout SD. 2012. Rib histomorphometry for adult age estimation. In Bell L editor. Forensic Microscopy for Skeletal Tissues: Methods and Protocols. Berlin: Springer Science+Business Media. P.109-127.

Cuijpers AGFM. 2006. Histological identification of bone fragments in archaeology: Telling humans apart from horses and cattle. International Journal of Osteoarchaeology 16:465-480.

Cunningham SL, Kirkland SA, Ross AH. 2011. Bone weathering of juvenile-sized remains in the North Carolina Piedmont. In: Ross AH, Abel SM eds. The Juvenile Skeleton in Forensic Abuse Investigations. Berlin: Springer Science+Business Media. P.179-196.

Damann FE, Carter DO. 2014. Human decomposition ecology and postmortem microbiology. In: Pokines J and Symes SA eds. Manual of Forensic Taphonomy. Boca Raton: CRC Press. P.37-50.

Damann FE, Williams DE, Layton AC. 2015. Potential use of bacterial community succession in decaying human bone for estimating postmortem interval. Journal of Forensic Sciences 60(4):844-850.

de Boer HH, Aarents MJ, Maat GJR. 2013. Manual for the preparation and staining of embedded natural dry bone tissue sections for microscopy. International Journal of Osteoarchaeology 23:83-93.

Dix J, Graham M. 2000. Time of death, decomposition and identification: An atlas. Boca Raton: CRC Press.

Dupras TL, Schultz JJ. 2014. Taphonomic bone staining and color changes in forensic contexts. In: Pokines J and Symes SA eds. Manual of Forensic Tahonomy. Boca Raton: CRC Press. P.315-340.

Evans FG. 1973. Mechanical properties of bone. Springfield: Charles C. Thomas.

Fiorillo AR. 1995. Possible influence of low temperature on bone weathering in Curecanti National Recreation Area, southwest Colorado. Current Research in the Pleistocene 12:69-71.

Fitter AH, Stickland TR. 1992. Fractal characterization of root system architecture. Functional Ecology 6(6):632-635.

Galloway A, Birkby WH, Jones AM, Henry TE, and Parks BO. 1989. Decay Rates of Human Remains in Arid Environment. Journal of Forensic Sciences 34(3):607-616.

Garland AN, Janaway RC, Roberts CA. 1988. A study of the decay processes of human skeletal remains from the Parish Church of the Holy Trinity, Rothwell, Northamptonshire. Oxford Journal of Archaeology 7(2):235-252.

Garland AN. 1993. An introduction to the histology of exhumed mineralized tissue. In: Grupe G and Garland AN editors. Histology of Ancient Human Bone: Methods and Diagnosis Proceedings of the "Paleohistology Workshop" held from 3-5 October 1990 at Gottingen. P. 1-16.

Gennard DE. 2007. Forensic entomology: An introduction. West Sussex: John Wiley & Sons.

Goff ML. 1992. Problems in the estimation of postmortem interval resulting from wrapping of the corpse: A case study from Hawaii. Journal of Agricultural Entomology 9(4):237-243.

Green AE. 2015. An examination of the progression of fracture propagation in long bones during the postmortem period in Central Florida. University of Central Florida.

Grupe G. 1993. Decomposition phenomena in thin sections of excavated human bone. In: Grupe G and Garland AN editors. Histology of Ancient Human Bone: Methods and Diagnosis Proceedings of the "Paleohistology Workshop" held from 3-5 October 1990 at Gottingen. P. 27-36.

Hackett CJ. 1981. Microscopical focal destruction (tunnels) in exhumed human bones. Medicine, Science and the Law 21(4): 243-265.

Haglund WD, Reay DT, Swindler DR. 1989. Canid scavenging/disarticulation sequence of human remains in the Pacific Northwest. Journal of Forensic Sciences 34(3):587-606.

Hawksworth DL, Wiltshire PEJ. 2011. Forensic mycology: The use of fungi in criminal investigations. Forensic Science International 206:1-11.

Hedges REM. 2002. Bone diagenesis: An overview of processes. Archaeometry 44(3):319-328.

Hedges REM, Millard AR, Pike AWG. 1995. Measurements and relationships of diagenetic alteration of bone from three archaeological site. Journal of Archaeological Science 22:201-209.

Hillier ML, Bell LS. 2007. Differentiating human bone from animal bone: A review of histological methods. Journal of Forensic Science 52(2):249-263.

Hobischak NR, Anderson GS. 1999. Freshwater-related death investigations in British Colombia in 1995-1996. A review of coroner's cases. Canadian Society of Forensic Sciences Journal 32:97-106.

Hopkins DW, Wiltshire PEJ, Turner BD. 2000. Microbial characteristics of soils from graves: An investigation at the interface of soil microbiology and forensic science. Applied Soil Ecology 14:283-288.

Huculak MA, Rogers TL. 2009. Reconstructing the sequence of events surrounding body disposition based on color staining of bone. Journal of Forensic Science 54(5):979-984.

Janjua MA, Rogers TL. 2008. Bone weathering patterns of metatarsal v. femur and the postmortem interval in Southern Ontario. Forensic Science International 178:16-23.

Jans MME. 2008. Microbial bioerosion of bone – A review. In: Wisshak M and Tapanila L, eds. Current developments in bioerosion. Springer-Verlag Berlin Heidelberg. P397-413.

Jans, MME. 2014. Microscopic destruction of bone. In: Pokines J and Symes SA eds. Manual of Forensic Tahonomy. Boca Raton: CRC Press. P.19-36.

Jans MME, Kars H, Nielsen-Marsh CM, Smith CI, Nord AG, Arthur P, Earl N. 2002. *In situ* preservation of archaeological bone: A histological study within a multidisciplinary approach. Archaeometry 44(3):343-352.

Jans MME, Nielsen-Marsh CM, Smith CI, Collins MJ, Kars H. 2004. Characterisation of microbial attach on archaeological bone. Journal of Archaeological Science 31:87-95.

Junod CA, Pokines JT. 2014. Subaerial weathering. In: Pokines J and Symes SA eds. Manual of Forensic Tahonomy. Boca Raton: CRC Press. P.287-314.

Katz JL, Yoon HS, Lipson S, Maharidge R, Meunier A, Christel P. 1984. The effects of remodeling on the elastic properties of bone. Calcified Tissue International 36:31-36.

Kjorlien YP, Beattie OB, Peterson AE. 2009. Scavenging activity can produce predictable patterns in surface skeletal remains scattering: Observations and comments from two experiments. Forensic Science International 188:103-106.

Komar DA, Beattie OB. 1998. Effects of carcass size on decay rates of shade and sun exposed carrion. Canadian Society of Forensic Science Journal 31(1):35-43.

Komar DA, Buikstra JE. 2008. Forensic anthropology: Contemporary theory and practice. New York: Oxford University Press.

Madgwick R, Mulville J. 2012. Investigating variation in the prevalence of weathering in faunal assemblages in the UK: A multivariate statistical approach. International Journal of Osteoarchaeology 22:509-522.

Maggiano CM. 2012. Making the mold: A microstructural perspective on bone modeling during growth and mechanical adaptation. In: Crowder C and Stout S, editors. Bone Histology: An Anthropological Perspective. P45-90.

Mann RW, Bass WM, Meadows L. 1990. Time since death and decomposition of the human body: Variables and observations in case and experimental field studies. Journal of Forensic Science 35(1):103-111.

Marchiafava V, Bonucci E, Ascenzi A. 1974. Fungal osteoclasia: A model of dead bone resorption. Cal. Tiss. Res. 14:195-210.

Martiniakova M, Grosskopf B, Omelka R, Vondrakova M, Bauerova M. 2006a. Differences among species in compact bone tissue microstructure of mammalian skeleton: Use of a discriminant function analysis for species identification. Journal of Forensic Science s 51(6):1235-1239.

Martiniakova M, Vondrakova M, Omelka R. 2006b. Manual preparation of thin sections from historical human skeletal material. Timisoara Medical Journal 56(1):15-17.

Maurer A, Person A, Tutken T, Amblard-Pison S, Segalen L. 2014. Bone diagenesis in arid environments: An intra-skeletal approach. Palaeogeography, Paleaeoclimatology, Palaeoecology 416:17-29.

Megyesi MS, Nawrocki SP, Haskell NH. 2005. Using accumulated degree-days to estimate the postmortem interval from decomposed human remains. Journal of Forensic Science 50(3):618-626.

Mulhern DM, Ubelaker DH. 2001. Differences in osteon banding between human and nonhuman bone. Journal of Forensic Sciences 46(2):220-222.

Nawrocki SP. 2009. Forensic taphonomy. In Blau S, Ubelaker DH eds. Handbook of Forensic Anthropology and Archaeology. San Francisco: Left Coast Press. P.284-294.

Nicholson RA. 1996. Bone degradation, burial medium and species representation: Debunking the myths, an experiment-based approach. Journal of Archaeological Science 23:513-533.

Nielsen-Marsh CM, Hedges REM. 2000. Patterns of diagenesis in bone I: The effects of site environments. Journal of Archaeological Science 27:1139-1150.

Nielsen-Marsh CM, Smith CI, Jans MME, Nord A, Kars H, Collins MJ. 2007. Bone diagenesis in the European Holocene II: Taphonomic and environmental considerations. Journal of Archaeological Science 34:1523-1531.

Piepenbrink H. 1986. Two examples of biogenous dead bone decomposition and their consequences for taphonomic interpretation. Journal of Archaeological Science 13(5):417-430.

Pokines JT. 2014. Introduction: Collection of macroscopic osseous taphonomic data and the recognition of taphonomic suites of characteristics. In: Pokines J and Symes SA eds. Manual of Forensic Tahonomy. Boca Raton: CRC Press. P. 1-18.

Pokines JT, Baker JE. 2014. Effects of burial environment on osseous remains. In: Pokines J and Symes SA eds. Manual of Forensic Tahonomy. Boca Raton: CRC Press. P. 51-114.

Potmesil M. 2005. Bone dispersion, weathering, and scavenging of cattle bones. Nebraska Anthropologist, Paper 6.

Reeves NM. 2009. Taphonomic effects of vulture scavenging. Journal of Forensic Science 54(3):523-528.

Safadi FF, Barbe MF, Abdelmagid SM, Rico MC, Aswad RA, Litvin J, Popoff SN. 2009. Bone structure, development and bone biology. In: Khurana JS, editor. Bone pathology. P. 1-50.

Saville PA, Hainsworth SV, Rutty GN. 2007. Cutting crime: The analysis of the "uniqueness" of saw marks on bone. International Journal of Medicine 121:349-357.

Schoenly K, Goff ML, Early M. 1992. A BASIC algorithm for calculating the postmortem interval from arthropod successional data. Journal of Forensic Sciences 37(3):808-823.

Shalaby OA, deCarvalho LML, Goff ML. 2000. Comparison of patterns of decompistion in a hanging carcass and a carcass in contact with soil in xerophytic habitat on the island of Oahu, Hawaii. Journal of Forensic Science 45(6):1267-1273.

Shattuck RE. 2010. Perimortem fracture patterns in South-central Texas: A preliminary investigation into the perimortem interval. Thesis: Texas State University, San Marcos.

Shean BS, Messinger L, Papworth. 1993. Observations of differential decomposition on sun exposed v. shaded pig carrion in Coastal Washington State. Journal of Forensic Science 38(4):938-949.

Smith CI, Nielsen-Marsh CM, Jans MME, Collins MJ. 2007. Bone diagenesis in the European Holocene I: Patterns and mechanisms. Journal of Archaeological Science 34:1485-1493.

Sowemimo-Coker SO. 2002. Red blood cell hemolysis during processing. Transfusion Medical Reviews 16(1):46-60.

Steadman DW, Worne H. 2007. Canine scavenging of human remains in an indoor setting. Forensic Science International 173:78-82.

Stout SD. 1978. Histological structure and its preservation in ancient bone. Current Anthropology 19(3):601-604.

Stout SD, Teitelbaum SL. 1976. Histological analysis of undecalcified thin sections of archaeological bone. American Journal of Physical Anthropology 44(2):263-269.

Tappen M. 1994. Bone weathering in the tropical rain forest. Journal of Archaeological Science 32:667-673.

Tappen M. 1995. Savanna ecology and natural bone deposition: Implications for early hominid site formation, hunting, and scavenging. Current Anthropology 36:223-260.

Tersigni MA. 2007. Frozen human bone: A microscopic investigation. Journal of Forensic Science 52(1):16-20.

Thali MJ, Lux B, Losch S, Rosing FW, urlimann J, Feer P, Dirnhofer R, Konigsdorfer U, Zollinger U. 2011. "Brienzi" – The blue Vivanite man of Switzerland: Time since death estimation of an adipocere body. Forensic Science International 211:34-40.

Todisco D, Monchot H. 2008. Bone weathering in a periglacial environment: The Tayara Site (KbFk-7), Qikirtaq Island, Nunavik (Canada). Arctic 61(1):87-101.

Trueman CN, Martill DM. 2002. The long-term survival of bone: The role of bioerosion. Archaeometry 44(3):371-382.

Turner B, Wiltshire P. 1999. Experimental validation of forensic evidence: A study of the decomposition of buried pigs in a heavy clay soil. Forensic Science International 101:113-122.

Turner-Walker G. 2008. The chemical and microbial degradation of bones and teeth. In: Pinhasi R, Mays S eds. Advances in Human Palaeopathology. West Sussex: John Wiley & Sons P. 3-28.

Turner-Walker G. 2012. Early bioerosion in skeletal tissues: Persistence through deep time. Neues Jahrbuch für Geologie ud Paläontologie – Abhandlugen 256(2):165-183.

Turner-Walker G, Jans M. 2008. Reconstructing taphonomic histories using histological analysis. Paleogeography, Paleoclimatology, Paleoecology 266:227-235.

Ubelaker DH, Buchholz BA. 2005. Complexities in the use of bomb-curve radiocarbon to determine time since death of human skeletal remains. Forensic Science Communications 8.1:1-8.

Ubelaker DH, Buchholz BA, Stewart. 2006. Analysis of artificial radiocarbon in different skeletal and dental tissue types to evaluate date of death. Journal of Forensic Science 51(3):484-488.

US Department of Agriculture Food Safety and Inspection Service. 2003. FSIS Directive 6900.2, Rev 1: Humane handling and slaughter of livestock. Washington: Government Printing Office.

VanLaerhoven SL. 2008. Blind validation of postmortem interval estimates using developmental rates of blow flies. Forensic Science International 180:76-80.

Weitzel MA. 2005. A report of decomposition rates of a special burial type in Edmonton, Alberta from an experimental field stud. Journal of Forensic Sciences 50(3):641-647.

Wells JD, LaMotte LR. 2001. Estimating the postmortem interval. In: Byrd JH, Castner JL eds. Forensic Entomology: The Utility of Arthropods in Legal Investigations. Boca Raton: CRC Press. P. 263-286.

White T, Black MT, Folkens PA. 2011. Human osteology. Cambridge: Academic Press.

White L and Booth TJ. 2014. The origin of bacteria responsible for bioerosion to the internal bone microstructure: Results from experimentally-deposited pig carcasses. Forensic Science International 239:92-102.

Wieberg DAM. 2005. Establishing the perimortem interval: Correlation between bone moisture content and blunt force trauma characteristics. University of Missouri-Columbia.

Wieberg DAM and Wescott DJ. 2008. Estimating the time of long bone fractures: Correlation between postmortem interval, bone moisture content, and blunt force trauma fracture characteristics. Journal of Forensic Sciences 53:1028-1034.

Wild EM, Arlamovsky KA, Golser R, Kutschera W, Priller A, Puchegger S, Rom W, Steier P, Vycudilik W. 2000. ^{14}C dating with the bomb peak: An application to forensic medicine. Nuclear Instruments and Methods in Physics Research B 172:944-950.

Yoshino M, Kimijima T, Miyasaka S, Sato H, Seta S. 1991. Microscopical study on estimation of time since death in skeletal remains. Forensic Science International 49:143-158.